ROLE OF HIV-1 NEF AND VPU IN VIRAL REPLICATION AND $CD4^+$ T CELL DEPLETION.

Richard L Watkins

A dissertation submitted to the faculty of the University of North Carolina at Chapel Hill in partial fulfillment of the requirements for the degree of Doctor of Philosophy in the Department of Microbiology and immunology

Chapel Hill
2014

Approved by:

J. Victor Garcia-Martinez

Ronald Swanstrom

Kristina De Paris

David Margolis

Ralph Baric

ABSTRACT

Richard L Watkins: Role of HIV-1 Nef and Vpu in viral replication and $CD4^+$ T cell depletion. (Under the direction of J Victor Garcia-Martinez)

HIV-1, within its 9-gene genome, encodes a set of accessory proteins regarded as non-essential for *in vitro* replication, but that are critical for optimal viral replication *in vivo*. Specifically, Nef and Vpu, two proteins with some overlap in function, have been implicated in robust viral replication and disease progression.

As part of my dissertation I used an LAI with a simple frame-shift in *nef*, ablating the expression of Nef, and demonstrated the *in vivo* pressure to restore the *nef* ORF. I went on to show, that the protein resulting from the reopening of the *nef* ORF was defective for CD4 downmodulation. Mice infected with LAI containing these *in vivo* generated *nef*s displayed reduced viral loads and the CD4 depletion compared to mice infected with wild type LAI. When the infections with a more severally defective *nef* that was irreversibly inactivated are compared to infections with LAI containing Nefs defective for CD4 downmodulation, I found that nearly 50% of the pathogenic phenotype of wild type LAI could be attributed to Nef's ability to downmodulate surface expression of CD4.

I also examined the role that Vpu plays in replication and $CD4^+$ T cell depletion during an LAI infection in BLT-humanized mice. These investigations demonstrate that Vpu is required for rapid $CD4^+$ T cell depletion and high viral loads. Of interest is that Vpu-defective HIV-1 expressing no Vpu and HIV-1 expressing Nef specifically lacking the ability to downmodulate CD4 have strikingly similar replicative and pathogenic phenotypes.

I also examined the contribution *nef* makes to high viral loads and $CD4^+$ T cell depletion during the infection of the CCR5-tropic virus, HIV-1 JRCSF. Mice infected with JRCSF expressing defective *nef*s have lower viral loads and maintain a higher percentage of their $CD4^+$ T cells than mice infected with wild type JRCSF. I also demonstrate that like LAI, JRCSF expressing a frame-shifted *nef* restores the *nef* ORF. I show in this dissertation that the Nef produced by one of these *in vivo*-generated *nef* mutants is also specifically defective for CD4 downregulation. I also performed a longitudinal analysis of peripheral blood $CD8^+$ T cell activation to demonstrate that Nef is required for increased T cell activation during JRCSF infection.

My dissertation demonstrates that the high viral loads and $CD4^+$ T cell depletion seen during HIV infection depends on the presence of Nef and Vpu. Specifically, Nef has a critical role in determining the outcome of infection. The presence of Nef is required for immune activation, which may explain differences in pathogenic outcomes.

“If you don’t fall from your bike once in a while you’re not going fast enough.”

-Richard L Watkins Jr.

ACKNOWLEDGEMENTS

I would like to express my gratitude to my mentors, Dr. Victor Garcia-Martinez and Dr. John Foster. Dr. Garcia and Dr. Foster have been very supportive in guiding me through my graduate training. I would also like to thank all of the members in Garcia lab both past and present for their friendship and support. Working in the Garcia lab has been a great experience.

I would also like to thank all of my family and friends. Specifically, my mother, father, brother, and sister for providing me with the confidence to pursue anything I desire. I would also like to thank my lovely wife, Charity, who represents my greatest accomplishment in life; thank you for pushing me through the tough times.

Life has provided me with numerous opportunities. I plan to take full advantage of every one.

TABLE OF CONTENTS

LIST OF TABLES

LIST OF FIGURES

ABBREVIATIONS

°C	degree Celsius
AIDS	acquired immune deficiency syndrome
AP-1	adaptor protein 1
AP-2	adaptor protein 2
APOBEC3	apolipoprotein B mRNA editing enzyme, catalytic polypeptide-like
ASK1	Apoptosis signal-regulating kinase 1
BLT	humanized mouse bone marrow liver thymus humanized mouse
BST2	bone marrow stromal antigen 2
CCR5	C-C chemokine receptor type 5
CD134	cluster of differentiation 134
CD3	cluster of differentiation 3
CD4	cluster of differentiation 4
CD38	cluster of differentiation 38
CD8	cluster of differentiation 8
cDNA	complementary Deoxyribonucleic acid
CTL	cytotoxic T lymphocyte
CXCR4	C-X-C chemokine receptor type 4

DMEM	Dulbecco's modified Eagle's medium
DNA	Deoxyribonucleic acid
ELISA	enzyme-linked immunosorbent assay
ER	endoplasmic reticulum
ERV	endogenous retrovirus
FACS	Fluorescence-activated cell sorting
FasL	Fas ligand
FBS	Fetal Bovine Serum
FIV	Feline Immunodeficiency virus
HeLa	Henrietta Lacks
HeLa MAGI	Henrietta Lacks -CD4-LTR-beta-gal cells
HIV-1	Human immunodeficiency virus type 1
HIV-1 JRCSF	JRCSF Human immunodeficiency virus type 1 J.R. Cerebral Spinal Fluid
HIV-1LAI	Human immunodeficiency virus type 1 LAI
HLA-DR	human leukocyte antigen DR
IFNα	Interferon alpha
IL-2	Interleukin 2
IVKA	*In vitro* kinase assay

JRCSFNef*fs*Δ-78	Human immunodeficiency virus type 1 J.R. Cerebral Spinal Fluid containing a 78 base pair deletion within frame shifted *nef*.
LAINef*fs*	Human immunodeficiency virus type 1 LAI containing a frame shifted *nef*
LAINef*fs*Δ-1	Human immunodeficiency virus type 1 LAI containing a 1 base pair deletion within frame shifted *nef*.
LAINef*fs*Δ-13	Human immunodeficiency virus type 1 LAI containing a 13 base pair deletion within frame shifted *nef*.
LAINefP72A/P75A	Human immunodeficiency virus type 1 LAI containing two alinines substitutions and proline positions 72 and 75 with Nef.
LAIΔvpu	Human immunodeficiency virus type 1 LAI containing large deletion with *vpu*.
mg	milligram
MHC1	major histocompatibility complex class one
mL	milliliter
mM	millimolar
MOI	multiplicity of infection
Nef	negative factor
NFκ-B	nuclear factor kappa-light-chain-enhancer of activated B cells
NIH	National Institutes of Health
NK cells	Natural Killer Cells

NOD	Non-obese diabetic
NSG	NOD/SCID IL-2$\gamma^{-/-}$
Orf	open reading frame
gp120env	envelope glycoprotein 120
p55gag	gag 55kd protein
PACS-1	Phosphofurin acidic cluster sorting protein 1
Pak2	p21 protein activated kinase 2
PBS	Phosphate Buffered Saline
PCR	Polymerase Chain Reaction
PD1	Programmed cell death protein 1
RELIK	Rabbit Endogenous Lentivirus type K
RNA	Ribonucleic acid
RPMI medium	Roswell Park Memorial Institute medium
S.E.M.	standard error of the mean
SCID mice	severe combined immune deficient mice
SH3	SRC Homology 3
SIV	simian immunodeficiency virus
SIVcpz	simian immunodeficiency virus chimpanzee

SIVgor	simian immunodeficiency virus gorilla
SIVrcm	simian immunodeficiency virus red capped mangabey
TCIU	Tissue Culture Infectious Units
TRIM5a	Tripartite motif-containing protein 5 alpha
ug	microgram
Vpu	viral protein unique
Wpi	weeks post infection
WT	wild type

CHAPTER 1: INTRODUCTION

1.1 The evolution of the AIDS pandemic

If untreated, Human Immunodeficiency Virus (HIV) infection leads to the near total depletion of $CD4^+$ T cells [1-3]. The consequence of this depletion is that the infected individual is left with a crippled immune system and is vulnerable to opportunistic infections and, consequently, the subsequent development of Acquired Immune Deficiency Syndrome (AIDS) [3-6]. AIDS, according to the World Health Organization (WHO), has claimed the lives of 35.9 million, making it one of the worst public health concerns in modern human history [7].

The pandemic that is AIDS is caused by HIV-1, which is the consequence of the cross-species transmission of simian immunodeficiency viruses (SIVcpz) from chimpanzees to humans [8-10]. SIVcpz spawned from transmission and recombination events involving at least two separate lineages of SIV, an SIV strain from red-capped mangabeys (SIVrcm) and from *Cercopithecus* monkeys [11]. SIVcpz strains were transmitted into humans on at least three occasions, one of which resulted in the cross-species transmission of the precursor of HIV-1 group M (major) [8]. Other episodes resulted in the cross-species transmission of the precursor

of HIV-1 group O and the rare HIV-1 group N [12]. HIV-1 group M strains have accounted for the infection nearly 60 million people [9, 13].

After entry into humans, HIV-1 group M has diverged into multiple subtypes (A, B, C, D, F, G, H, J, and K) and over 50 recombinant forms [14, 15]. Despite the high degree of divergence in HIV-1, the lentiviruses found in chimpanzees are even more diverse [16]. Underlying this diversity is the fact that humans and chimpanzees all have the same gene structure; in 5' to 3' order they are *gag*, *pol*, *vif*, *vpr*, *tat*, *rev*, *vpu, env,* and *nef*. Monkey viruses exhibit differences in gene structure from the chimpanzee/human lentivirus, which are *gag*, *pol*, *vif*, *vpx/vpr*, *tat*, *rev*, *env,* and *nef* [8, 12]. The non-primate lentivirus feline immunodeficiency virus (FIV) is closely related to HIV-1 [17, 18]; the genes in FIV are *gag*, *pol*, *vif*, *orfA*, *rev, and env*. *orfA* has multiple functions reminiscent of those of *vpr*, *tat,* and *nef* [18]. Viral tropisms in the case of feline and primate viruses are similar in that both types are able to infect T cells and cells of monocytic lineage [17, 19-21]. The T lymphocytic tropism of FIV derives from using CD134 as its primary receptor [19]. Both HIV and FIV viruses also have a co-receptor, CXCR4 [22]. However, HIV-1 uses CD4 as the primary receptor and CCR5 as the co-receptor [23, 24]. Late in infection, virus can emerge that uses CXCR4 as co-receptor [4, 25]. Interestingly, the *orfA*-encoded protein downregulates its primary receptor, CD134, from the cell surface analogous to the downregulation of CD4 by Nef [26, 27].

In humans, HIV-1 infects $CD4^+$ T cells via receptor- and co-receptor-mediated adsorption. Once inside the cell, HIV-1 uncoats and then reverse transcribes its RNA-based viral genome into a provirus [28, 29]. The provirus is permanently integrated into the host genome where host factors produce viral transcripts, splice the transcript into multiple mRNAs, and translate viral proteins. The nascent virion buds from the cell membrane and coats the virus in a lipid layer. Upon viral release, immature virions are converted into mature infectious virions by the viral protease [30-32], a process that leads to the production of thousands of progeny virions and provides several steps that innate host cell defenses can attack [33, 34]. However, while the defenses of the human host may have been sufficient at stopping retroviral infections in our ancestors, our current defense repertoire against HIV-1 is insufficient.

The susceptibility of the host to viral infections and the likelihood of cross-species transmission depend heavily on the ability of the virus to evade different host mechanisms of the host immune system [35]. These restriction factors limit progression at various stages of the viral lifecycle; for example, APOBEC3G (A3G), TRIM5α, and tetherin [8, 34], whose functions are the 1) creation of lethal hypermutations, 2) untimely uncoating of reverse transcription complexes, and 3) inhibition of viral release from infected cells, respectively [34]. HIV-1 has mechanisms to antagonize every host cell restriction factor.

HIV-1 reverse transcriptase makes an error in transcribing RNA to DNA approximately once in every 10,000 nucleotides [36]. In addition, HIV-1 is also highly recombinogenic [8, 37-39]. In HIV-1 infected individuals, billions of progeny viruses are produced each day [40, 41]. The viral generation of HIV-1 is 1.2 days [42]; thus, the potential for variation among HIV-1 quasispecies within an infected individual is great. HIV-1 evolves rapidly to counter various aspects of the host's immune system [8]. Although HIV-1 contains just nine genes, four (*vif*, *vpr*, *vpu*, and *nef*) are used to avoid and antagonize host cell factors that limit viral replication [8]. The activity of accessory proteins has been viewed as dispensable, due to the lack of observable effects on *in vitro* replication upon their ablation [8, 43]. However, these accessory proteins are strongly conserved in regards to natural infection, demonstrating their importance [44]. In fact, the presence of these accessory genes has allowed the successful cross-species transmission of SIV that resulted in the virus that created the HIV-1/AIDS pandemic [8, 45].

1.1.2 Human and HIV-1 ancestors

Primates originated from an ancestor that lived in the trees of tropical forests; many primate characteristics represent adaptations to life's challenges, which include both environmental and viral factors [44, 46]. For example, most primate species remain at least partly arboreal [47]. On the other hand, examples of adaptations to viral challenges can be seen in the arsenal that the primate host welds against viral infection, specifically to SIV and HIV.

HIV and SIV are members of a family of viruses known as retroviruses, whose ancestral fossils can be found littered throughout the genomes of primates, both human and non-human; these genomic relics are known collectively as endogenous retrovirus (ERVs). Implicit in each ERV is the victory over a retroviral infection by the host immune system, specifically factors of the immune system intrinsic to the host cell. The host cell possesses measures to effectively thwart viral infection at multiple steps in the viral life cycle.

HIV-1 belongs to the genus of lentiviruses. Many lentiviruses exist; one of the oldest is rabbit endogenous lentivirus type K (RELIK) [8, 48]. RELIK, like HIV-1, contains the structural and regulatory genetic elements *gag*, *pol*, *env*, *tat*, and *rev* but, unlike HIV-1, lacks homologs of the genes *vif*, *vpr*, *vpu*, and *nef* [8], genes that were acquired over the course of 12 million years in which RELIK-like lentiviruses jumped from species to species. The absence of homologs suggests that *vif*, *vpr*, *vpu*, and *nef* gave the predecessors to HIV-1 a selective advantage over their evolutionarily forgotten peers. For example, the younger (~ 2 million years) endogenous lentivirus, the gray mouse lemur prosimian immunodeficiency virus (pSIVgml) from a Madagascan lemur, contains a *vif* gene [8]. With *vif*, lentiviruses were able to counter the anti-viral function of the APOBEC3 genes that have deep roots in mammalian evolution [8]. From here the prosimian virus, pSIVgml, could serve as the precursor to a virus capable of transmission into simians, which would require acquiring the genes *vpx*, *vpr,* and *nef*. Although

the acquisition of the genes *vpr* and *nef* allowed for transmission into simian hosts, the acquisition of these genes was insufficient for transmission into chimpanzees, an event that would require the acquisition of yet another gene, *vpu*.

Vpu is an 81 amino acid type I membrane protein and functions to decrease the surface expression of both tetherin and CD4 [34, 49]. Tetherin, a crucial hurdle in the cross-species transmission of SIV, is also antagonized by Nef. The antagonism of tetherin by both *vpu* and *nef* is a result of the co-evolution of SIV with its respective primate host, as not all SIVs contain the *vpu* gene. In fact, it was a recombination event within an infected chimpanzee that introduced *vpu* into what is now HIV-1 [45]. *vpu* is believed to have been introduced into chimpanzee SIV (SIVcpz) via the recombination of an ancestor to an SIV found in *cercopithecus* monkeys (SIVsun) and SIV in the red-capped mangabey (SIVrcm) [8, 12, 50]. The recombined SIVcpz spread in chimpanzees and later transmitted to both gorillas and humans to create what is now SIVgor and HIV-1 [8].

The antagonism of tetherin by HIV-1 Vpu represents the co-evolution of primate lentiviruses with their host, with the host evolving to thwart the viruses of its ancestors only to later succumb to the descendants of those very same viruses [8]. Specifically, mammalian cells evolved restriction factors to protect themselves from lentiviruses among other viruses; however, lentiviruses specifically have accessory proteins to overcome these restriction factors [34, 44].

Moreover, the countering of these restriction factors has allowed HIV-1 to become one of the worst pandemics in human history [8].

1.2 Tetherin and CD4

Bone marrow stromal antigen 2 (BST2) or tetherin, is a lipid raft-associated innate restriction factor [51]. Tetherin is not constitutively expressed, but is interferon-dependent and prevents virion release from the cell surface of the infected cell [52, 53]. Tetherin antagonism by Vpu has been shown to decrease the susceptibility of HIV-infected cells to antibody-dependent cell mediated cytotoxicity [54]. Another investigation showed that in the absence of Vpu, natural killer (NK) cell-activating FcgRIIIa signaling and NK cell degranulation and NK cell-mediated antibody-dependent-cell-mediated-cytotoxicity were enhanced, although the mechanism of this effect is unknown [55]. The second major role of Vpu is downregulating CD4. Vpu prevents newly translated CD4 from being expressed on the cell surface via endoplasmic reticulum associated degradation as opposed to internalizing cell surface-expressed proteins, as in the case of tetherin antagonism [56, 57].

1.3 The HIV Negative factor (Nef) contribution to pathogenesis

HIV-1 Nef is a multifunctional accessory protein of about 27-35kDa that is abundantly expressed early in replication [58, 59]. Myristoylated and mainly localized in the perinuclear region, HIV-1 Nef lacks enzymatic activity of its own, but despite this, large deletions in *nef*

have been implicated in the lack of progression to AIDS following eight accidental exposures by blood transfusions from a single donor [60-62]. After 17 years, of the nine individuals exposed, three infections led to a sufficient drop of $CD4^+$ T cells, classifying these individuals as slow progressors. Of the remaining six, three died from causes unrelated to HIV before their progression status could be determined. The remaining three have been defined as elite controllers [60]. In addition to this clinical observation, experiments in the rhesus macaque SIV-infection model have demonstrated the importance of the *nef* gene for SIV-induced pathogenesis and robust virus replication *in vivo* [63]. Transgenic mouse models have also been used to assess the role Nef plays in the pathogenesis of HIV-1 *in vivo* [64-66]. Humanized mice have demonstrated that Nef is necessary for robust viral replication and depletion of $CD4^+$ T cells [60].

Bone marrow, liver, and thymus (BLT) humanized mice were used to investigate the role of Nef in viral replication and systemic $CD4^+$ T cell loss. BLT humanized mice infected with an HIV-1 defective for *nef* displayed reduced virus replication and $CD4^+$ T cell cytotoxicity [60]. This experiment demonstrates that Nef is critical for virus replication and $CD4^+$ T cell cytotoxicity [35, 58, 67].

However, it will be of great interest to determine which of Nef's functions are directly involved in virus replication and $CD4^+$ T cell cytotoxicity. Although numerous functions have

been ascribed to Nef, four *in vitro* functions have been extensively documented [68-74]: 1) downregulatation of cell surface expression of major histocompatibility complex class 1, 2) enhanced virion infectivity, 3) activation of p21 protein-activated kinase, and 4) downregulation of surface expression of CD4 in infected cells [58].

1.3.1 Major Histocombatibility Complex type 1 (MHC1) down regulation by Nef

MHC1 molecules are found on nearly every nucleated cell and function to display peptides generated from within the cells to cytotoxic T cells lymphocytes (CTL) [75, 76]. Presentation of foreign peptides by MHC1 generally leads to their destruction by CTLs [77, 78]. Foreign peptide presentation by MHC1 is specifically designed to eliminate infected cells before virus spreads [79, 80]. The process of spreading from infected to uninfected cells is essential to the survival of HIV-1; thus, inhibiting foreign peptide presentation by MHC1 is critical. HIV-1 Nef antagonizes MHC1; understanding the mechanism of this particular Nef activity is still ongoing. Nef interacts with the cytoplasmic tail of MHC1 to recruit AP-1 to the cytoplasmic tail of MHC-1 and redirects it to the Trans Golgi network on its way to lysosomes where it is degraded [81-83]. It has also been proposed that MHC-1 is endocytosed by Nef in an adaptor protein 1 (AP-1), phosphofurin acidic cluster sorting protein-1 (PACS-1), and clathrin-dependent fashion [84, 85].

The downmodulation of MHC1 by Nef has been shown to be important for HIV-1 replication [86]. Nef-mediated downmodulation of MHC1 is important for the rapid decline of $CD4^+$ T cells during HIV-1 infection; however, Nef-induced downregulation of MHC1 does not block the development of a dramatic CTL response, which is responsible for the sharp reduction in viral load following the acute phase of HIV-1 infection [6]. It has also been shown that HIV-1 develops escape mutations over the course of the infection [87]. However, Nefs from viremic long-term non-progressors were shown to be fully capable of MHC1 downmodulation [88].

Two largely incompatible models have been generated that differ as to whether or not Nef accelerates MHC1 endocytosis from the cell surface or diverts MHC1 from its normal transit to the cell surface directly to the lysosomes for degredation. In the first model, it was proposed that a Nef-induced signal to ARF6 initiated endocytosis from the cell membrane [84]. Initially, Nef is directed to the TGN by PACS-1 to be primed by a tyrosine kinase in order to then activate PI3K to activate ARNO and subsequently activate ARF6. By an unknown mechanism ARF6 triggers endocytosis of MHC1. Independently, Nef also acts to prevent recycling of internalized MHC1 back to the cell surface but no mechanisms have been forthcoming for this process. In recent years, further elaborations have been made to the model with involvement of PACS-2 and ZAP70/Syk added [85].

Several critical interactions sites on Nef are known to be necessary for the MHC1 downregulation activity. In the above model, it is proposed that four glutamate residues (the acidic cluster (AC) in Nef (^{62}EEEE^{65}) engage the furin binding region (fbr) of PACS-1. PACS-2 may bind to other sorting molecules to target Nef to the *trans*-Golgi network (TGN). The mutation of the AC in Nef to four alanines abrogates the MHC-1 downregulationfunction. At the TGN a second structural motif of Nef, which is proposed to be an SH3 binding domain (^{72}PXXP^{75}), engages an unidentified *src* family kinase (SFK) that displaces PACS-2 [84]. SFK/Nef complex would then bind and phosphorylate ZAP70/Syk on tyrosine, enabling ZAP70/Syk to bind the SH2 domain of phosphatidylinositol 3-kinase (PI3K) [84]. The resulting activation of PI3K would lead to elevated levels of phosphatidylinositol (3,4,5)-triphosphate, the stimulation of the guanine nucleotide exchange factor ARNO, and the GTP loading of ARF6 [84]. This completes the series of events initiated by Nef/PACS-2 binding. To achieve MHC1 downregulation, the model continues with activated ARF6 inducing the rapid internalization of MHC1 [84]. For the increased rate of MHC1 internalization to be effective in reducing MHC1 cell surface levels, Nef also blocks the recycling of MHC1 back to the plasma membrane by an unknown mechanism. This last Nef activity is specifically disabled by the M20A mutation. In summary, the steps leading to the ultimate sequestration of MHC1 to the TGN are defined by

three mutant Nefs, (^{62}AAAA^{65}, ^{72}AXXA^{75}, and M20A), all of which result in the crippling of MHC1 downregulation.

An alternate model proposes a ternary complex between Nef, adaptor protein 1 (AP-1) and the cytoplasmic tail of MHC1. This complex is responsible for the misdirection of MHC1 away from the cell surface [89-91]. The roles for ^{62}EEEE^{65} and ^{72}PXXP^{75} are radically different in this model. The tetraglutamate is not viewed as an acidic cluster and ^{72}PXXP^{75} is not an SH3 domain-binding site. These interpretations were confirmed by fine structure-function mapping [92, 93]. Specifically only two of four glutamates were sufficient for full function. Also, mutation of the ^{72}PXXP^{75} putative SH3 domain binding failed to conform to the canonical expectation that activity would be completely lost by single mutations AXXP or PXXA [94-97]. Critically, mutation to alanine of a highly conserved proline at positions 78 (and hence outside of the proposed SH3 domain binding site) did eliminate MHC1 downregulation activity [93, 98, 99]. The validity of the second model was confirmed by X-ray crystal analysis of the Nef, MHC1 cytoplasmic tail and AP-1 complex. The glutamates interacted with a basic patch on AP-1 to stabilize the ternary complex, and the three prolines (72,75, and 78) were strung out in a unique confirmation unlike Sh3 binding domains. A critical interaction was observed between P78 of Nef and a pocket formed by the cytoplasmic tail of MHC1 in association with the YXXΦ site of AP-1 [82].

The role of M20 remains obscure though a computer model predicts binding of a region of Nef around M20 to the YXXΦ site of AP-1 [100]. The above-mentioned X-ray crystal structure and the computer model have not been reconciled.

Finally, the mutation of the highly conserved, multifunctional residue aspartate-123 eliminated MHC1 downreulation activity [101, 102]. Until the roles of M20 and D123 are resolved the full mechanism of Nef's downregulation of MHC1 will remain unknown. However, much has been learned about the mechanism of Nef's MHC1 downreulation activity that should provide a basis for developing small molecule inhibitors [103]. What remains to be determined is the importance of this activity for the development of AIDS.

1.3.2 Downregulation of cell surface expression of CD4 by Nef

The downregulation of CD4 from the cell surface by Nef was the first and is the most extensively characterized function of the Nef protein [26, 104]. This particular function of Nef is highly conserved with Nefs from HIV-1 groups M, N, and O as well as Nefs from SIVcpz, all of which are capable of downregulating surface expression of CD4 [105]. Differences between group M subtypes have been reported in Nef's ability to downmodulate CD4 [106]. Downmodulation of CD4 by Nef involves internalizing surface CD4 [107], which requires the clathrin-associated adaptor protein 2 (AP-2) [108]. In addition, the internalization of surface CD4 is independent of the phosphorylation of serine residues in the CD4 cytoplasmic tail [26].

As mentioned, Nef has no enzymatic activity of its own and the internalization of CD4 requires cellular components. X-ray crystallography and nuclear magnetic resonance studies have demonstrated that Nef has flexible N-terminal (amino acids 1-68), a central structured core (amino acids 69-197) and a short C-terminal segment (amino acids 198-206). Within the structured core is a flexible loop (amino acids 146-179) [109-111]. Within this loop are two motifs critical for CD4 downregulation – a canonical dileucine trafficking motif (Leu164 and Leu165) and diacidic motif (aspartate or glutamate at 174 and aspartate at 175) that is specific to Nef [108, 112, 113]. The dileucine sequence in SF2 Nef is ^{160}ENNSLL^{165}. The glutamate and two leucines are highly conserved but the internal residues are not [114]. Position 174 of the acidic motif is highly conserved as an acidic residue and position 175 is strictly conserved as aspartate. Yeast-3-hybrid assays have shown that the two motifs are both involved in the binding of Nef to AP-2 with the formation of a ternary complex with the cytoplasmic tail of CD4 [108, 113]. The Nef-directed binding of CD4 to AP-2 has been proposed as the mechanism for enhanced endocytosis of CD4.

The dileucine motif in Nef has been investigated by mutational analysis. Mutation of E160, N161, N162, or S163 to glycine has little effect on the capacity of Nef to downregulate CD4 [115]. However, the charge reversing mutation of E160 to lysine reduces activity by 50%. A possible role for the three internal residues (N161, N162, or S163) has been tested by

replacing them with RQP, which is found in the dileucine motif of tyrosinase [108]. The mutant Nef was fully active for CD4 downregulation and this activity was only marginally dependent on the diacidic motif. Hence, the Nef dileucine motif (ENNSLL) is suboptimal relative to the tyrpsinase motif (ERQPLL) and it is compensated for by the contribution of the diacidic motif to binding. The diacidic residues have been proposed to stabilize the ternary complex by interacting with two basic residues present in AP-2, lysine-297 and arginine-340, on the alpha-adaptin trunk domain [113]. The mutation of these residues specifically inhibits the ability of Nef to bind AP-2 and downregulate CD4.

A possible explanation for this complex situation instead of a direct canonical interaction between the Nef dileucine motif and AP-2 is that the Nef dileucine motif is multifunctional and interacts with not only AP-2 but also AP-1. The diacidic motif allows the dileucine motif that is otherwise optimized for AP-1 binding to also function for AP-2 binding. The direct dileucine-dependent binding of Nef to AP-1 has been demonstrated by *in vitro* pull down assays [89, 91, 115]. This Nef interaction with AP-1 is distinct from the MHC1 cytoplasmic tail, Nef and AP-1 non-canonical interaction described above. A functional role for a direct Nef/AP-1 binding has not yet been discovered.

In addition to the diacidic and dileucine motifs, the internalization of CD4 from the cell surface requires Nef to be myristoylated, which allows Nef to be relocated from the cytosol to

cellular membranes [116]. It is at the plasma membrane that the Nef flexible loop (amino acid 146-179) engages AP-2, which allows binding to the cytoplasmic tail of CD4 and results in the internationalization of CD4 followed by trafficking to the lysosomes [107, 112, 113, 116-123].

Additional Nef residues are necessary for the CD4 internalization. Mutation of tryptophan 57 and leucine 58 to alaninie on the N-terminal flexible arm also renders Nef inactive for CD4 downregulation as does the mutation of aspartate 123 in the structured core [101, 124]. In the results section, we discovered a new pair of residues that are required for CD4 downregulation -aspartate 36 and leucine 37. As was the case for MHC1 downregulation much remains to be resolved before understanding of CD4 downregulation by Nef is complete.

1.3.3 Enhancement of virion infectivity

In vitro single-round infectivity assays have demonstrated that, in the absence of Nef, HIV-1 infectivity is decreased [125, 126]. However, full infectivity can be rescued in assays in which a *nef*-defective virus is complemented by exogenous expression of Nef in the producer cell [126, 127]. This effect does not involve the downregulation of CD4 as production of virus in cells, like 293T, that does not express CD4 yields defective virus without Nef. The precise mechanism behind this effect is poorly understood; however, investigations have shown that Nef-mediated enhancement of infectivity occurs early in infection [128, 129]. Two investigations have supported this claim but propose different mechanisms: 1) Nef may increase viral DNA

synthesis and 2) Nef affects viral entry [129-132]. Early reports demonstrated that Nef has no impact on viral entry, but does impact viral replication [126, 131, 133].

An important study of the mechanism of enhancement of HIV-1 infectivity by Nef has uncovered a role of dynamin 2. Co-immunoprecipitation assays following expression of HA-tagged Nef in 293T cells revealed a prominent protein band of 100kD that was absent from control precipitation [134]. This protein was shown by liquid chromatography-coupled tandem mass spectrometry to be dynamin-2. The specificity of the Nef-dynamin-2 interaction was shown by the fact that dynamin-1 and dynamin-3 do not bind Nef [134]. A mutational analysis of Nef was performed and it was determined that three surface-exposed domain residues, leucine 112, phenylalanine 121 and aspartae 123 were critical for dynamin-2 binding. Mutation of each of there residues to alanine blocked the capacity of Nef to enhance viral infectivity. The SH3 binding domain (PXXP) and dileucine motif (EXXXLL) of Nef were not important for dynamin-2 binding but did inhibit enhancement of viral infectivity by 50 and >90 percent respectively when mutated to alanine. The dramatic dependence of viral infectivity on the dileucine motif suggests that Nef bound to dynamin-2 also interacts with an adaptor protein.

Pizzato reported that the unusual murine leukemia virus protein, glycosylated Gag can replace Nef the enhancement of virion infectivity [135]. This MLV protein is produced from a CUG initiation codon upstream of the Gag AUG codon. GlycoGag contains a membrane

spanning domain and inserts into the ER membrane with the N-terminus in the cytoplasm and the usual Gag sequence in the lumen of the ER where it becomes glycosylated. There are about 60 amino acids in the cytoplasm derived from the upstream coding sequence before the standard *gag* AUG. This suggests that glycosylated Gag functions at the inner surface of the cell membrane which is the site of virion budding. In the case of Nef-induced enhancement of viral infectivity the site of virion budding at the inner surface of the cell membrane could also be the site where Nef acts since this activity requires myristylation of the N-terminus [134].

1.3.4 Activation of p21 activated protein kinase 2 (Pak2) by Nef

Immune activation is associated with increased viral loads and disease progression [136]. Fackler and colleagues postulated that Nef can regulate activation of the infected cell through interactions with Pak2. Investigations have also demonstrated that Nef forms a complex with Pak2 and induces its autophosphorylation and activation [93]. Pak2 is a member of a family of proteins whose common functions include modulating the signaling cascades that lead to cytoskeletal remodeling, regulating apoptosis, and regulating transcription [137]. The biological importance of the Nef-Pak2 interaction is poorly understood and not all Nefs activate Pak2 equally [138-140]. However, it has been determined that a cellular SH3 domain protein is involved. By precise mutational analysis it can be determined if the protein is interacting with an unknown SH3 domain protein by the unique characteristics of proline rich SH3 domain binding

site interaction with SH3 domain proteins [94, 96, 97]. The full type II SH3 domain binding motif is PXXPXR which corresponds to the Nef sequence – ^{72}PQVPLR^{77}. Mutations of either of the prolines or the arginine should massively reduce the ability of the motif to bind to its SH3 domain partner. The identities of the "X" residues vary and provide specificity for the binding, which is critical as the human genome contains 300 SH3 domain proteins [141]. As noted above, the single mutation of the prolines of the Nef SH3 binding domain does not fully block the MHC1 downregulation activity, nor was the mutation of arginine 77 effective in preventing Nef from downregulating MHC1 [93]. In contrast each of these mutations prevented Nef from activating Pak2 [93]. This was also the case for the binding of Nef to the SH3 domain of the tyrosine kinase, Hck [93, 142-144]. Consistent with the SH3 domain binding motif model the effect of mutating internal residues ("X") varied between Pak2 activation and Hck binding [93]. Therefore the Nef SH3 binding site is capable of binding to different SH3 domain proteins and exhibits a similar flexibility to the dileucine motif to be involved with different host proteins to bring about different functions.

Pak2 activation, enhancement of virion infectivity, and MHC1 downmodulation by Nef, all rely on the presence of the polyproline segment P_{69}VR<u>PQVPLR</u>P_{78} [93]. However, the PXXPXR motif is dispensable for pathogenesis. Rhesus macaques infected with a virus with a mutated PXXPXR motif had high viral loads and developed AIDS-like symptoms [145, 146].

These results indicate that MHC1 downmodulation, Pak2 activation, and enhanced virion infectivity are all functions of Nef that are dispensable for robust viral replication and $CD4^+$ T cell depletion.

1.4 CD4 as an innate restriction factor of HIV-1

Two genes, namely *nef* and *vpu*, are not found in lentiviruses that infect horses, cows, goats, sheep, or cats [8, 17]. While both Nef and Vpu are multifunctional, which functions of these two proteins have a major impact on the ability of HIV-1 to actively replicate and induce pathogenesis remains unclear [43]. Of particular interest is the genes' role in adapting primate viruses to infect $CD4^+$ T cells [147]. Using CD4 as the primary viral receptor is difficult because there are 100,000 molecules of CD4 on the surface of $CD4^+$ T cells [148]. Presumably this is not a problem for viral entry but it is very likely that CD4 within the infected cell can block the production of infectious virions by binding of CD4 to Env in the ER [149].

In human lymphoid tissue, Nef-mediated downmodulation of CD4 has been shown to correlate with both viral replication and $CD4^+$ T cell depletion [150]. Nefs from an AIDS patient have enhanced CD4 downmodulation when compared to Nefs from an asymptomatic patient [146, 150, 151]. Of interest is that the infectivity of virus from AIDS patients is also higher than infectivity of viruses from asymptomatic patients [146]. Taken together, these two observations,

an *ex vivo* and an *in vitro* investigation, suggest that CD4 downmodulation is important for both $CD4^+$ T cell depletion and robust viral replication [146, 150].

Using the BLT humanized mouse I have determined that HIV-1 LAI containing a Nef mutated to be specifically defective for CD4 downregulation is attenuated in replication and pathogenesis [152]. The $CD4^+$ T cell cytotoxic phenotype represents approximately 50% of the overall defective phenotype of virus devoid of Nef expression [60]. The highly significant impairment of HIV-1 fitness that results from specifically mutating *nef* to be defective for CD4 downregulation demonstrates the importance of this function for the simian/human lentiviruses, which appears concomitant with the expansion of viral tropism to include CD4-expressing T cells. Remarkably, we have also found that the complete inactivation of *vpu* gives a phenotype similar to that observed for *nef* specifically mutated to lack CD4 downregulation [153]. Vpu, like Nef, acts to reduce the cellular content of CD4 [154]. The similarity of the phenotypes suggests a common mechanism of incomplete blocking of the capacity of intracellular CD4 to interfere with HIV-1 replication.

1.5 Other Nef activities that may be important for HIV-1 replication and pathogenesis.

There are Nef activities in addition to Pak2 and Hck activation that are dependent on an intact SH3 binding site, including upregulation of FasL and PD-1 and Lck-dependent activation Ras-Erk signaling to promote the production of the T lymphocyte survival factor IL-2 [155-158].

To address the possibility that these activities may significantly impact HIV-1 replication and pathogenesis in BLT humanized mice I mutated prolines 72 and 75 to alanine to prevent interactions between Nef and host cell SH3 domain proteins [152]. This mutation did not exhibit a negative effect on Nef function in BLT humanized mice. One explanation for this counter intuitive observation is that high levels of replication and rapid reduction in $CD4^+$ T cell and $CD4^+$ $CD8^+$ thymocytes depends on only a few Nef activities.

CHAPTER 2: *IN VIVO* ANALYSIS OF HIGHLY CONSERVED NEF ACTIVITIES IN HIV-1 REPLICATION AND PATHOGENESIS[1]

2.1 Summary

Background: The HIV-1 accessory protein, Nef, is decisive for progression to AIDS. *In vitro* characterization of the protein has described many Nef activities of unknown *in vivo* significance including CD4 downregulation and a number of activities that depend on Nef interacting with host SH3 domain proteins. Here, we use the BLT humanized mouse model of HIV-1 infection to assess their impact on viral replication and pathogenesis and the selection pressure to restore these activities using enforced *in vivo* evolution.

Results: We followed the evolution of HIV-1_{LAI} (LAI) with a frame-shifted *nef* (LAINef*fs*) during infection of BLT mice. LAINef*fs* was rapidly replaced in blood by virus with short deletions in *nef* that restored the open reading frame (LAINef*fs*Δ-1 and LAINef*fs*Δ-13). These *in vivo* generated mutations were incorporated into Nef expression vectors for *in vitro* analysis.

---

[1] This chapter appeared as an article in the journal Retrovirology. The original citation is as follows: Richard L Watkins, Wei Zou, Paul W Denton, John F Krisko, John L Foster and J Victor Garcia. In vivo analysis of highly conserved Nef activities in HIV-1 replication and pathogenesis. Retrovirology 2013, 10:125. RW, WZ, PD, JK, and JF performed experiments

The LAINef*fs*Δ-1 and LAINef*fs*Δ-13 were stably expressed and specifically defective for CD4 downregulation. Subsequently, LAINef*fs*Δ-1 was often replaced by wild type LAI. Unexpectedly, LAINef*fs*Δ-1 three-fold reduced viral replication (compared to LAI) and a 50% reduction of systemic $CD4^+$ T cells (>90% for LAI) demonstrating the importance of CD4 downregulation. These results also demonstrate that functions other than CD4 downregulation enhanced viral replication and pathogenesis of LAINef*fs*Δ-1 and LAINef*fs*Δ-13 compared to Nef-defective LAI. To gain insight into the nature of these unknown activities, we constructed the double mutant P72A/P75A. Multiple Nef activities can be negated by mutating the SH3 domain-binding site (P72Q73V74P75L76R77) to P72A/P75A and this mutation does not affect CD4 downregulation. Virus with *nef* mutated to P72A/P75A closely resembled the wild-type virus *in vivo* as viral replication and pathogenesis was not significantly altered. Unlike LAINef*fs* described above, the P72A/P75A mutation had a very weak tendency to revert to wild type sequence.

Conclusions: The *in vivo* phenotype of Nef is significantly dependent on CD4 downregulation but minimally on the numerous Nef activities that require an intact SH3 domain binding motif. These results suggest that CD4 downregulation plus one or more unknown Nef activities contribute to enhanced viral replication and pathogenesis and are suitable targets for anti-HIV

therapy. Enforced evolution studies in BLT mice will greatly facilitate identification of these critical activities.

2.2 Introduction

Patients infected with *nef*-defective HIV-1, have strongly attenuated viral replication and pathogenesis [62, 159-161]. *In vitro* studies have defined numerous Nef activities but how this 206 amino acid protein has such a major effect on the outcome of HIV-1 infection in patients is unknown [8, 124, 162-164]. One view of Nef's overall impact on HIV-1 infection is that there is a cumulative effect of multiple activities to achieve high viral loads resulting in the development of AIDS [35, 165]. In support of this view, a number of Nef activities have been found to be conserved in monkey, ape and human immunodeficiency viruses [105, 166-170]. A difficulty with this interpretation is that there are so many Nef activities that the effect of any given activity on replication and pathogenesis would be small. Alternatively, one or a few Nef functionalities may be the major contributors to viral replication and pathogenesis. In this regard CD4 downregulation, a highly conserved Nef function, is of particular interest. *Ex vivo* studies with activated peripheral blood T cells and cultures of tonsil tissue support a dominant role for CD4 downregulation in establishing high rates of viral replication [150, 171, 172]. Another factor that may be critical is the Src homology region 3 (SH3) domain-binding site in Nef's polyproline helix [93, 173, 174]. This ten amino acid segment (PVRPQVPLRP) is the most highly

conserved stretch of amino acids in the protein [175]. Evidence exists for SH3 domain binding site involvement with enhanced viral replication [93, 134, 174], cytotoxic effects [155, 156, 176-178], activation of Hck [144] and antagonism of host immune responses [84, 179-182]. Nef structure/function studies have documented that the CD4 downregulation activity and the SH3 domain protein dependent activities are genetically distinct [93, 127, 183].

To gain greater understanding of the roles of Nef's diverse activities during HIV-1 replication we have employed the BLT humanized mouse model. This model has stable reconstitution of a full spectrum of human immune cells and has been used to investigate a number of different aspects of HIV-1 infection [60, 87, 184-187]. With regard to Nef, we have previously compared the replicative properties of HIV-1_{LAI} (LAI) and LAI with two large deletions in *nef* coding sequence (LAINef*dd*) in BLT mice [60]. LAI exhibited high levels of viral replication and near total depletion of $CD4^+$ T cells in blood and tissues, as well as, depletion of $CD4^+$ $CD8^+$ thymocytes from the human thymic organoid. LAINef*dd* had significantly reduced viral replication and dramatically reduced capacity for inducing $CD4^+$ T cell and $CD4^+$ $CD8^+$ thymocyte loss [60]. However, one important aspect of HIV-1 infection of BLT humanized mice that has not yet been investigated is the ability of *nef* to evolve during HIV-1 infection. In patients, HIV-1 *nef* extensively mutates resulting in tremendous sequence diversity but it has not been possible to clearly relate these changes to Nef activities or the

pathogenic potential of the virus [146, 151, 175, 188-190]. Here, we investigate three critical features of Nef's role during HIV-1 infection: 1) the ability of the virus to mutate *nef* sequences to gain enhanced replicative fitness, 2) the role of CD4 downregulation in viral replication and pathogenesis and 3) the importance of Nef's interactions with host SH3 domain proteins in replication and pathogenesis. We find that Nef induced CD4 downregulation is highly significant for active viral replication and pathogenesis. In addition, there are unidentified function(s) that contribute to viral replication and/or $CD4^+$ T cell depletion and are necessary for Nef's full pathogenic potential. Importantly, this latter function or functions does not depend on interactions with host cell SH3 domain proteins.

2.3 Experimental Procedure

2.3.1 Preparation of BLT humanized mice

BLT humanized mice were prepared as previously described [60, 87, 185, 186, 191-198]. Briefly, thymus/liver implanted or NOD/SCID IL-$2\gamma^{-/-}$ mice (The Jackson Laboratories, Bar Harbor, ME) were transplanted with autologous human $CD34^+$ cells isolated from fetal liver (Advanced Bioscience Resources, Alameda, CA). Human reconstitution in the peripheral blood of these mice was monitored periodically by flow cytometry (FACSCanto; BD Biosciences). Mice were maintained either at the Animal Resources Center, UT Southwestern Medical Center at Dallas (UTSWMC) or at the Division of Laboratory Animal Medicine, University of North

Carolina at Chapel Hill (UNC-CH) in accordance with protocols approved by the UTSWMC or UNC-CH Institutional Animal Care and Use Committees.

To ensure genetic diversity, fifteen different tissue donors were used to generate five groups of mice used for the experiments presented in this manuscript. The overall level of engraftment for all the mice used for these experiments was 60.9% $\pm$ 3.2% (n = 27). None of the groups (Naïve, LAI, LAINef*fs*Δ-1, LAINef*fs*Δ-13 and LAINefP72A/P75A) had significantly different engraftment levels compared to any of the other groups ($p \geq 0.1535$). All groups had at least two different human genetic backgrounds included in the evaluation of infection. LAINef*fs*Δ-1, LAINef*fs*Δ-13 and LAINefP72A/P75A infected groups each shared a common donor with the LAI infected group.

2.3.2 Cell lines and culture conditions

HeLa Magi and TZM-bl cells were maintained in Dulbecco's modified Eagle's medium (DMEM; Cellgro, Herndon, VA) supplemented with 10% fetal bovine serum (FBS; Cellgro), 100 IU/ml of penicillin, 100 µg/ml streptomycin, and 2 mM glutamine (Cellgro) in 10% CO_2 at 37°C. Similarly, 293T cells were cultured under the same conditions as TZM-bl and HeLa Magi cells but in 5% CO_2. The human CEM T cell line was cultured in RPMI 1640 medium supplemented with 10% fetal bovine serum (Hyclone), 50 IU of penicillin per ml, 50 µg streptomycin per ml, 2 mM L-glutamine and 1 mM sodium pyruvate in 10% CO_2 at 37°C.

2.3.3 Proviral clones

The proviral clone, pLAI (accession # K02013), was described by Peden et al [199]. pLAINef*fs* was constructed to be defective for *nef* by cutting with XhoI, filling in with Klenow and re-ligating. This leaves *nef* sequence intact but introduces a four-base frame-shift after *nef* codon 35. The one base deletion (8501) and thirteen base deletion (8511-8523) found in *nef* sequences from LAINef*fs* infected mice were inserted into pLAINef*fs* by site directed mutagenesis to produce pLAINef*fs*Δ-1 and pLAINef*fs*Δ-13, respectively.

2.3.4 Virus production, exposure of BLT mice to HIV-1_{LAI} and HIV-1_{LAI} with mutated *nef*s, tissue harvesting and flow cytometric analyses.

Stocks of LAI, LAINef*fs*, LAINef*fs*Δ-1, LAINef*fs*Δ-13 and LAINefP72A/P75A were prepared and titered as we previously described [200, 201]. Briefly, proviral clones were transfected into 293T cells. Viral supernatant was collected 48 hours after transfection and diluted in Dulbecco's modified Eagle's medium (DMEM) supplemented with 10% fetal bovine serum, 100 IU penicillin/ml, 100 ug/ml streptomycin, and 2 mM glutamine. TZM-bl cells were infected in 12-well tissue culture plates with 0.4 ml of virus at multiple dilutions in medium for two hours. Then, 1.0 ml of supplemented DMEM was added and the plates incubated overnight. Virus containing medium was removed the next day, replaced with fresh DMEM plus 10% fetal bovine serum and the incubation continued for 24 hours. The cells were fixed and stained with 5-

bromo-4-chloro-3-indolyl-β-D-galactopyranoside (40 hours after first exposure to virus). Individual blue cells were counted directly to determine infectious particles per ml (TCIU). Each titer of these viral stocks was performed in triplicate and at least two different titer determinations were performed for each virus preparation.

Intravenous exposure of BLT mice with infectious virus was conducted via tail vein injection with the indicated tissue culture infectious units (TCIU). Viral load in peripheral blood of infected mice was monitored longitudinally by quantitative real-time PCR using Taqman RNA to-C_T^{TM} 1-step kit from Applied Biosystems, USA [192, 193, 202]. The sequences of the forward and reverse primers and the Taqman probe for PCR were: 5'-CATGTTTTCAGCATTATCAGAAGGA-3', 5'-TGCTTGATGTCCCCCCACT-3', and 5'-FAM CCACCCCACAAGATTTAAACACCATGCTAA-Q-3', respectively.

$CD4^+$ and $CD8^+$ T cell levels were monitored by flow cytometric analysis as previously described [185, 196, 198]. Immunophenotyping was performed on blood samples collected longitudinally and on mononuclear cells isolated from tissues at harvest. Whole peripheral blood (PB) from humanized mice was analyzed according to the BD Biosciences Lyse/Wash protocol (Cat. No. 349202) as we have previously described [203]. Briefly, following antibody labeling of whole blood, red blood cells were lysed. The remaining cells were washed, fixed and the sample was analyzed by flow cytometry. Tissue mononuclear cell isolations and immunophenotyping

analyses were also performed according to published methods [185, 196, 198]. Flow cytometric gating for CD4 and CD8 cell surface expression was performed as follows: (step 1) forward and side scatter properties were utilized to set a live cell gate; (step 2) live cells were then analyzed for expression of the human pan-leukocyte marker CD45; (step 3) human leukocytes were then analyzed for hCD3 and (step 4) these T cells or thymocytes were analyzed for hCD4 and hCD8 expression.

The panel of antibodies for analysis of $CD8^+$ T cells double positive for $CD38^+$ and HLA-DR^+ was CD8 FITC (SK1), HLA-DR, PE (TU36) or IgG2bκ PE, CD4 PerCP (SK3), CD3 PE-Cy7 (SK7), CD38 APC (HB7) or IgG1κ APC, and CD45 APC-Cy7 (2D1) (all purchased from BD Biosciences). Gating was performed as follows: (step 1) forward and side scatter properties were utilized to set a live cell gate; (step 2) live cells were then analyzed for expression of the human pan-leukocyte marker CD45; (step 3) human leukocytes were then analyzed for CD3; (step 4) T cells were analyzed for CD4 and/or CD8 expression; (step 5) activation of human $CD8^+$ T cells was analyzed for HLA-DR and CD38 expression [186]. Gates defining HLA-DR and CD38 expression were set with isotype-matched flourophore-conjugated antibodies.

2.3.5 Viral Replication *in vitro*

The human T-cell line A3.01 (NIH AIDS Reagent Program) was used to propagate both wild-type and *nef*-mutant HIV-1_{LAI}. Cells were infected with virus stocks at a multiplicity of

infection (MOI) of 0.05 in complete RPMI (containing 10% fetal bovine serum (Hyclone), 50 IU of penicillin per ml, 50 μg streptomycin per ml, 2 mM L-glutamine, and 1 mM sodium pyruvate) plus 2 μg/ml polybrene at 37° C, 5% CO_2 for 4 hours. The cells were washed extensively with PBS and cultured at 37° C, 5% CO_2 in complete RPMI. Cell cultures were passaged twice weekly at which time a sample of the culture supernatant was collected for quantification of viral capsid protein by $p24^{gag}$ ELISA (HIV-1 p24 Antigen Capture Assay (Advance Biosciences Library, Inc., #5421).

2.3.6 *In vitro* analysis of Nef activities

The site directed mutations of *nef* in pLAINef*fs*Δ-1, pLAINef*fs*Δ-13 and pLAINefP72A/P75A were subcloned into pLXSN, a retroviral vector for transduction of CEM T cells and into pcDNA3.1 for transfection into 293T cells [93]. Assays for CD4 downregulation, MHCI downregulation, and activation of PAK2 were described previously [93]. Enhancement of virion infectivity was determined by single infection assays using HeLa-MAGI indicator cells with virus produced from proviral clones transfected into 293T cells [93, 204]. Protein expression was determined by Western Blot analysis with sheep anti-Nef antibody or mouse monoclonal anti-Nef [93, 205].

2.3.7 Sequence analysis of plasma virion RNA

Viral RNA was extracted from 20 μl of plasma from infected mice using the QIAamp Viral RNA Mini kit (Qiagen Sciences, USA). RNA was then reverse transcribed into cDNA, which was then subjected to nested PCR. The outer primers for *nef* amplification are 5'-AGCTTGCTCAATGCCACAGCC-3' and 5'-GCTGCATATAAGCAGCTGCTTTTTG-3'. The inner primers are 5'-TAGAGCTATTCGCCACATACC-3' and 5'-GCTTGCTACAAGGGACTTTCCGC-3'. Gel purified PCR products were sequenced and the sequences were aligned to HIV_{LAI} sequences to determine if nucleotide changes had occurred.

2.3.8 Statistics

Mann-Whitney tests were performed in Prism version 5 (Graph Pad). All data plotted as mean $\pm$ S.E.M.

2.4 Results

With the exceptions of *vif* and *pol*, the ability of HIV-1 to correct defective genes *in vivo* and regain function has not been investigated [206, 207]. Determining the selection pressure for Nef functions is a key component for characterizing the overall importance of Nef and the phenotypic contribution of its individual activities. In addition, it provides an opportunity to use enforced selection to discern what structural/functional motifs of Nef are important *in vivo*. To address the mutational response of the virus to a defective *nef*, we generated an inactivating

mutation by filling in the 5' four-base overhang generated by the XhoI restriction endonuclease at codon 35 with Klenow (Figure 2.1 A). This insertion resides 5' of the polypurine tract and does not alter the synthesis of *gag*-encoded proteins (Figure 2.1 B) or alter the *in vitro* replication properties of the virus (Figure 2.1 C).

LAI and the *nef* frame-shifted LAI (LAINef*fs*) were injected intravenously (iv, 360,000 TCIU) into BLT mice. Three LAI infected mice were monitored over eight weeks for virus in the blood. These mice had peak viral loads of $12.2 \pm 4.7 \times 10^6$ copies of viral RNA. No changes were observed in *nef* sequence after eight weeks of the infection (Figure 2.2 A). The LAINef*fs* inoculated mice were also monitored longitudinally for the presence of virus in plasma. LAINef*fs* infected mice exhibited active viral replication with peak viral loads of $2.26 \pm 0.72 \times 10^6$ copies of viral RNA per ml of blood (n = 7). We sequenced *nef* from viral RNA in blood from two to eight weeks post-infection and found that the frame-shifted LAINef*fs* (designated "+4") was initially replaced by one of two *nef* sequences with restored open reading frames (Figure 2.2 A). One mouse (LAINef*fs* 1) had a thirteen base deletion downstream of the original four base insertion (Δ-13). In the other six cases (LAINef*fs* 2-7), the *nef* coding sequence also retained the four base insertion but lost one base in a run of five adenines just downstream of the original insertion site (Δ-1). The original LAINef*fs* (+4) was not detectable in blood by five weeks post infection in any of the seven mice. In two mice, and by a slower process, wild type

nef appeared by 4-7 weeks (LAINef*fs* 4, 5). After eight weeks, four mice (LAINef*fs* 3, 4, 5 and 6) were predominantly infected with a virus containing wild type *nef* (not shown). In summary, in the blood of all of the mice inoculated with LAINef*fs* the original defective *nef* was replaced by a *nef* mutant that restored the open reading frame. Sequences determined at eight weeks yielded four mice with exact removal of the four base insertion (WT), two mice with Δ-1 and one mouse with Δ-13. These results support the conclusion that a strong positive selection exists for a functioning *nef*.

The amino acid sequences of the restored *nef*s are reported in Figure 2.2 B. The changes in Nef sequence resulting from the one base deletion (LAINef*fs*Δ-1) and the thirteen base deletion (LAINef*fs*Δ-13) were the replacement of three amino acids (DLE, 36-38) in wild type LAINef with four missense amino acids (SRPG) and the replacement of ten wild type amino acids (DLEKHGAITS, 36-45) with seven missense amino acids (SRPGKTC), respectively (Figure 2.2 B). The sequencing data suggested that virus with *fs*Δ-1 and *fs*Δ-13 *nef*s had a strong replicative advantage over the *nef*-defective virus. However, the replacement of LAINef*fs*Δ-1 with wild type (WT) virus in four mice further suggests a replicative advantage for wild type *nef* over revertant *nef*s. Based on these *in vivo* findings, we were interested in characterizing the *in vitro* activities of the Δ-1 and Δ-13 mutant Nefs.

2.4.1 *In vitro* functional analysis of *nef* mutants that evolved *in vivo*

To assess *in vitro* phenotypes of the Nefs expressed by LAINef*fs*Δ-1 and LAINef*fs*Δ-13, we transferred the coding sequences into the retroviral expression plasmid, pLXSN, and produced retroviral vectors [26]. CEM T cells expressing wild type and mutant Nefs were assayed for level of expression, CD4 downregulation and MHC Class I (MHCI) downregulation activities (Figure 2.3 A). The mutant forms of Nef were expressed at the same level as wild type Nef (Figure 3A, *Upper Panel*, α-Nef). Flow cytometric analysis of cell surface CD4 and MHCI expression of CEM T cells that were transduced to express LAI Nef yielded the well-known patterns for the downregulation of these proteins (Figure 2.3 A, *Lower Panel*, [26, 93, 208]). Both LAI Nef*fs*Δ-1 and LAI Nef*fs*Δ-13 proteins were fully active for MHCI downregulation but devoid of CD4 downregulation activity. To assess the effect of the two mutations on Nef's interaction with p21 activated protein kinase (PAK2), we expressed the Nef*fs*Δ-1 and Nef*fs*Δ-13 proteins from pcDNA3.1 in transfected 293T cells. We determined the capacity of these Nefs to activate PAK2 using an *in vitro* kinase assay (IVKA, [93, 200, 209]). Again, both mutant proteins were expressed at the same level as wild type LAI Nef (Figure 2.3 B, α-Nef) and both proteins activated PAK2 although at a reduced level for LAI Nef*fs*Δ-13 (Figure 2.3 B, α-PAK2 IVKA). We also generated the proviral clones, pLAINef*fs*Δ-1 and pLAINef*fs*Δ-13, to characterize the enhancement of infectivity function of these Nefs. Virus was produced from

transfected 293T cells and assayed with HeLa MAGI indicator cells. In this single infection assay, a reduction in the number of infected cells per ng of virion $p24^{gag}$ is observed for LAINef*fs* relative to LAI (Figure 2.3 C). LAINef*fs*Δ-1 and LAINef*fs*Δ-13 both exhibited higher infectivities than LAINef*fs* in this assay but were not significantly different from LAI (Figure 2.3 C). Finally, in Figure 3D, the capacities of LAINef*fs*Δ-1 and LAINef*fs*Δ-13 to replicate in A3.01 cells were observed to be the same as LAI (Figure 2.3 D). On the basis of this data, we concluded that LAINef*fs*Δ-1 and LAINef*fs*Δ-13 exhibited a specific loss of the CD4 downregulation activity and were potentially useful to investigate the impact of CD4 downregulation by Nef on HIV-1 infection in BLT mice. However, the question remained whether these *nef*s could revert to wild type sequence *in vivo* as four of seven mice infected with LAINef*fs* had predominantly the wild type *nef* sequence in blood after eight weeks (Figure 2.2 A). It should be noted that reversion of the Δ-1 mutation to wild type would require two steps, a four-base deletion and a one base insertion of adenosine. We judged this two-step process to be unlikely to occur within the time frame of the experiments. Accordingly, the wild type *nef*s found in four of the seven mice by week eight may have been directly generated from the frame-shifted *nef* in LAINef*fs* by the exact removal of the four-base insertion.

2.4.2 Infection of BLT humanized mice with *in vivo* generated *nef* mutations

LAI, LAINef*fs*Δ-1 and LAINef*fs*Δ-13 were intravenously injected (90,000 TCIU) into BLT mice. In Figure 2.4, the positive control, wild type LAI, and the negative control, uninfected mice (Naïve), are compared to LAINef*fs*Δ-1 and LAINef*fs*Δ-13 infected mice. In Figures 2.4 A and C, LAI inoculation was followed with rapid appearance of viral RNA in blood and replication to high levels (peak viral loads, $3.03 \pm 0.54 \times 10^6$ copies viral RNA per ml of plasma, n = 7). The time course for the infections with LAINef*fs*Δ-1 and LAINef*fs*Δ-13 revealed a reduction in viral replication compared to LAI (Figure 2.4 A and C). The average peak viral load (in millions of RNA copies per ml of plasma) for LAINef*fs*Δ-1 was 1.19 ± 0.26 (n = 4) which was significantly different from LAI (Figure 2.4 A, 3.03 ± 0.54 (n = 7); p = 0.0242). Similarly, in Figure 2.4 C, the average peak viral load for LAINef*fs*Δ-13 was lower than LAI (0.93 ± 0.23 (n = 4); p = 0.0061). Thus, there appears to be about a threefold reduction in peak viral load relative to wild type for LAINef*fs*Δ-1 and LAINef*fs*Δ-13.

During infection with LAI, $CD4^+$ T cell levels in blood were dramatically reduced (Figure 2.4 B and D) while $CD4^+$ T cells in the blood of uninfected mice were maintained at approximately 80% of total blood T cells (Figure 2.4 B and D). For LAI, the average time to reduce $CD4^+$ T cells to 50% of total blood T cells was 21.6 ± 2.4 days post infection (dpi, n = 7). For mice inoculated with LAINef*fs*Δ-1 or LAINef*fs*Δ-13, an intermediate loss of $CD4^+$ T cells

was evident (Figure 2.4 B and D). The time for $CD4^+$ T cells in blood to decline to 50% of total T cells was determined and compared to LAI (Figure 2.4 B and D). As noted, LAI gave 21.6 $\pm$ 2.4 dpi (n = 7), which was significantly shorter than LAINef*fs*Δ-1 at 65.1 $\pm$ 13.4 dpi (n = 4, p = 0.0106) and LAINef*fs*Δ-13 at 52.5 $\pm$ 13.5 dpi (n = 4, p = 0.0294). LAINef*fs*Δ-1 and LAINef*fs*Δ-13 infected mice were not statistically different from each other. Together, the results from Figure 2.4 document an intermediate *in vivo* Nef phenotype for LAINef*fs*Δ-1 and LAINef*fs*Δ-13.

We have previously reported the phenotypes of LAI and LAI with a totally inactivated *nef* (LAINef*dd*, [60]). The observation that LAI expressing a Nef specifically defective for CD4 downregulation has a significant level of replication and cytotoxicity was not expected based on previous reports [150, 171, 210]. In support of our conclusion, we also noted that a partial loss of $CD4^+$ T cells from blood is established by six weeks. At this time point, the percent of $CD4^+$ T cells in LAINef*fs*Δ-1 and LAINef*fs*Δ-13 infected mice were significantly lower than in Naïve mice but significantly higher than in LAI-infected mice (Figure 2.4 B and D). For LAINef*fs*Δ-1 inoculated mice, the percent $CD4^+$ T cells of total T cells present in blood was 55.4 $\pm$ 3.3 (n = 4) compared to 77.5 $\pm$ 2.8 (n = 4) for Naïve (Figure 2.4 B) with p = 0.0286. For LAINef*fs*Δ-13 inoculated mice, the percentages were 47.0 $\pm$ 11.7 (n = 4) versus 77.5 $\pm$ 2.8 (n = 4) with p = 0.0286. Also at six weeks, LAINef*fs*Δ-1 and LAINef*fs*Δ-13 infected mice had higher percentages of $CD4^+$ T cells than LAI infected mice (Figure 2.4 B and D). Percent of $CD4^+$ T cells for LAI

was 12.5 ± 4.5 (n = 6), versus 55.4 ± 3.3 (n = 4, p = 0.0095) for LAINef*fs*Δ-1. Percent of $CD4^+$ T cells for LAI versus LAINef*fs*Δ-13 was 12.5 ± 4.5 (n = 6) versus 47.0 ± 11.7 (n = 4, p = 0.0190).

At eight weeks, $CD4^+$ T cells in blood of LAI infected mice are nearly depleted while Naïve mice maintained $CD4^+$ T cells at approximately 80% of total $CD4^+$ T cells (Figure 2.4 B and D, [60, 198]). It was of interest to allow the LAINef*fs*Δ-1 and LAINef*fs*Δ-13 infections to continue past eight weeks to determine if these viruses would slowly deplete $CD4^+$ T cells from blood. By 14 weeks, substantial levels of $CD4^+$ T cells were still evident in blood for both viruses, which emphasizes the persistence of the partial Nef phenotype in the absence of CD4 downregulation (Figure 2.4 B and D).

2.4.3 Systemic loss of $CD4^+$ T cells in BLT humanized mice infected with LAINef*fs*Δ-1 and LAINef*fs*Δ-13

We previously observed that systemic loss of human $CD4^+$ T cells from organs closely paralleled loss of human $CD4^+$ T cells from blood during infection with wild type (LAI) and *nef*-defective (LAINef*dd*) virus [60, 198]. For LAINef*fs*Δ-1 and LAINef*fs*Δ-13 infected mice, we also determined that the loss of $CD4^+$ T cells in peripheral blood is matched by the loss of these cells from bone marrow, lymph node, liver, lung and spleen (Figure 2.5 A). Statistical analysis of Naïve versus LAI, LAINef*fs*Δ-1 and LAINef*fs*Δ-13 infected mice demonstrated significant losses in the percent of $CD4^+$ T cells in the five tissues (fifteen comparisons to Naive, all gave p

< 0.05). Also, the fraction of total T cells that were $CD4^+$ was consistently higher in LAINef*fs*Δ-1 infected mice compared to LAI (all five comparisons, $p < 0.05$). In the case of LAINef*fs*Δ-13 versus LAI, three of five organs had statistically higher levels of $CD4^+$ T cells in LAINef*fs*Δ-13 infected mice, with the higher levels of $CD4^+$ T cells not reaching statistical significance for bone marrow and lymph node. The comparisons between LAINef*fs*Δ-1 and LAINef*fs*Δ-13 infected mice were not significantly different in any tissue. Therefore, the partial reduction of $CD4^+$ T cells in blood seen with LAINef*fs*Δ-1 and LAINef*fs*Δ-13 infection is systemic.

We previously reported a devastating impact of LAI infection on $CD4^+$ $CD8^+$ thymocytes. However, LAI lacking a functional *nef* failed to reduce double positive thymocytes [60]. In Figure 5B, drastic depletion of $CD4^+$ $CD8^+$ thymocytes was confirmed following inoculation with LAI. Intermediate losses were observed with LAINef*fs*Δ-1 and LAINef*fs*Δ-13 (Naive, 76.3 $\pm$ 3.0%; LAI, 1.7 $\pm$ 1.2%; LAINef*fs*Δ-1, 35.0 $\pm$ 17.1%; LAINef*fs*Δ-13, 29.3 $\pm$ 10.2%). On the basis of the above results, we conclude that the partial losses of LAINef*fs*Δ-1 and LAINef*fs*Δ-13 found for $CD4^+$ T cells appeared to extend to $CD4^+$ $CD8^+$ thymocytes as well.

The mechanistic interpretation of the intermediate phenotype of the LAINef*fs*Δ-1 and LAINef*fs*Δ-13 viruses depends on the status of the sequence of *nef.* We sequenced *nef* in plasma virion RNA of LAINef*fs*Δ-1 and LAINef*fs*Δ-13 and found no reversions over the course of infection. Specifically, for LAINef*fs*Δ-1, the four base insertion and the Δ-1 deletion remained

intact. For LAINef*fs*Δ-13, the four base insertion and the thirteen base deletion remained intact. There were no second site mutations present in *nef* either (not shown). The absence of wild type *nef* sequence from LAINef*fs*Δ-1 and LAINef*fs*Δ-13 infected BLT mice implies the stability of the phenotypic properties of these two *nef*s during infection. This failure of *nef*s from LAINef*fs*Δ-1 and LAINef*fs*Δ-13 to revert to wild type supports the hypothesis that the appearance of wild type *nef* sequence found in four of seven mice (Figure 2.2) infected with LAINef*fs* was the result of an exact four base deletion and not a two-step removal of the four base insertion plus a one base addition. Therefore, our investigations of LAINef*fs*Δ-1 and LAINef*fs*Δ-13 demonstrate that LAIs stably lacking Nef's CD4 downregulation activity have the *in vivo* phenotype of a reduced capacity for viral replication, for $CD4^+$ T cell depletion and for $CD4^+$ $CD8^+$ thymocyte depletion relative to LAI [60].

2.4.4 LAI, LAINef*fs*Δ-1 and LAINef*fs*Δ-13 and systemic T cell activation

One explanation for the intermediate infection phenotypes of LAINef*fs*Δ-1 and LAINef*fs*Δ-13 would be an inability of these mutated HIV-1s to induce systemic T cell activation [211, 212]. It has been previously reported that naïve BLT mice have approximately 2% of $CD8^+$ T cells that are $CD38^+$ HLA-DR^+ double positive in blood. Infection with LAI or LAINef*dd* elevates this fraction to approximately 8% [60, 186]. We observed similar effects of LAINef*fs*Δ-1 and LAINef*fs*Δ-13 infection on T cell activation. At six weeks post infection,

LAINef*fs*Δ-1 and LAINef*fs*Δ-13 were determined to have 8.2 $\pm$ 3.5 % (n = 4) and 6.1 $\pm$ 2.3 % (n = 4) $CD38^+$ $HLA\text{-}DR^+$ double positive $CD8^+$ T cells in blood, respectively. Thus, LAINef*fs*Δ-1 and LAINef*fs*Δ-13 exhibit the same enhancements of peripheral blood T cell activation as LAI and LAINef*dd*.

2.4.5 The role of SH3 domain dependent activities on LAI infection of BLT mice

A large number of diverse activities of Nef have been shown to be dependent on the highly conserved SH3 domain-binding site. We considered the possibility that these activities may account for the observed selective advantage of the LAINef*fs*Δ-1 and LAINef*fs*Δ-13 over LAINef*fs* despite the absence the CD4 downregulation activity. SH3 domain-binding dependent activities are blocked by mutating two key prolines in Nef's polyproline helix (P72A/P75A, [124, 173]). To investigate the role of the P72A/P75A mutant Nef *in vivo* we generated isogenic, replication competent LAINefP72A/P75A. In 293T cells, LAINefP72A/P75A expressed similar levels of Nef and $p24^{gag}$ compared to LAI (Figure 2.6 A) and actively replicated in A3.01 T cells (Figure 2.6 B). We assayed the enhancement of virion infectivity for LAI and LAINefP72A/P75A and observed the expected loss of this activity for the SH3 domain binding site mutant (Figure 2.6 C, [93, 127, 134]). Also, we expressed the mutated *nef* from LAINefP72A/P75A with the retroviral vector, LXSN, in CEM T cells and found it to be functional for CD4 downregulation but consistent with previous reports largely defective for

MHCI downregulation (Figure 2.6 D [84, 98, 179]). On the basis of these results, we concluded that infecting BLT mice with LAINefP72A/P75A would distinguish between the phenotypic impacts of SH3 domain binding protein dependent activities and CD4 downregulation.

BLT mice were infected with 90,000 TCIU of LAINefP72A/P75A mutant virus (Figure 2.7). Under these experimental conditions, a 1.9-fold higher peak viral load was observed for LAINefP72A/P75A versus LAI (Figure 2.7 A). This difference was not statistically different (5.83 ± 1.84 (n = 4) versus 3.03 ± 0.54 (n = 7); p = 0.1091). In addition, the P72A/P75A Nef mutant and the wild type virus showed a similar time course for reduction of peripheral blood $CD4^+$ T cells to 50% of total T cells in blood with LAINefP72A/P75A at 29.5 ± 4.1 dpi (n = 4) versus LAI at 21.6 ± 2.4 dpi (n = 7); p = 0.1554 (Figure 2.7 B). These results indicate that a functional SH3 domain-binding site in Nef is not required *in vivo* for either high levels of virus replication or for $CD4^+$ T cell depletion.

2.4.6 Systemic depeltion of $CD4^+$ T cells and thymocytes by LAINefP72A/P75A

In transgenic mice, it has been reported that expression of HIV-1 Nef from a CD4 promoter is cytotoxic to $CD4^+$ T cells in multiple organs [64]. In addition, this cytotoxic effect is lost when the polyproline helix is mutated [177]. Therefore, we determined the impact LAINefP72A/P75A infection in BLT mice on $CD4^+$ T cells in bone marrow, lymph node, liver, lung and spleen (Figure 2.8 A). LAI and LAINefP72A/P75A effectively depleted $CD4^+$ T cells.

All differences in levels of $CD4^+$ T cells between Naïve mice and either LAI or LAINefP72A/P75A mice are statistically significant. In contrast, comparisons between the levels of residual $CD4^+$ T cells in mice infected with LAI versus LAINefP72A/P75A were not significantly different (Figure 2.8 A). $CD4^+$ $CD8^+$ thymocytes in the human thymic organoid were also analyzed. We found that these cells were efficiently depleted by LAINefP72A/P75A (Figure 2.8 B). We, therefore, conclude that contrary to expectations the mutation, P72A/P75A has little to no effect on the systemic depletion of $CD4^+$ T cells or $CD4^+$ $CD8^+$ thymocytes *in vivo*.

2.4.7 *In vivo* selection pressure to correct the P72A/P75A mutation is weak

Our conclusion that an intact SH3 domain-binding site is not a major factor in determining the level of HIV-1 replication suggests that there is little or no selection pressure for reversion of the alanines to prolines. LAINefP72A/P75A virion RNA from plasma of the LAINefP72A/P75A infected mice from Figures 2.7 and 2.8 was processed for sequencing. No nucleotide changes in *nef* were noted through six weeks for the entire *nef* sequence from all four mice. Also, no changes were seen to fourteen weeks for three of four mice (not shown). At week eight, however, *nef* sequence from one of the four mice infected with the P72A/P75A mutant virus had a clear shift from guanine to mostly cytosine at the first base of the codon for position 75 (Figure 2.9). This transversion converted the mutant alanine codon (GCT) to the wild type

proline codon (CCT). Even though the $CD4^+$ T cells in LAINefP72A/P75A infected mice were nearly depleted, we continued monitoring the infection past eight weeks to determine if further mutations would occur during LAINefP72A/P75A infection. Interestingly, for the mouse presented in Figure 2.9, the virus with an alanine codon at 72 and proline codon at 75 completely replaced the input virus but failed to revert the alanine codon at position 72 (Figure 2.9, Weeks 10-14). There were no other changes in the *nef* sequence from this mouse (not shown). Since no reversion to original SH3 domain binding site (P72/P75) occurred within the eight week time frame, the high levels of viral replication and peripheral blood $CD4^+$ T cell depletion could not be explained by appearance of wild type virus. However, it should be noted that *in vitro* studies have documented an intermediate MHC1 downregulation activity for the proline 75 mutation [93]. Thus, our results support a model where CD4 downregulation plus one or a few additional activities- not dependent on the SH3 domain binding site- largely account for Nef's impact on viral replication and/or pathogenesis. Loss of the capacity for SH3 domain binding has little effect on viral replication and pathogenesis and exhibits at best a small reduction in viral fitness.

2.5 Discussion

Previously, we established that there are large phenotypic differences between infection of BLT mice with wild type LAI and the *nef*-defective LAINef*dd in vivo* [60]. LAI replicates to high viral loads concomitantly with aggressive and systematic depletion of $CD4^+$ T cells and

$CD4^+$ $CD8^+$ thymocytes. LAINef*dd* exhibits 6-7 fold lower peak viral loads and has little to no capacity to deplete $CD4^+$ T cells or thymocytes [60]. These two large effects of Nef make it feasible to characterize the importance of Nef's individual activities in BLT mice [162]. Here, we have demonstrated a third important property of *nef* in the BLT mouse model- the ability to evolve and restore functionality. Viruses expressing Nef proteins have a decisive replicative advantage over the frame-shifted LAINef*fs* and replace the *nef*-defective virus within a few weeks. Hence, in seven mice, the input LAINef*fs* was lost after four weeks with either LAINef*fs*Δ-1 (six mice) or LAINef*fs*Δ-13 (one mouse) being the sole virus in peripheral blood. By eight weeks, four of seven mice further evolved to be predominantly wild type virus.

The strong *in vivo* selection of LAINef*fs*Δ-1 and LAINef*fs*Δ-13 over LAINef*fs* led us to characterize these *in vivo* selected mutant proteins *in vitro*. We discovered them to be stable but with a total loss of CD4 downregulation activity. Three other *in vitro* Nef activities, MHCI downregulation, PAK2 activation and enhancement of virion infectivity, remained intact. When BLT mice are infected with LAINef*fs*Δ-1 and LAINef*fs*Δ-13, we observed an approximate 3-fold reduction in peak viral load and a partial loss of $CD4^+$ T cells and $CD4^+$ $CD8^+$ thymocytes relative to that observed for LAI. These observations suggest that the *in vivo* selection of the two viruses with mutant *nef*s relative to LAINef*fs* relied on activities beyond CD4 downregulation.

Conversely, the partial reduction of Nef effectiveness observed for LAINef*fs*Δ-1 and LAINef*fs*Δ-13 demonstrates a significant role for CD4 downregulation.

Our data provided evidence that there is selective pressure for restoration of Nef activities other than CD4 downregulation. The identity of these activities is unknown. We considered likely candidates to be one or more of the SH3 domain binding site dependent activities. These activities include enhancement of virion infectivity [93, 127, 134], PAK2 activation [93, 173, 174], upregulation of Fas ligand (FasL) and programmed cell death 1 (PD1) [155, 156], activation of Hck [144], downregulation of MHCI [84, 179, 180] and Lck-dependent activation Ras-Erk signaling to promote the production of the T lymphocyte survival factor IL-2 [158, 213]. We mutated prolines 72 and 75 to alanine to prevent interactions between Nef and host cell SH3 domain proteins [93, 173]. This mutation did not exhibit a negative effect on Nef function in BLT mice. One explanation for this counter intuitive observation is that high levels of replication and rapid reduction in $CD4^+$ T cell and $CD4^+$ $CD8^+$ thymocytes depend on only a few Nef activities.

Future studies with BLT mice will investigate Nef activities that are potentially responsible for the CD4 downregulation-independent aspects of Nef function *in vivo*. Possible activities include elevated secretion of exosomes, blocking the anti-viral effect of autophagy and inhibition of ASK1 [71, 214-218]. Conversely, these studies may lead to the important result

that known Nef activities may not account for a substantial portion of its impact on HIV-1 infection *in vivo* [219]. In this regard, our mutational strategy of introducing palindromic insertions into Nef coding sequence can be extended to scan the protein for regions of special significance for viral replication and pathogenesis. The HIV-1/BLT mice infection model described here is a feasible experimental platform for resolving these questions.

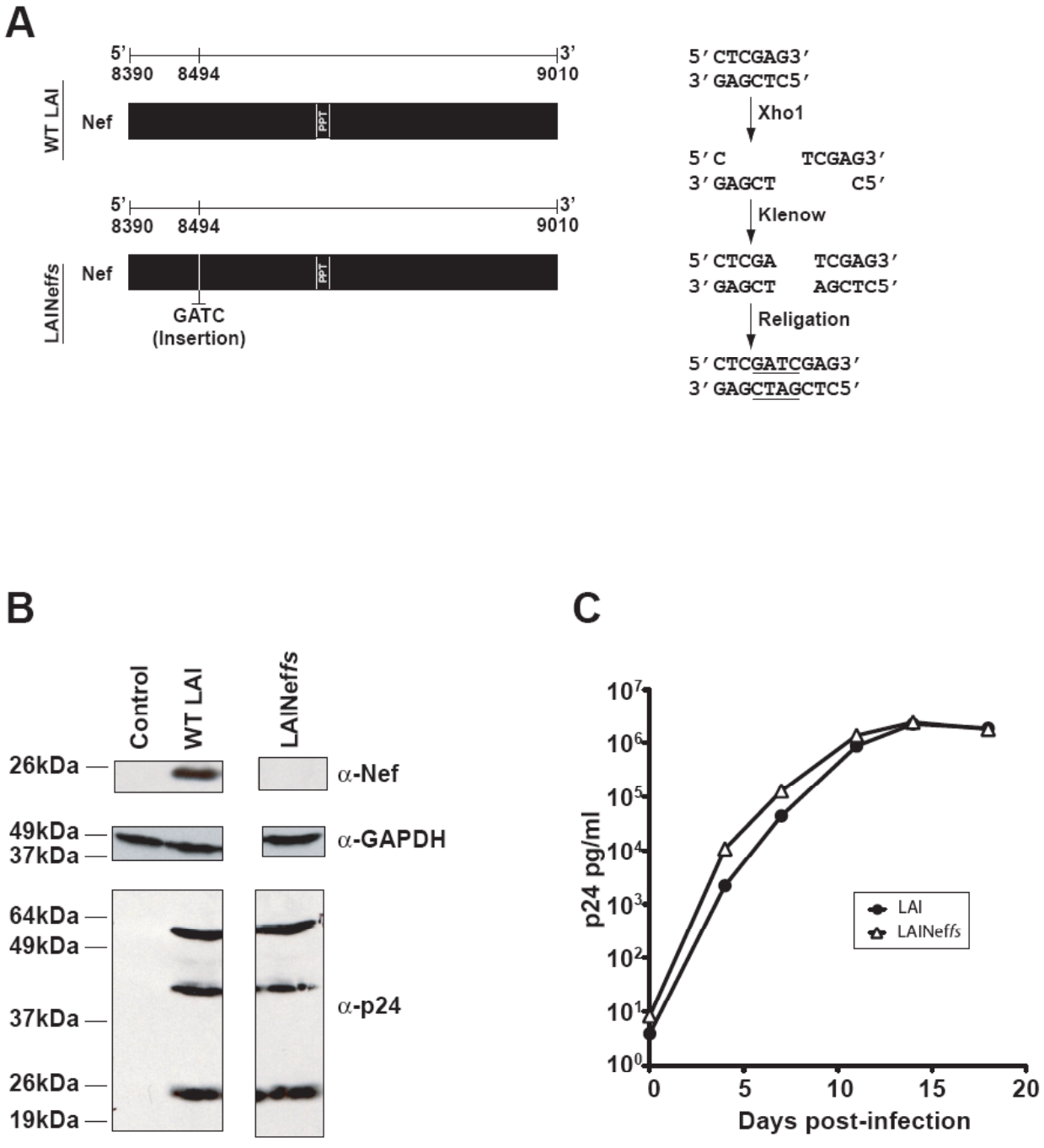

Figure 2.1. A frame shift in *nef* ablates expression of Nef but does not affect viral replication.

(A) *Upper Panel, Left*, Schematic representation of wild type LAI (WT LAI) is presented.

Nucleotides 8390 to 9010 in NCBI accession number, K02013, represent the *nef* coding sequence. *Lower Panel*, *Left*, A schematic of frame shifted *nef* (LAINef*fs*) is presented. The insertion of GATC following nucleotide 8494 is indicated. PPT, polypurine tract. *Upper Panel*, *Right,* Flow chart describing the generation of the GATC insertion is presented. (B) The frame shift in *nef* eliminates Nef expression but does not alter the expression of Gag. *nef* (α-Nef) and *gag* (α -p24) encoded proteins were detected by Western blot analysis of 293T producer cell lysates. GAPDH (α -GAPDH) is a protein loading control. (C) A3.01 cells were infected with LAI or LAINef*fs* at a multiplicity of infection of 0.05 and viral production was followed for 20 days with ELISA for $p24^{gag}$.

A

Mouse[a]	2-4 Weeks[b]	4-7 Weeks[c]
LAINef*fs* 1	30 dpi, Δ-13	51 dpi, Δ-13
LAINef*fs* 2	30 dpi, +4/Δ-1	51 dpi, Δ-1
LAINef*fs* 3	16 dpi, +4	37 dpi, Δ-1
LAINef*fs* 4	15 dpi, +4/Δ-1	29 dpi, WT
LAINef*fs* 5	21 dpi, Δ-1/+4	44 dpi, Δ-1/WT
LAINef*fs* 6	15 dpi, +4	29 dpi, Δ-1
LAINef*fs* 7	15 dpi, Δ-1	44, dpi Δ-1
LAI 1	---	58 dpi, WT
LAI 2	---	58 dpi, WT
LAI 3	---	58 dpi, WT

[a] Mouse identification
[b] Mutations found in amplified *nef* sequences from mice at 2-4 weeks
[c] Mutations found in amplified *nef* sequences from mice at 4-7 weeks

B

```
LAI             MGGKWSKSSVVGWPTVRERMRRAEPAADGVGAASRDLE-KHGAITSSNTA 50
LAINeffsΔ-1     MGGKWSKSSVVGWPTVRERMRRAEPAADGVGAASRSRPGKHGAITSSNTA 50
LAINeffsΔ-13    MGGKWSKSSVVGWPTVRERMRRAEPAADGVGAASRSRPGKTC----SNTA 50
                ************************************    *      ****
LAI             ATNAACAWLEAQEEEEVGFPVTPQVPLRPMTYKAAVDLSHFLKEKGGLEG 100
LAINeffsΔ-1     ATNAACAWLEAQEEEEVGFPVTPQVPLRPMTYKAAVDLSHFLKEKGGLEG 100
LAINeffsΔ-13    ATNAACAWLEAQEEEEVGFPVTPQVPLRPMTYKAAVDLSHFLKEKGGLEG 100
                ************************************************
LAI             LIHSQRRQDILDLWIYHTQGYFPDWQNYTPGPGVRYPLTFGWCYKLVPVE 150
LAINeffsΔ-1     LIHSQRRQDILDLWIYHTQGYFPDWQNYTPGPGVRYPLTFGWCYKLVPVE 150
LAINeffsΔ-13    LIHSQRRQDILDLWIYHTQGYFPDWQNYTPGPGVRYPLTFGWCYKLVPVE 150
                ************************************************
LAI             PDKVEEANKGENTSLLHPVSLHGMDDPEREVLEWRFDSRLAFHHVARELH 200
LAINeffsΔ-1     PDKVEEANKGENTSLLHPVSLHGMDDPEREVLEWRFDSRLAFHHVARELH 200
LAINeffsΔ-13    PDKVEEANKGENTSLLHPVSLHGMDDPEREVLEWRFDSRLAFHHVARELH 200
                ************************************************
LAI             PEYFKNC                                             206
LAINeffsΔ-1     PEYFKNC                                             207
LAINeffsΔ-13    PEYFKNC                                             203
                *******
```

Figure 2.2. LAINef*fs* mutates to have one of three *nefs* with an open reading frame. (A) At several time points during the eight week infection, viral RNA was reverse transcribed from plasma. After amplification by PCR, *nef* was sequenced. By four weeks, six of seven mice exhibited *nef* sequence with a one base deletion just downstream of the four base insertion in a

run of five adenines. This one base deletion (Δ-1) restored the *nef* reading frame. In the remaining mouse, a 13 base deletion occurred downstream of the four base insertion (Δ -13) which also restored the *nef* open reading frame. Three of the seven mice had a mixture of two different sequences in plasma which are indicated by the "majority sequence / the minority sequence." By seven weeks, there were two mice with reversions to wild type sequence (WT) by the removal of four inserted bases from CTCGATCGAG to yield CTCGAG. +4, *nef* with the original four base insertion intact. (B) The conceptual translations of the LAINef*fs* Δ -1 and LAINef*fs*Δ-13 mutated *nef*s are aligned with wild type LAI Nef amino acid sequence. Bold indicates missense amino acids encoded by LAINef*fs* Δ -1 and LAINef*fs* Δ -13.

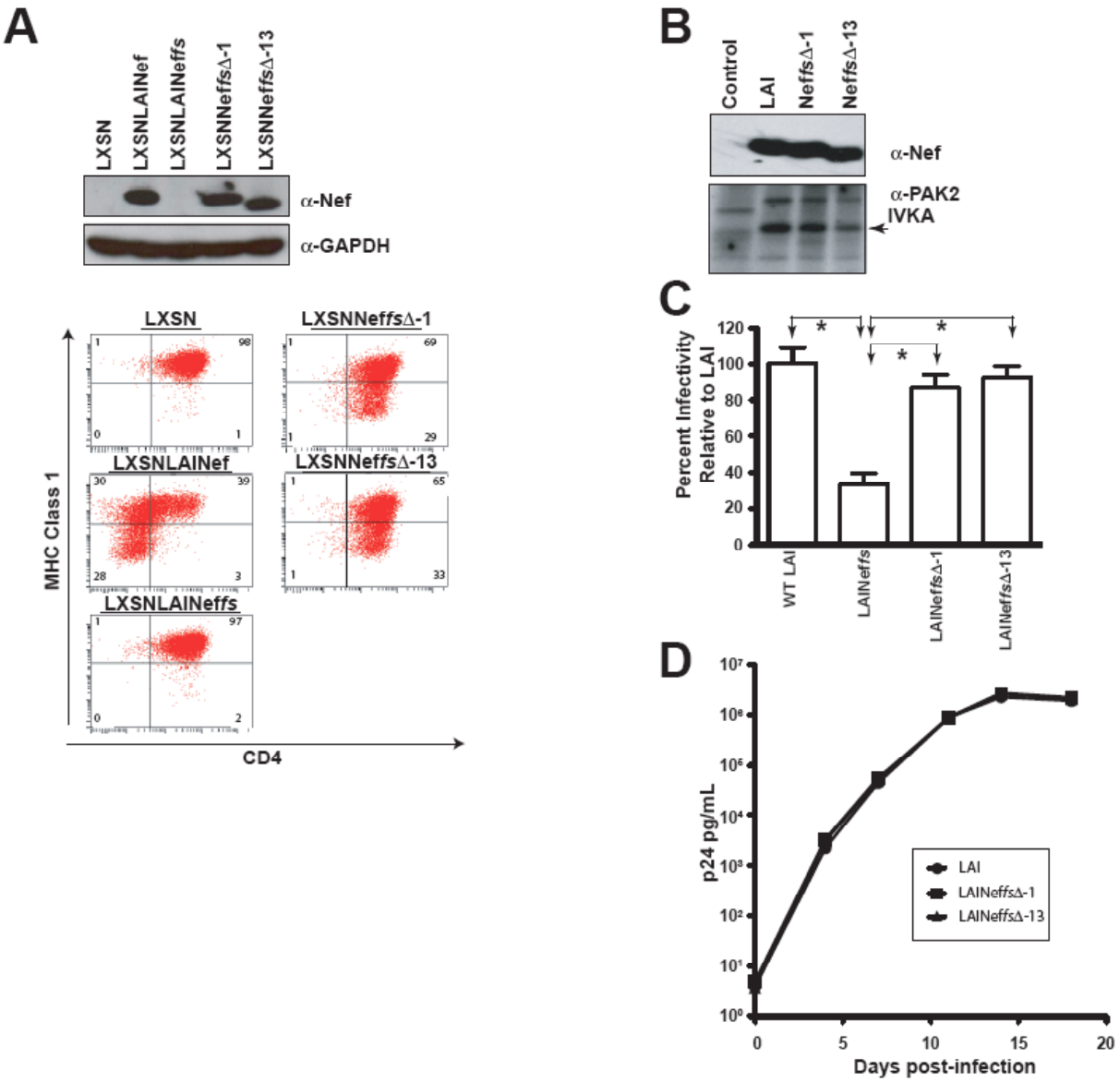

Figure 2.3. LAINef*fs*Δ−1 and LAINef*fs*Δ−13 encode Nefs that are specifically defective for downregulating surface expression of CD4. (A) Nefs encoded by LAINef*fs* Δ-1, LAINef*fs* Δ-13 and LAI were expressed in CEM cells following transduction with retroviral vectors (LXSN). *Upper Panel*, A Western blot demonstrates LAI Nef*fs* Δ-1 and LAI Nef*fs* Δ-13 were expressed at comparable levels as wild type (α-Nef). LXSN and LXSNNef*fs* served as negative controls.

GAPDH is a protein loading control (α -GAPDH). *Lower Panel*, CEM cells expressing LAI Nef, LAI Nef*fs*, LAI Nef*fs* Δ -1 and LAI Nef*fs* Δ -13 were analyzed by flow cytometry for cell surface CD4 and MHC Class I (MHCI) expression. LXSNLAINef was the positive control. LXSN and LXSNLAINef*fs* were negative controls. LAI Nef*fs*Δ-1 and LAI Nef*fs*Δ-13 were fully defective for CD4 downregulation but functional for MHCI downregulation. Percentage of cells in each quadrant out of total cells is indicated. (B) Nefs encoded by LAI, LAINef*fs*Δ-1 and LAINef*fs*Δ-13 were expressed in transfected 293T cells. Control, 293T cells transfected with empty vector. *Upper Panel*, Lysates from transfected cells were analyzed by Western blot and comparable expression of the three Nefs was observed (α-Nef). *Lower Panel*, Total p21 activated protein kinase-2 (PAK2) in lysates of transfected cells lysates were immunoprecipitated with anti-PAK2 antiserum (α-PAK2) and analyzed by the *in vitro* kinase assay (IVKA). Control cells with no Nef expression had no activated PAK2. Arrow, autophosphorylated PAK2. (C) pLAI, pLAINef*fs*, pLAINef*fs*Δ-1 and pLAINef*fs*Δ-13 proviral clones were transfected into 293T cells and virus harvested from the media. LAI, LAINef*fs*, LAINef*fs*Δ-1 and LAINef*fs*Δ-13 were titered using HeLa-MAGI indicator cells [204] and $p24^{gag}$ contents were quantified by ELISA. Infectivities (blue cells per ng $p24^{gag}$) from six determinations of each virus were normalized relative to LAI (100%). Significant comparisons

are indicated by lines and arrows above respective bars (*, $p < 0.05$). (D) A3.01 cells were infected with LAI, LAINef*fs*Δ-1 and LAINef*fs*Δ-13 at multiplicity of infection of 0.05 and viral production followed for 20 days with ELISA for $p24^{gag}$.

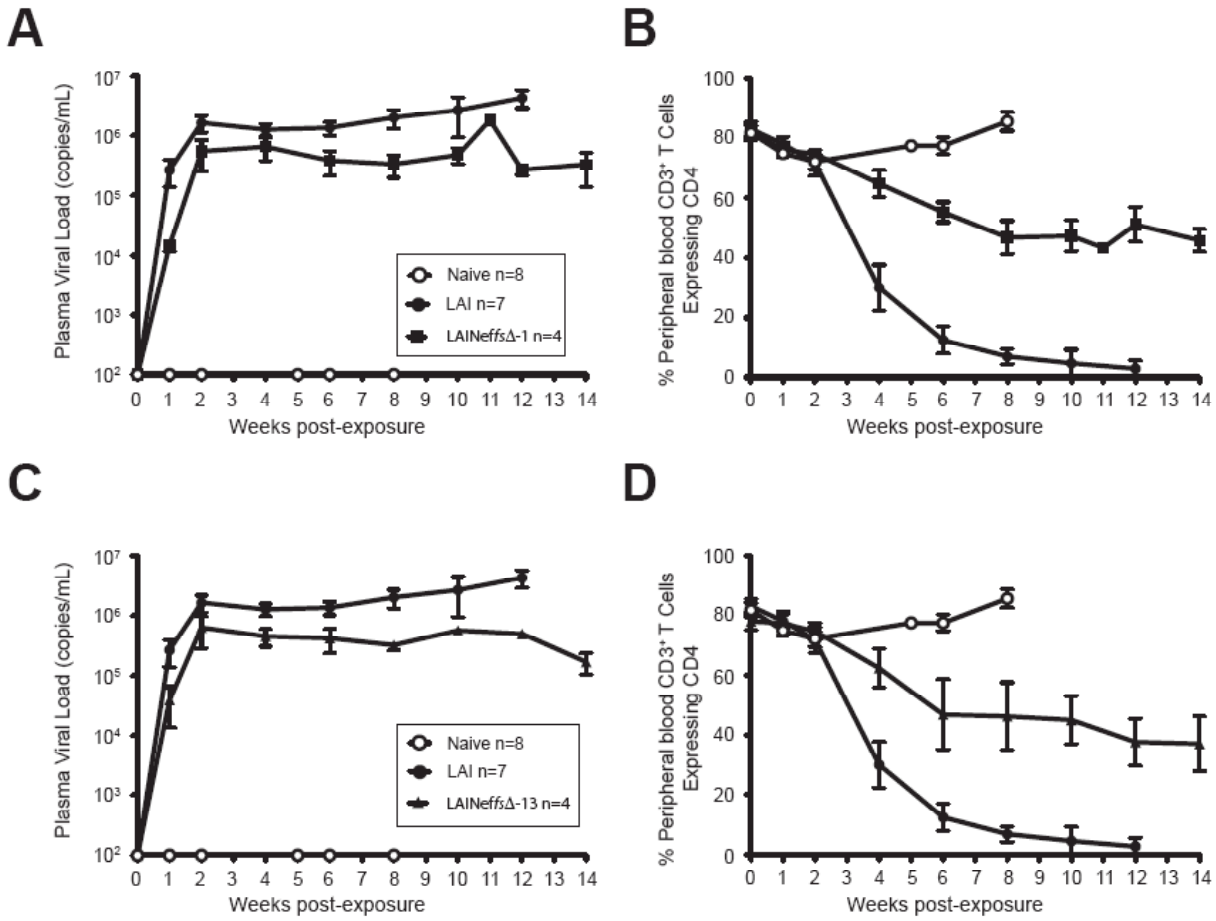

Figure 2.4. Viral load analysis and peripheral blood $CD4^+$ T cell depletion in mice infected with LAI. (A) Viral loads (copies of LAI RNA per milliliter of plasma) of BLT humanized mice exposed to 90,000 TCIU of LAI or LAINef*fs*Δ-1 were plotted. Uninfected mice (Naïve) served as negative controls (open circle, n = 8); LAI (filled circle, n=7); and LAINef*fs*Δ-1 (filled square, n = 4). (B) Plot of percent peripheral blood $CD3^+$ T cells expressing CD4. Naïve mice, LAI and LAINef*fs*Δ-1 as in (A). (C) Viral loads were plotted following inoculation of 90,000

TCIU of LAI or LAINef*fs*Δ-13. Naïve mice as negative controls (open circle, n = 8); LAI (filled circle, n=7); and LAINef*fs*Δ-13 (filled triangles, n = 4). (D) Plot of percent peripheral blood $CD3^+$ T cells expressing CD4. Naïve mice, LAI and LAINef*fs*Δ-13 as in (C).

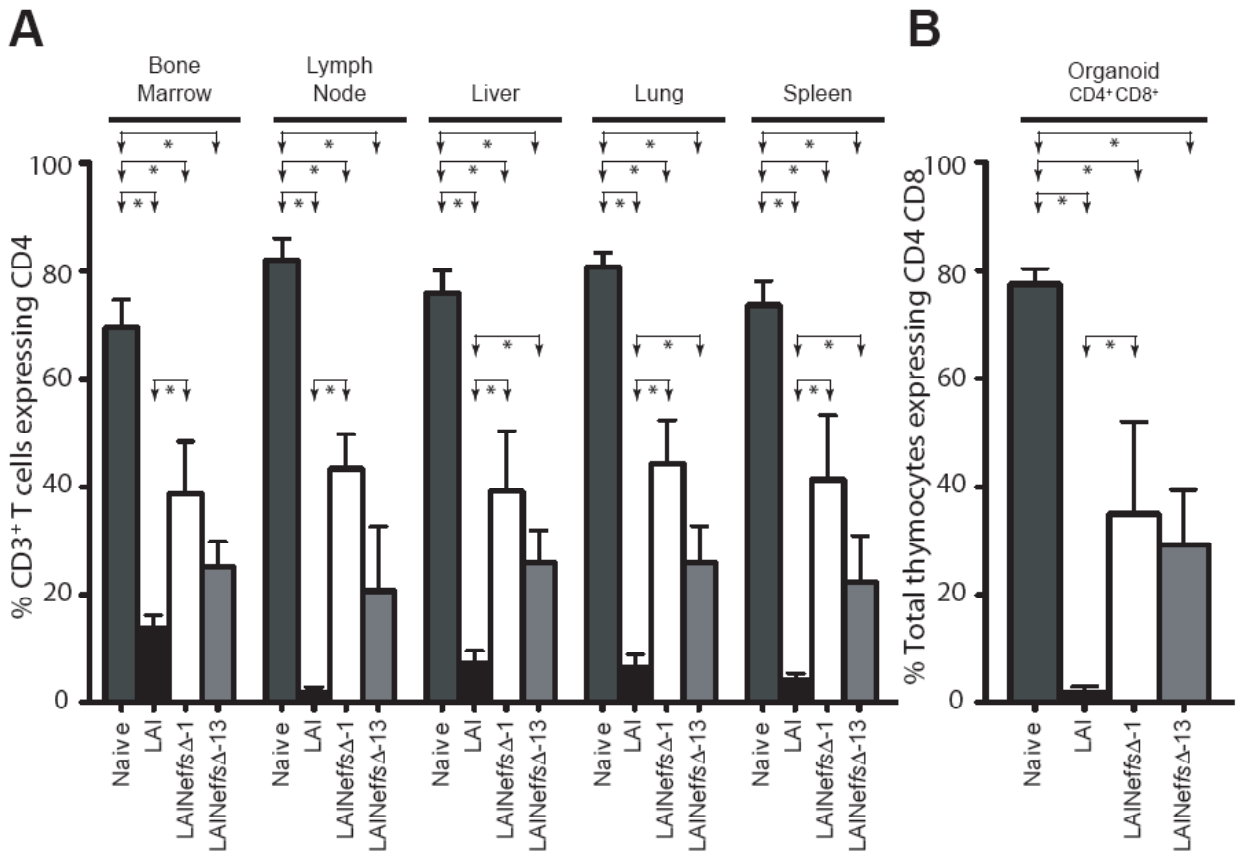

Figure 2.5. Analysis of $CD4^+$ T cells from tissues in mice exposed to LAI, LAINef*fs*Δ−1 or LAINef*fs*Δ−13. **(A)** Percent $CD4^+$ T cells of total T cells in five organs from unexposed BLT mice (Naive, n = 8) were compared to groups of BLT mice exposed to one of three viruses: LAI (n = 6), LAINef*fs*Δ-1 (n = 4), or LAINef*fs*Δ-13 (n = 4). Statistical comparisons reaching significance are indicated by lines and arrows above respective bars (*, $p < 0.05$). **(B)** The same groups as in (A) were compared for $CD4^+CD8^+$ double positive thymocytes relative to total thymocytes.

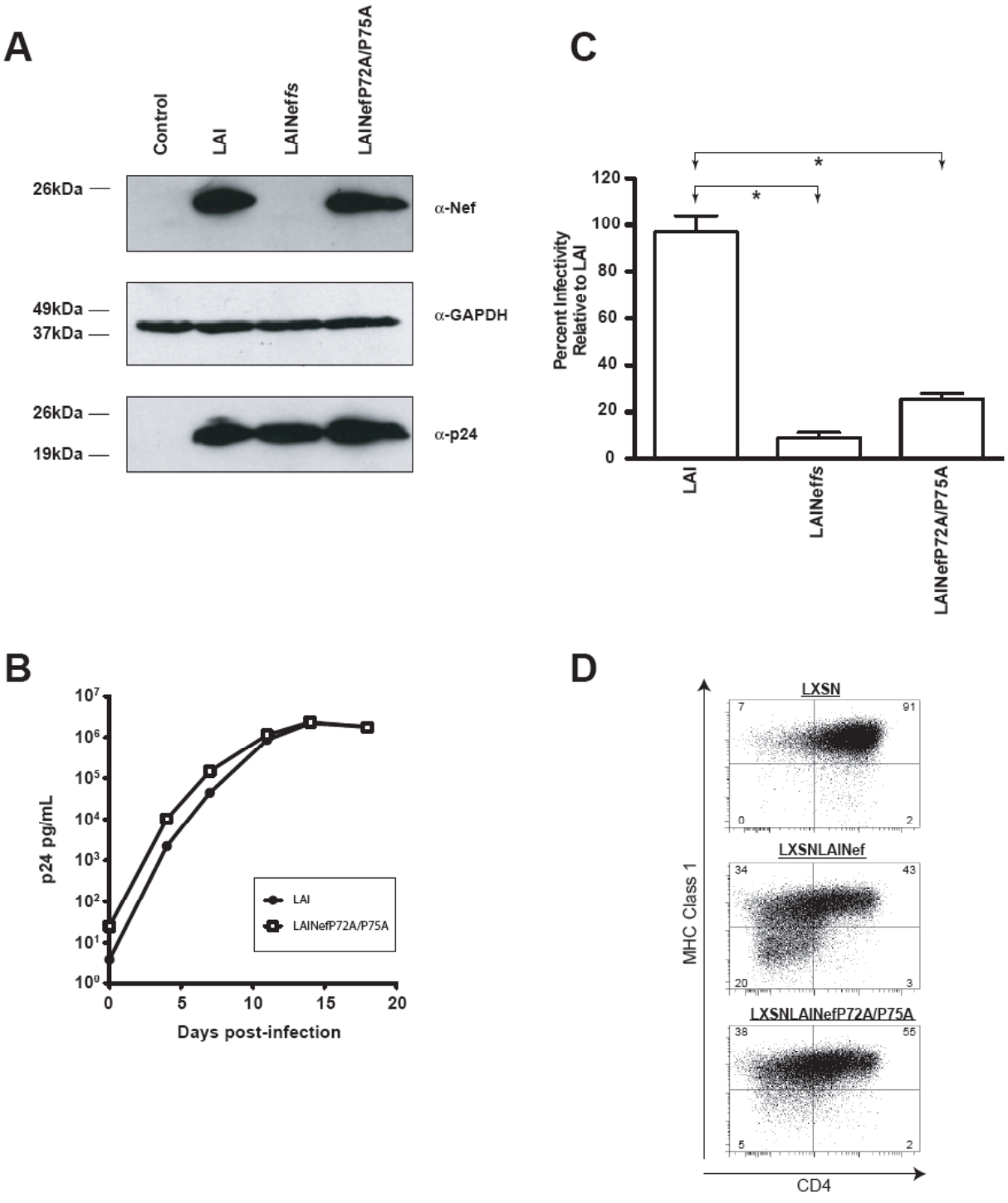

Figure 2.6. LAINefP72A/P75A replicates in A3.01 T cells and is functional for CD4 downregulation. pLAI, pLAINef*fs* and pLAINefP72A/P75A proviral clones were transfected

into 293T cells and virus harvested from the media. **(A)** Nef (α-Nef) and $p24^{gag}$ (α-p24) proteins were detected by Western blot analysis of 293T producer cell lysates. Control is non-transfected 293T cells. GAPDH (α-GAPDH) is a protein loading control. **(B)** A3.01 cells were infected with LAI and LAINefP72A/P75A at multiplicity of infection of 0.05 and viral production followed for 20 days with ELISA for $p24^{gag}$. **(C)** LAI, LAINef*fs* and pLAINefP72A/P75A were titered using HeLa-MAGI indicator cells [204] and $p24^{gag}$ quantitated by ELISA. Infectivities were normalized to LAI (100%). **(D)** Nefs encoded by LAINefP72A/P75A and LAI were expressed in CEM cells following transduction with retroviral vectors (LXSN). CEM cells expressing LAI Nef and LAI NefP72A/P75A were analyzed by flow cytometry for cell surface CD4 and MHC Class I expression. LXSN is the negative control. Percentage of cells in each quadrant out of total cells indicated.

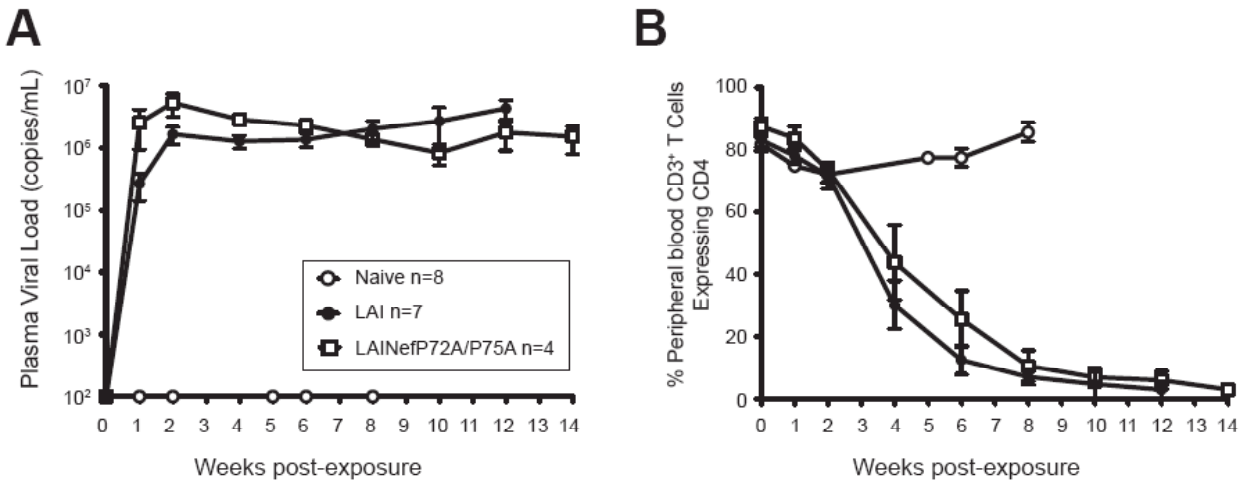

Figure 2.7. Viral load analysis and peripheral blood $CD4^+$ T cell depletion in mice infected with LAINefP72A/P75A. (A) Viral loads of BLT mice were plotted for BLT humanized mice that were exposed to 90,000 TCIU of LAI (n = 7) and LAINefP72A/P75A (n = 4). Uninfected mice (Naïve) served as negative controls. (B) The percent of $CD4^+$ T cells out of total T cells in peripheral blood are plotted for mice in (A).

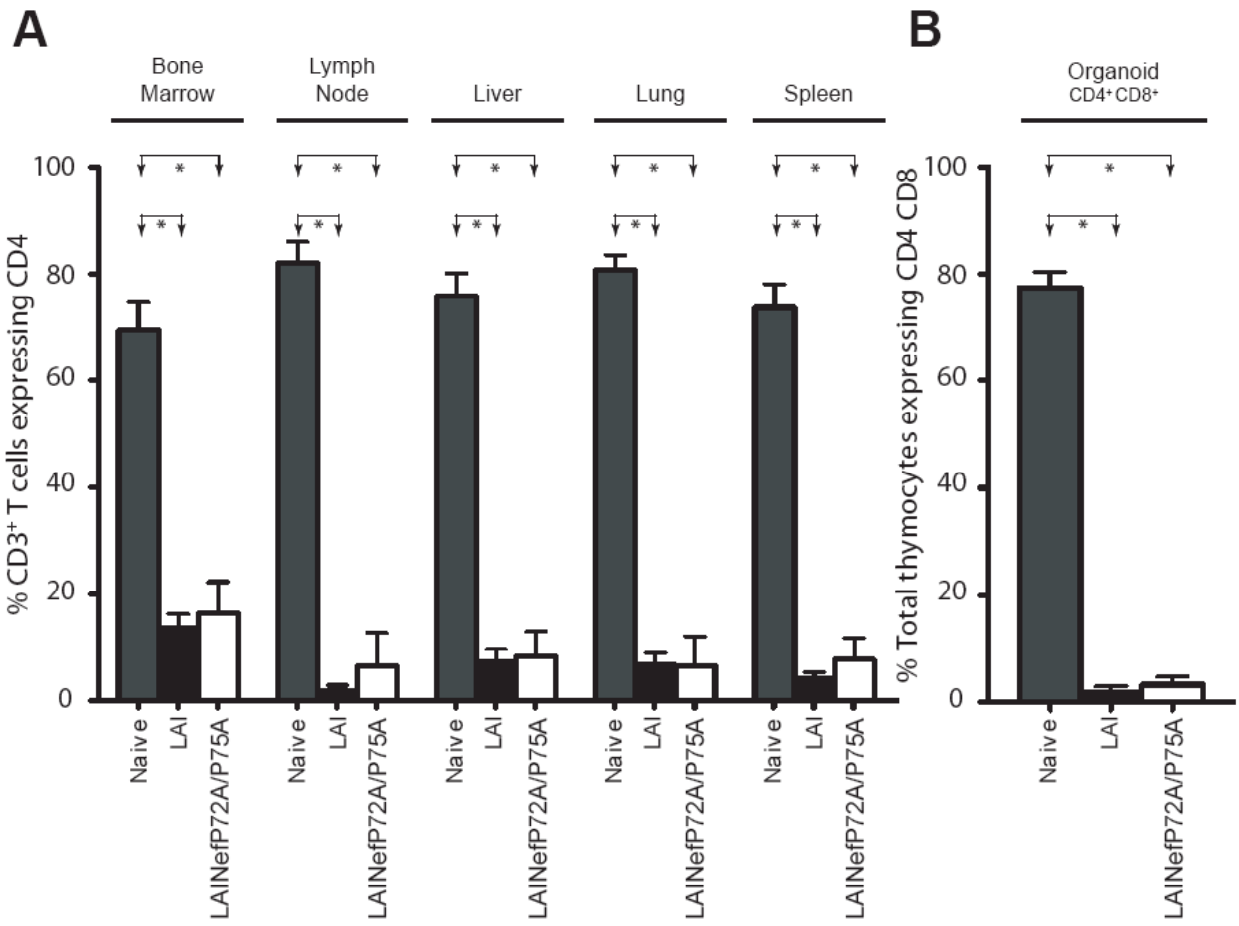

Figure 2.8. Analysis of $CD4^+$ T cells from tissues from mice exposed to LAI or LAINefP72A/P75A. (A) Percent of $CD4^+$ T cells out of total T cells from bone marrow, lymph node, liver, lung and spleen from unexposed BLT mice (Naive, n = 8) were compared to groups of BLT mice exposed to LAI (n = 7) or LAINefP72A/P75A (n = 4). Statistical comparisons reaching significance are indicated by lines and arrows above respective bars (*, $p < 0.05$). (B) The same analysis as in (A) is presented for $CD4^+CD8^+$ double positive thymocytes relative to total thymocytes. Statistical comparisons reaching significance are indicated by lines and arrows above respective bars (*, $p < 0.05$).

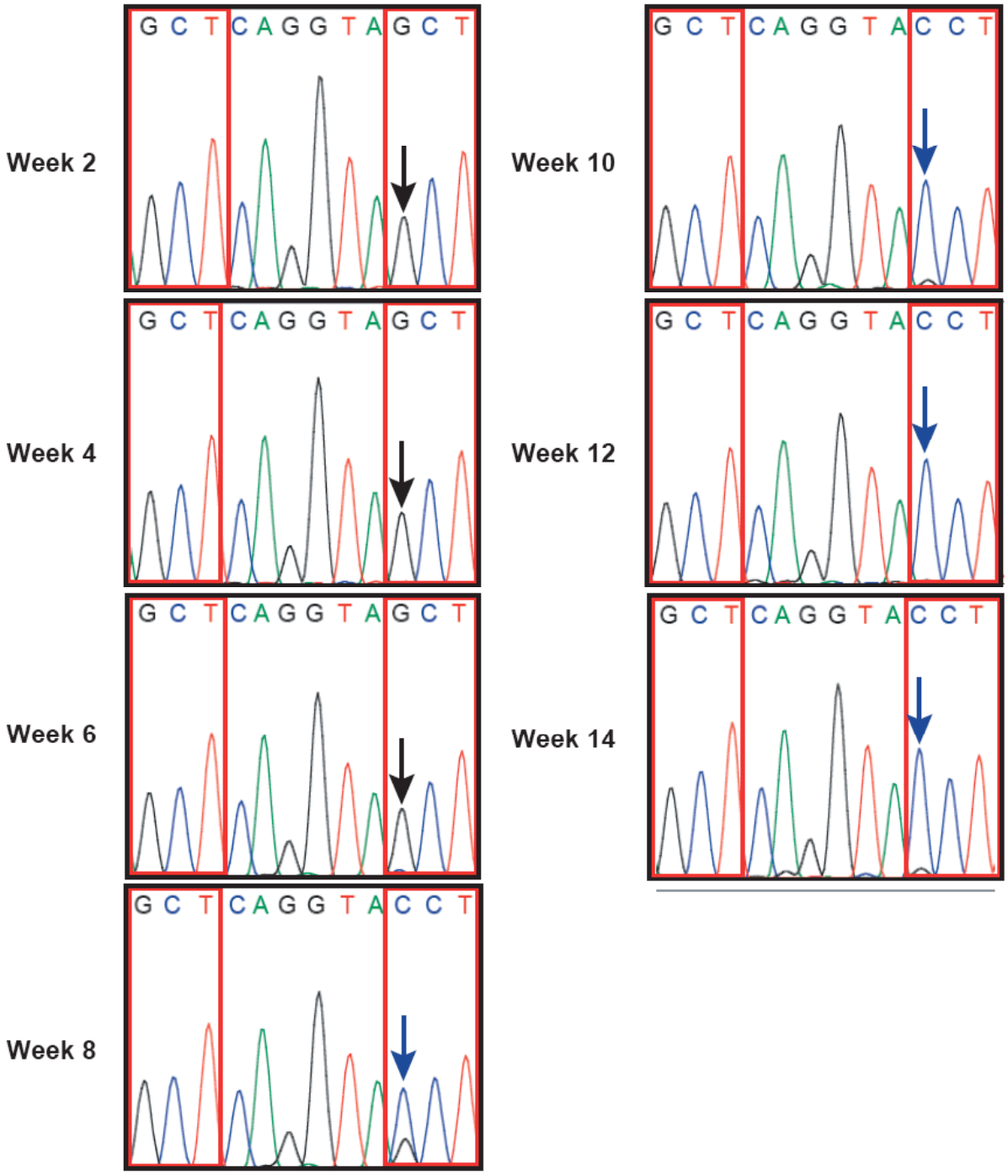

Figure 2.9. Delayed partial reversion of P72A/P75A. *nef* sequences were obtained from viral RNA in plasma of four LAINefP72A/P75A infected mice from Figure 2.7. Only one of four mice had a change in *nef* sequence which is shown in the panels here. This was the reversion of

the P75A mutation back to proline. The delayed and limited appearance of this mutation may be the result of the low probability of a transversion (G to C) coupled to a small enhancement of viral fitness. The twelve nucleotides encoding the SH3 domain binding motif core (P72Q73V74P75) are presented. The wild type proline codons that were mutated to alanine are P72A (left panel headed by GCT) and P75A (right panel headed by GCT). The replacement of guanine with cytosine that restores the P75 codon is seen in the right panels of weeks 8, 10, 12 and 14 headed with CCT instead of GCT. Arrow, guanine mutated to cytodine. A, green; C, blue; G, black: T, red. The four codons presented are GCT, alanine; CCT, proline; CAG, glutamine; GTA, valine.

CHAPTER 3: THE HIV-1 ACCESSORY PROTEIN, VPU, IS A MAJOR PATHOGENICITY FACTOR[2]

3.1 Summary

Background

Vpu is a multifunctional HIV-1 accessory protein that down-regulates two cellular antagonists of HIV-1, tetherin and CD4. Vpu may also facilitate sexual transmission and accelerate the epidemic spread of HIV-1 Group M.

Results

We employed BLT mice containing a humanized immune system to investigate the effects of Vpu on HIV-1 infection. A role for Vpu in pathogenesis has remained undefined. Intravenous injection of BLT mice with pathogenic CXCR4-tropic virus, HIV-1_{LAI} (LAI) or LAI with a deletion in *vpu* (LAIΔ*vpu*, 0.56 ng $p24^{gag}$) revealed an attenuated pathogenic phenotype for LAIΔ*vpu*. LAIΔ*vpu* reduced levels of $CD4^+CD8^+$ cells in human thymus and $CD4^+$ T cells in blood and tissues by 60% compared to >90% depletion for LAI. LAIΔ*vpu* exhibited a 4.4-fold lower peak viral load relative to LAI.

---

[2] Richard L Watkins, John F Krisko, John L Foster and J Victor Garcia. The HIV-1 Accessory Protein, Vpu, is a Major Pathogenicity Factor. RW, JK, and JF performed experiments

Conclusion

We concluded that Vpu is important for full $CD4^+$ T cell cytotoxicity and robust replication.

3.2 Introduction

The HIV-1 accessory protein Vpu counters the INFα-induced tethering of virions to the surface of the infected cell [220]. Vpu acts by neutralizing the membrane protein tetherin, which mediates this block in virus release [221, 222]. However, in chimpanzee, and nearly all simian immumodeficiency viruses, it is Nef not Vpu that blocks the inhibition of virus release by tetherin [223-228]. In the case of HIV-1 Group M, anti-tetherin activity resides solely in Vpu [8, 224, 226]. Group M (but not Groups N, O, or P) *vpu* acquired the capacity to down-regulate tetherin after zoonotic transfer from chimpanzees since SIV_{CPZ} Nef is ineffective against human tetherin [222, 229-231]. Based on *in vitro* studies of Group M, N, O and P Vpu's, it has been proposed that HIV-1 Group M *vpu*'s antitetherin activity may greatly enhance transmission resulting in the spread of HIV-1 Group M virus to epidemic proportions [8, 223, 226, 232, 233]. Therefore, it is expected that without Vpu expression, early viral propagation leading to systemic infection would be attenuated *in vivo* [8, 221, 224, 226, 230]. Unfortunately, direct experimental evidence for this hypothesis is lacking. Indeed, Dave et al. [234] and Sato et al. [235] that found intraperitoneal injection of low inoculums of vpu^- virus established systemic infections in mice

with humanized immune systems at an efficiency not statistically different from wild type *vpu*$^{+}$ virus.

Some investigators consider tetherin to be an HIV-1 restriction factor based on its capacity to prevent virion release from infected cells [236-238]. Other investigators have suggested a complex phenotype for tetherin even including situations in which tetherin expression is a positive factor for HIV-1 replication [239, 240]. One scenario for enhancement of viral replication by tetherin is during cell to cell spread though this effect remains controversial [238]. It has also been suggested that tetherin serves as a cellular signal of viral infection leading to NFκ-B activation [241, 242]. By down-regulating tetherin, Vpu may neutralize this signal [241-246].

Vpu is also known to retain and then direct the degradation of CD4 in the ER [154]. This Vpu activity is thought to be important to prevent the binding of CD4 to Env within the infected cell prior to virion budding [247]. Delivery of CD4-free Env to the virion surface allows the interaction of Env with HIV-1 receptors on new target cells [147, 246, 248, 249]. The importance of this Vpu activity for viral replication and pathogenesis is not known but it has been shown in SCID-hu mice and human lymphoid tissue *ex vivo* that Vpu expression is necessary for wild type levels of replication and pathogenesis [250, 251].

To address the significance of Vpu in HIV-1 infection, we have infected bone marrow liver thymus mice (BLT, [252]) humanized mice with wild type or *vpu*$^-$ HIV-1 by intravenous inoculation with CXCR4-tropic HIV-1_{LAI} (LAI) and LAI with a large deletion in *vpu*. We have then determined the *in vivo* effects of Vpu on viral replication, $CD4^+$ T cell loss, thymocyte loss and systemic T cell activation.

3.3 Experimental Procedures

3.3.1 BLT humanized mice

The mice were individually bioengineered by bone marrow transplant of $CD34^+$ hematopoietic progenitor cells into immunodeficient mice previously implanted with autologous liver and thymus tissue [184, 196, 203]. Briefly, NOD/SCID- IL-$2\gamma^{-/-}$ mice (NSG, The Jackson Laboratories, Bar Harbor, ME) implanted with thymus and liver tissue (Advanced Bioscience Resources, Alameda, CA) were irradiated and subsequently transplanted with $3.5X10^5$ autologous fetal liver $CD34^+$ cells and monitored for human engraftment. Human reconstitution in the peripheral blood of these mice was monitored by flow cytometry (FACSCanto; BD Biosciences). Mice were maintained at the Division of Laboratory Animal Medicine at the University of North Carolina at Chapel Hill (UNC-CH) in accordance with protocols approved by the Institutional Animal Care and Use Committee. To ensure genetic diversity, twenty-five different tissue donors were used to generate the groups of mice used for the experiments

presented in this manuscript. The overall level of engraftment for all the mice used in this manuscript was 63.5% ±2.4% (mean ±SEM, n = 56) with an interquartile range of 54.0% to 75.0%.

3.3.2 Proviral Clones

To generate *vpu*(-) virus, we introduced a 71 base pair deletion by by a site-directed mutagenesis strategy (QuickChange II Site-Directed Mutagenesis kit, Stratagene) into the HIV-1_{LAI} (LAI, K02013) proviral clone (JRCSF, M38429). The deletion in LAIΔ*vpu* (nucleotides 5656-5723, inclusive) was in the 5' end of *vpu* coding sequence just downstream of the *vpu* initiation codon.

3.3.3 Virus production and titering

Stocks of LAI, and LAIΔ*vpu* were prepared by transient transfection of 293T cells as previously described [200, 201]. Briefly, proviral clones were transfected into 293T cells, viral supernatant was collected 48 hours after transfection and concentrated by ultracentrifugation. Then viral titers in tissue culture infectious units (TCIU) were determined by the β-galactosidase TZM-bl cell assay as previously described [60, 185]. TZM-bl cells were infected in 12-well tissue culture plates with 0.4 ml of virus-containing medium for two hours. Dulbecco's modified Eagle's medium (DMEM) supplemented with 10% fetal bovine serum, 100 IU penicillin/ml, 100 mg/ml streptomycin, and 2 mM glutamine (1.0 ml) was added, and the plates incubated

overnight. Virus-containing medium was removed the next day and the incubation was continued for 24 hours. The cells were fixed and stained (40 hours after first virus exposure). The titers of these viral stocks were determined in triplicate and at least two different titer determinations were performed in each batch of virus used for all the experiments described in this manuscript. The $p24^{gag}$ content of the viral stocks and *in vitro* viral replication assays were determined by ELISA.

3.3.4 Exposure of BLT mice, tissue harvest and flow cytometric analyses

Intravenous exposure of BLT mice with LAI or LAIΔ*vpu* (30,000 TCIU) was conducted via tail vein injection as previously described [60, 191].

Infection of BLT mice with HIV was monitored in plasma by determining levels of viral RNA using one-step reverse transcriptase real-time PCR (ABI custom TaqMan Assays-by-Design) according to the manufacturer's instructions [primers (5'-CATGTTTTCAGCATTATCAGAAGGA-3') and (5'-TGCTTGATGTCCCCCCACT-3') and MGB-probe 5'FAM-CCACCCCACAAGATTTAAA CACCATGCTAA-Q 3'] as previously described [193, 202].

Flow cytometric analyses were performed on blood samples collected longitudinally and mononuclear cells isolated from tissues at harvest. Peripheral blood from BLT mice was analyzed according to the BD Bioscience Lyse/Wash protocol (Cat. No. 349202) as we have

previously described [185, 196, 198]. Briefly, following antibody labeling of whole blood, red blood cells were lysed. The remaining cells were washed, fixed and samples were analyzed by flow cytometry. Tissue mononuclear cell isolations and immuno-phenotyping analyses were also performed according to our published methods [60, 185, 193].

Flow cytometric data collection and analyses were performed on BD FACS Canto cytometer operated using FACSDiva software (V.5.0.3). Two flow cytometry antibody panels were used to analyze peripheral blood and cells isolated from tissues of BLT mice: Panel A - CD3 FITC (HIT3a), CD4 PE (RPA-T4), CD8 PerCP (SK1) and CD45 APC (HI30) and panel B – CD8 FITC (SK1), HLA-DR, PE (TU36) or IgG2bκ PE, CD4 PerCP (SK3), CD3 PE-Cy7 (SK7), CD38 APC (HB7) or IgG1| APC, and CD45 APC-Cy7 (2D1) (all purchased from BD Biosciences). Gating for all samples was performed as follows: (step 1) forward and side scatter properties were utilized to set a live cell gate; (step 2) live cells were then analyzed for expression of the human pan-leukocyte marker CD45; (step 3) human leukocytes were then analyzed for CD3, CD4 and/or CD8 expression

3.3.5 Sequence analyses of plasma virions

Sequence of *vpu* and *nef* was obtained from plasma virion RNA. HIV-RNA was extracted from 20 µl of plasma from infected mice using the QIAamp Viral RNA Mini kit (Qiagen Sciences, USA). RNA was then reverse transcribed into cDNA, which was subject to

nested PCR. The outer primers for *vpu* amplification are: 5′-GTCAGCCTAAGACTGCTTGTACC-3′ and 5′-GTGGGTACACAGGCATGTGTGG-3 and the inner primers are: 5′-GACAGCGACGAAGACCTCCTC-3′ and 5′-GATGCACAAAATAGAGTGGTGG-3′. The outer primers for *nef* amplification are: 5′-GAATAGTGCTGTTAGCTTGC-3′ and 5′-CTCAAGGCAAGCTTTATTGAG G-3′ and the inner primers are 5′-TAGAGCTATTCGCCACATACC -3′ and 5′-CTTTATTGAGGCTTAAGCAGT GG -3′. Gel purified PCR products were sequenced and the sequences aligned to LAIΔ*vpu* sequences to determine if sequence changes had occurred.

3.3.6 Viral Replication *in vitro*

The human T-cell line, CEM-SS (NIH AIDS Reagent Program), was modified to express CCR5 [207]. These cells were used to propagate LAI and LAIΔ*vpu*. Cells were infected with virus stocks at a multiplicity of infection (MOI) of 0.05 in complete RPMI (10% fetal bovine serum (Hyclone), 50 IU of penicillin per ml, 50 µg streptomycin per ml, 2 mM L-glutamine, and 1 mM sodium pyruvate) containing 2 µg/ml polybrene at 37^{o} C, 5% CO_2 for 4 hours. The cells were washed extensively with PBS and cultured at 37^{o} C, 5% CO_2 in complete RPMI. Cell cultures were passaged twice weekly at which time a sample of the culture supernatant was collected for quantification of viral capsid protein by p24^{gag} ELISA.

3.3.7 Analysis of $p55^{gag}$ and $gp120^{env}$ expression from LAI and LAIΔ*vpu*

Lysates from 293T cells transfected with proviral clones were analyzed for protein expression by Western blot. $p55^{gag}$ was detected with anti-$p24^{gag}$ (anti-HIV-1 p24 Gag Monoclonal, NIH AIDS Reagent Program) and $gp120^{env}$ was detected with anti-HIV-1 gp120 (HIV-1 gp120 antibody, Fitzgerald Industries International).

3.3.8 Statistical analyses

Bivariate statistical comparisons were performed using Mann-Whitney tests (Prism v5.0, Graph Pad). Data presented as mean ±SEM.

3.4 Results

3.4.1 Vpu and HIV-1 pathogenicity

In the pigtail macaque infection model, *vpu* is critical for the extreme pathogenicity of the CXCR4-tropic SHIV4 [253-256]. In contrast, HIV-1 Group N virus is pathogenic even though, in general, Group N Vpu's are minimally functional for CD4 down-regulation and tetherin antagonism [257, 258]. Further, infection of BLT mice with the CCR5 tropic viruses, made investigating of a possible role of Vpu in pathogenesis difficult, as these viruses are weakly pathogenic [234, 235]. Therefore, we tested the highly pathogenic CXCR4-tropic $HIV\text{-}1_{LAI}$ (LAI) for possible Vpu dependence as LAI Vpu has been shown to be functional for CD4 and tetherin down-regulation [60, 223]. LAI containing a 68 base deletion in *vpu* (LAIΔ*vpu*)

downstream of its initiation codon and upstream of the *env* initiation codon was constructed (Figure 3.1 A). LAI and LAIΔ*vpu* expressed similar levels of $p55^{gag}$ and $gp120^{env}$ (Figure 3.1 B). The two viruses also replicated similarly *in vitro* (Figure 3.1 C).

BLT mice were inoculated by intravenous injection with LAI or LAIΔ*vpu* (3000 TCIU, 0.54 ng $p24^{gag}$). High levels of viral RNA in plasma were observed at two weeks (Figure 3.2 A). In Figures 3.2 B and C, peak viral loads in blood were observed to be reduced 4.4-fold for LAIΔ*vpu* ($1.09X10^6$ $\pm 0.15X10^6$ copies viral RNA/ml, n=3) compared to LAI ($4.83X10^6$ $\pm 0.49X10^6$ copies viral RNA/ml, n=5; p=0.0357). This fold-difference was maintained throughout the course of the infection with viral loads at 11 weeks of $0.42X10^6$ $\pm 0.09X10^6$, n=3 for LAIΔ*vpu* and $2.21X10^6$ $\pm 0.67X10^6$, n=5 for LAI (p=0.0357, Figure 3.2 A). Therefore, loss of Vpu expression reduces overall viral replication for the CXCR4 tropic LAI by 4 to 5 fold compared to a minimal effect on viral replication for CCR5 tropic virus.

LAI infection results in massive loss of $CD4^+$ T cells from blood and tissues [60]. In Figure 3.3, we monitored the effect of inactivating *vpu* on $CD4^+$ T cell and $CD4^+CD8^+$ thymocyte depletion. As presented in Figure 3.3 A, uninfected mice maintained $CD4^+$ T cells at near constant levels, while LAI and LAIΔ*vpu* infected mice exhibited progressive loss of these cells. By eight weeks, five LAI infected mice had only 25.9% ±8.1% of the level of $CD4^+$ T cells in uninfected mice while three JRCSFΔ*vpu* infected mice had 62.3% ±8.6% (p=0.0357). By

eleven weeks, the level of $CD4^+$ T cells in LAI infected mice fell by 90% (10.1% ±3.2%, n=5) while in LAIΔ*vpu* infected mice there was only a partial reduction (41.7% ±11.9%, n=3; p=0.0357).

The different effects of LAI versus LAIΔ*vpu* on $CD4^+$ T cells in peripheral blood were reflected in tissues. In Figure 3.3 B, severe depletion of $CD4^+$ T cells in bone marrow, spleen, lymph nodes, liver and lung was found for LAI. In contrast, LAIΔ*vpu* exhibited an attenuated phenotype with $CD4^+$ T cells levels that was intermediate between uninfected mice and LAI infected mice in spleen, lymph nodes, liver, and lung (Figure 3.3 B). In bone marrow, LAI and LAIΔ*vpu* both reduced $CD4^+$ T cells relative to uninfected mice. Though LAIΔ*vpu* infected BLT mice had higher levels of $CD4^+$ T cells than LAI infected mice this difference was not statistically significant (LAI, 16.0% ±4.2%, LAIΔ*vpu*, 37.0% ±6.8%; p=0.0714). Similar to results from spleen, lymph nodes, liver and lung, $CD4^+CD8^+$ thymocytes in LAIΔ*vpu* infected mice exhibited an intermediate loss between that for uninfected mice and LAI infected mice (Figure 3.3 C). Thus, in five of six tissues, cells susceptible to infection by HIV-1 were present at significantly higher levels in LAIΔ*vpu* infected BLT mice than in LAI infected BLT mice (Figures 3.3 B and C) but LAIΔ*vpu* infected mice had uniformly lower levels of $CD4^+$ T cells in tissues than uninfected mice. Therefore, it appears that Vpu is an important factor for HIV-1 replication and pathogenesis.

In BLT mice, the overall impact on LAI infection of losing *vpu* function is qualitatively similar but of lesser magnitude compared to loss of *nef* function [60]. LAI with a defective *nef* is virtually devoid of pathogenic impact.

3.5 Discussion

Prominent defects were observed for the CXCR4-tropic *vpu*-deleted LAI relative to wild type, which establishes Vpu as an important pathogenesis factor (Figure 3.3). In this regard, it is of interest to compare LAIΔ*vpu* to *nef*-deleted LAI (LAIΔ*nef*). We previously reported that peak viral loads for BLT mice infected with a low dose of LAIΔ*nef* were reduced 7.1-fold relative to wild type LAI while here we found a 4.4-fold reduction when *vpu* was deleted (Figure 3.2 B, [60]). A greater impact on pathogenesis was also observed with LAIΔ*nef* which failed to deplete $CD4^+$ T cells in peripheral blood or in tissues while a partial loss of $CD4^+$ T cells was observed with LAIΔ*vpu* (Figure 3.3, [60]). Also, in contrast to LAI and LAIΔ*vpu*, LAIΔ*nef* had no cytotoxic impact on thymocytes [60]. Therefore, it appears that loss of *nef* has an overall greater negative effect on the virus than loss of *vpu*. However, it should be noted that the results with LAIΔ*vpu* are strikingly similar to our recent report with LAI expressing a Nef that was specifically defective for the CD4 down-regulation activity. With this mutated LAI, we observed intermediate reductions in viral replication, in loss of $CD4^+$ T cells and in loss of $CD4^+CD8^+$ thymocytes [152]. The similarity of the effect of losing Vpu expression and specific

loss of the Nef CD4 down-regulation function raises the possibility of a common mechanism. In this scenario, Nef and Vpu would act synergistically to counter the capacity of CD4 to act as a major restrictor of viral replication [149, 172, 259].

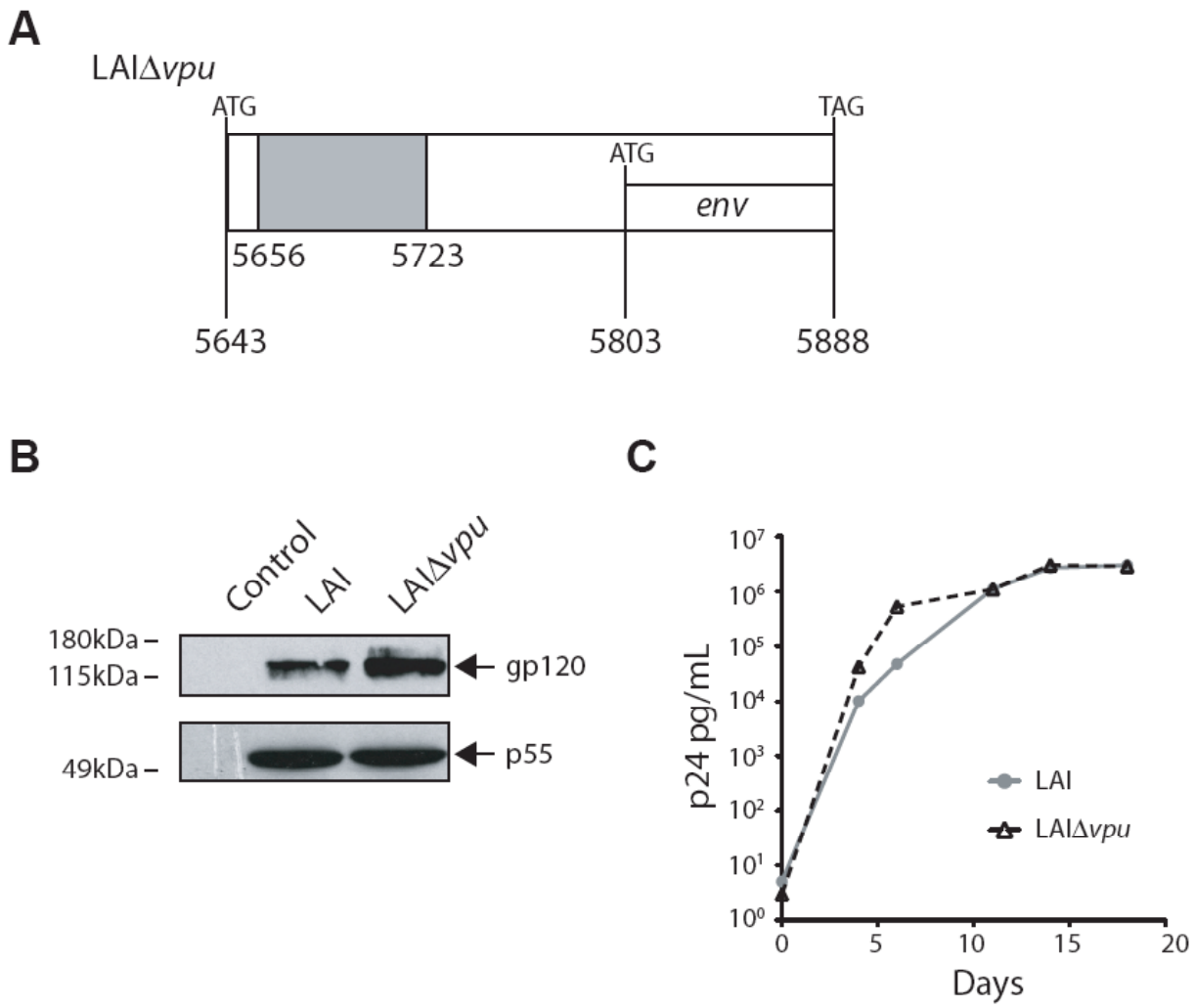

Figure 3.1. *In vitro* characterization of HIV-1LAI (LAI) with a 68 base deletion in *vpu*. (A) Schematic representation of LAI *vpu* with the 68 base deletion indicated (LAIΔ*vpu*) is presented. Nucleotides 5643 to 5888 (NCBI accession number, K02013) represent the *vpu* coding sequence. ATG represents the initiation codon of either *vpu* or *env*. TAG is the termination codon of *vpu*. The gray box is the 68 base pair deletion of nucleotides 5656 to 5723 inclusive. The inserted box at the 3' end of *vpu* represents the 5' *env* open reading frame. (B) The deletion in *vpu* does not alter expression of p55*gag* or gp120*env*. Cell lysates were analyzed for HIV-1 protein expression

by Western blot analysis with anti-gp120*env* or anti-p24*gag*. (C) CEM-SS cells as in Figure 3.1 were infected with LAI or LAIΔ*vpu* at a multiplicity of infection of 0.05 and viral production was followed for 20 days with ELISA for p24*gag*.

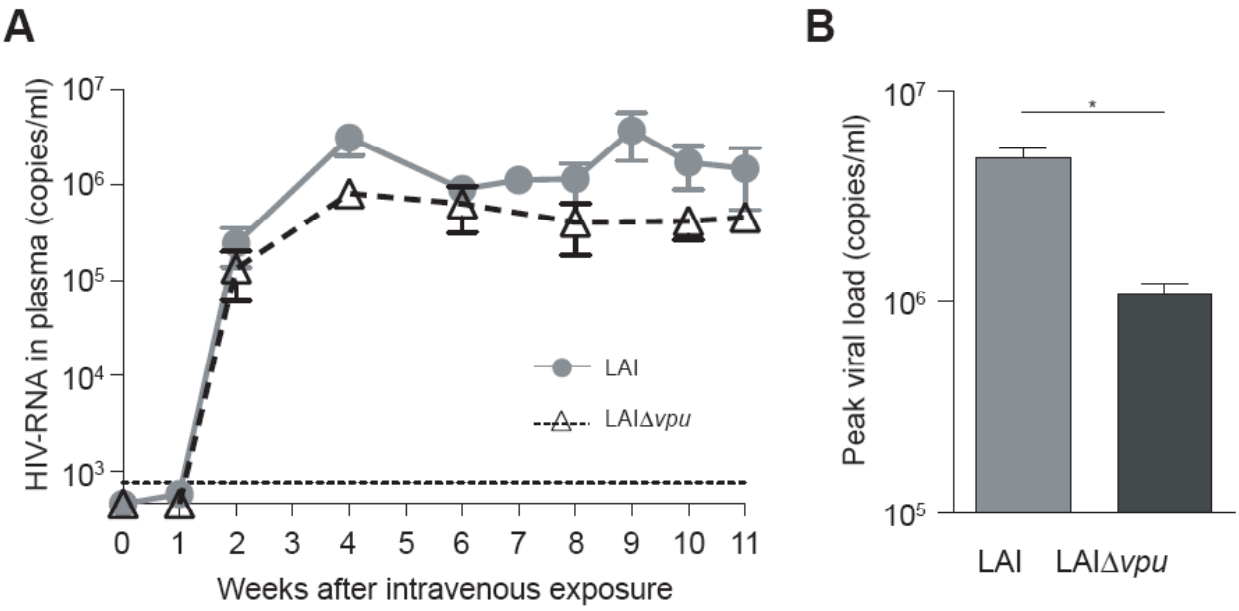

C

Peak viral loads in plasma for mice infected with LAI or LAIΔ*vpu*

Virus	Peak viral load (10^6 Copies/ml)	Week at peak viral load
LAI	6.19	4
LAI	5.63	9
LAI	4.64	4
LAI	4.25	11
LAI	3.44	4
LAIΔ*vpu*	1.25	4
LAIΔ*vpu*	1.22	6
LAIΔ*vpu*	0.80	8

Figure 3.2. Time courses of infection with wild type LAI and LAIΔ*vpu*. (A) Longitudinal analyses of viral RNA in plasma of BLT mice infected with 3,000 TCIU of either LAI (gray solid line, filled circles, n=5) or LAIΔ*vpu* (black dashed line, open triangles, n=3). Data represented as mean ±SEM. Light gray dotted line indicates limit of detection for viral RNA. (B)

Mean ±SEM of peak viral loads in copies of viral RNA per ml in plasma is reduced for LAIΔ*vpu*: LAI, 4.83X106 ± 0.49X106 and LAIΔ*vpu* 1.09X106 ± 0.15X106, Mann Whitney test, p=0.0357. Asterisk indicates $p < 0.05$. (C) Rank order of peak viral loads for mice in (A, B).

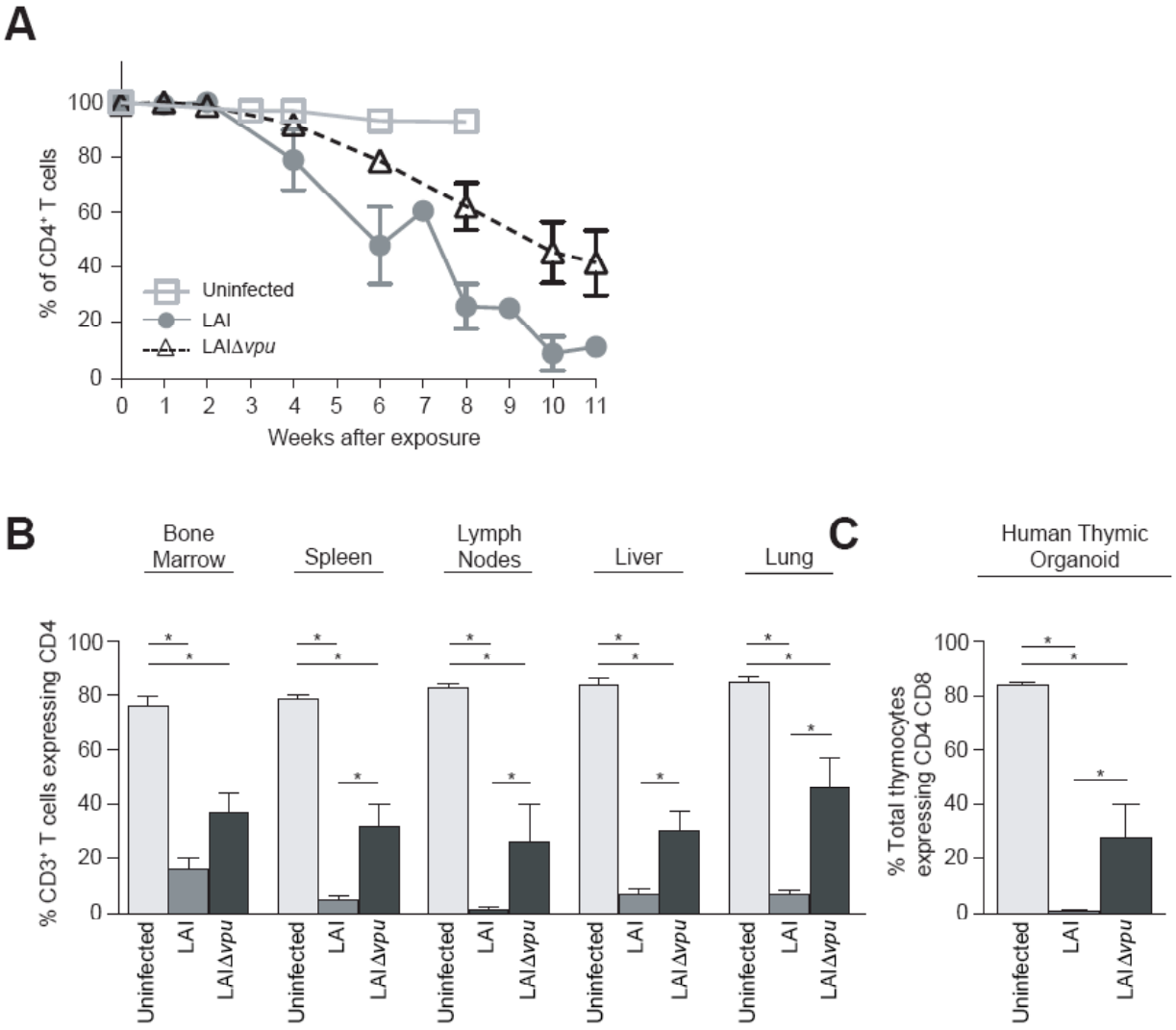

Figure 3.3. Infection with LAIΔ*vpu* exhibits an attenuated pathogenic phenotype relative to LAI. BLT mice from Figure 5 were analyzed for loss of $CD4^+$ T cells from peripheral blood. (A) The percentage of $CD4^+$ T cells relative to pre-exposure levels in peripheral blood of BLT mice infected with either LAI (gray solid line, filled circles, n=5), LAIΔ*vpu* (black dashed line, open triangles, n=3) or uninfected mice (light gray solid line, open squares, n=6) is presented. "%$CD4^+$ T cells" fraction of $CD4^+$ T cells out of total T cells with the pre-exposure level set to

100%. (B, C) BLT mice infected with 3000 TCIU of LAI (Figure 3.2) were sacrificed and analyzed for loss of CD4+ T cells and $CD4^+CD8^+$ thymocytes in tissues. (B) Flow cytometric analysis of cells from Bone Marrow, Spleen, Lymph Nodes, Liver and Lungs demonstrated decreases of the percentage of $CD3^+$ T cells expressing CD4 after infection with LAI (medium gray bars, n=5) or LAIΔ*vpu* (dark gray bars, n=3). Uninfected mice (light gray bars, n=10 except Lymph Node with n=5) are also presented. (C) Double positive ($CD4^+CD8^+$) thymocytes presented as percent of total thymocytes in human thymic organoid. LAI (medium gray bars, n=5) or LAIΔ*vpu* (dark gray bars, n=3). Uninfected mice (light gray bars, n=6) are also presented. * < 0.05

CHAPTER 4: THE ROLE OF NEF IN THE CONTEXT OF JRCSF INFECTION, A CCR5 TROPIC HIV-1 PRIMARY ISOLATE[3]

4.1 Summary

Background: The HIV-1 accessory protein Nef is critical for the development of AIDS. It has been shown that the highly pathogenic CXCR4-tropic virus LAI is rendered non-pathogenic in the absence of Nef and that LAI *nef* evolves to overcome a frame-shift to restore the *nef* open reading frame to regain partial Nef function, which ultimately leads to $CD4^+$ T cell loss. Conversely, if irreparable deletions are incorporated into *nef*, this virus lacks the ability to deplete peripheral blood $CD4^+$ T cells. It is not known, however, if Nef is needed for the depletion of $CD4^+$ T cells during the infection of CCR5-tropic viruses. Here we used the CCR5 tropic virus, HIV-1 JRCSF, to characterize the evolution of *nef in vivo* and the requirement of Nef for robust replication and depletion of $CD4^+$ T cells.

Results: I characterized the course of an intravenous infection with 90,000 TCIU of JRCSF

[3] Richard L Watkins, Nurjahan Begum, John L Foster and J Victor Garcia. The role of Nef in the context of JRCSF infection, a CCR5 tropic HIV-1 primary isolate. RW, NB, and JF performed experiments

(wild type) and compared this course of infection with that of viruses with defective *nef*s in BLT humanized mice: one with two large deletions in *nef* (JRCSFNef*dd*) and the other with a frame-shifted *nef* (JRCSFNef*fs*). JRCSF infection resulted in a 72.13% reduction in peripheral blood $CD4^+$ T cells, while infection with JRCSFNef*dd* did not. In contrast, JRCSFNef*fs* eventually depleted $CD4^+$ T cells, albeit at a much slower rate. We also tracked the evolution of *nef* throughout the course of infection of JRCSFNef*fs*. JRCSFNef*fs* was replaced by virus with deletions in *nef* that restored the ORF. A Nef representative of this *in vivo nef* evolution was determined through *in vitro* functional assays to lack the ability to downregulate CD4 but retain MHC1 downregulation.

Conclusions: Like the highly pathogenic X4 tropic virus, LAI, JRCSF depends on Nef for optimal replication and pathogenicity. In addition, as seen for LAINef*fs*, the frame shift in JRCSF is repaired but the resultant protein has lost the required ability to downregulate CD4. However, unlike in the case of LAI, JRCSF Nef is needed for the T cell activation seen in wild type JRCSF infection.

4.2 Introduction

nef-defective HIV-1 has strongly attenuated viral replication and pathogenesis [62, 159-161]. In addition, *nef* will evolve to overcome a four base insertion in codon 36 to restore its ORF, but in the process loses its ability to downregulate CD4. We now know that among the

many functions ascribed to Nef via *in vitro* investigation, its ability to downregulate surface expression of CD4 is responsible for nearly half of the $CD4^+$ T cell depletion seen during HIV-1 infection of BLT humanized mice [152]. Therefore, Nef's overall impact on HIV-1 infection is due to its effect on CD4 downregulation activity and other Nef functions that together result in high viral loads and eventually the development of AIDS [60, 152].

To gain a better understanding of the function *in vivo* in the context of an R5 tropic HIV-1 *nef*, we created a frame-shift in JRCSF *nef* (JRCSFNef*fs*) and used this virus to infect BLT humanized mice. We followed the course of infection of this virus and compared it to wild type virus. We specifically monitored viral replication and peripheral blood $CD4^+$ T cell depletion and tracked the evolution of *nef* throughout the infection at two time points. Because in the case of LAINef*fs* infection the ORF was restored rapidly, the reversion of JRCSFNef*fs* is also likely, making it difficult to determine the need for Nef to achieve high viral load and $CD4^+$ T cell depletion. To assess Nef's requirement for the maintenance of high viral loads and $CD4^+$ T cell depletion we created irreparable deletions in the *nef* of JRCSF (JRCSFNef*dd*) and used this *nef*-defective virus to infect BLT humanized mice. We then compared the course of infection with those of mice infected with JRCSF and JRCSFNef*fs*. The characterization of infection included 1) $CD4^+$ T cells in the blood, 2) plasma viral RNA levels, 3) and $CD8^+$ T cell activation levels.

4.3 Experimental Procedure

4.3.1 Preparation of BLT humanized mice

BLT humanized mice were prepared as described [60, 87, 185, 186, 191-198]. Briefly, thymus/liver implanted NOD/SCID IL-2$\gamma^{-/-}$ mice (The Jackson Laboratories, Bar Harbor, ME) were transplanted with autologous human $CD34^{+}$ cells isolated from fetal liver (Advanced Bioscience Resources, Alameda, CA). Human reconstitution in the peripheral blood of these mice was monitored periodically by flow cytometry (FACSCanto; BD Biosciences). Mice were maintained at the Division of Laboratory Animal Medicine, University of North Carolina at Chapel Hill (UNC-CH) in accordance with protocols approved by the UNC-CH Institutional Animal Care and Use Committees.

To ensure genetic diversity, seven different tissue donors were used to generate four groups of mice used for the experiments. All groups had at least two different human genetic backgrounds included in the evaluation of infection. JRCSFNef*fs* and JRCSFNef*dd* infected groups each shared a common donor with the JRCSF infected group.

4.3.2 Cell lines and culture conditions

TZM-bl cells were maintained in Dulbecco's modified Eagle's medium (DMEM; Cellgro, Herndon, VA) and supplemented with 10% fetal bovine serum (FBS; Cellgro), 100 IU/ml of penicillin, 100 μg/ml streptomycin, and 2 mM glutamine (Cellgro) in 10% CO_2 at 37°C.

Similarly, 293T cells were cultured under the same conditions as TZM-bl cells but in 5% CO_2. The human CEM T cell line was cultured in RPMI 1640 medium supplemented with 10% fetal bovine serum (Hyclone), 50 IU of penicillin per ml, 50 µg streptomycin per ml, 2 mM L-glutamine, and 1 mM sodium pyruvate in 10% CO_2 at 37°C.

4.3.3 Proviral clones

The proviral clone, pYK-JRCSF (accession # M38429), was described by Koyanagi *et al*. [260]. JRCSFNef*fs* was constructed to be defective for *nef* by digesting pYK-JRCSF with XhoI, filling in with Klenow and re-ligating, which, leaves the *nef* sequence intact but introduces a four-base frame-shift after *nef* codon 35. JRCSFNef*dd* was constructed by cutting with Xho1 and Acc65I, filling in with Klenow and religating. The junction retained the Xho1 site and was in frame. The Xho1 site was then cut, filled, and ligated to create a frame shift. The 292 base deletion was made by site-directed mutagenesis.

4.3.4 Virus production, exposure of BLT mice to HIV-1_{JRCSF} and HIV-1_{JRCSF} with mutated *nef*s, and flow cytometric analyses

Stocks of JRCSF, JRCSFNef*fs*, and JRCSFNef*dd* were prepared and titered as previously described [200, 201]. Briefly, proviral clones were transfected into 293T cells. Viral supernatant was collected 48 hours after transfection and diluted in DMEM, and supplemented with 10% fetal bovine serum, 100 IU penicillin/ml, 100 mg/ml streptomycin, and 2 mM glutamine. TZM-

bl cells were infected in 12-well tissue culture plates with 0.4 ml of virus at multiple dilutions in DMEM plus 10% fetal bovine serum containing DEAE dextran for 2 hours. Then, 1.0 ml of DMEM plus 10% fetal bovine serum was added and the plates were incubated overnight. Virus-containing medium was removed the next day, replaced with fresh DMEM plus 10% fetal bovine serum, and the incubation continued for 24 hours. The cells were fixed with formaldehyde and glutaraldehyde and stained with 5-bromo-4-chloro-3-indolyl-β-D-galactopyranoside (40 hours after first exposure to virus). Individual blue cells were counted directly to determine infectious units per ml (TCIU). Viral stocks were tittered in triplicate and at least two different titer determinations were performed for each virus preparation.

BLT mice were exposed to infectious virus via tail vein injection with 90,000 TCIU. Viral load in peripheral blood of infected mice was monitored longitudinally by quantitative real-time PCR using Taqman RNA to-C_T^{TM} 1-step kit from Applied Biosystems, USA [192, 193, 202]. The sequences of the forward and reverse primers and the Taqman probe for PCR were 5'-CATGTTTTCAGCATTATCAGAAGGA-3', 5'-TGCTTGATGTCCCCCCACT-3', and 5'-FAM CCACCCCACAAGATTTAAACACCATGCTAA-Q-3', respectively.

$CD4^+$ and $CD8^+$ T cell levels were monitored by flow cytometric analysis as previously described [185, 196, 198]. Immunophenotyping was performed on blood samples collected longitudinally and on mononuclear cells isolated from tissues at harvest. Whole peripheral blood

(PB) from humanized mice was analyzed according to the BD Biosciences Lyse/Wash protocol (Cat. No. 349202), as previously described [203]. Briefly, following antibody labeling of whole blood, red blood cells were lysed. The remaining cells were washed and fixed and the sample was analyzed by flow cytometry. Tissue mononuclear cell isolations and immunophenotyping analyses were also performed according to published methods [185, 196, 198]. Flow cytometric gating for CD4 and CD8 cell surface expression was performed as follows: (step 1) forward and side scatter properties were used to set a live cell gate, (step 2) live cells were analyzed for expression of the human pan-leukocyte marker CD45, (step 3) human leukocytes were analyzed for hCD3, and (step 4) these T cells or thymocytes were analyzed for hCD4 and hCD8 expression.

The panel of antibodies for analysis of $CD38^+$ and $HLA\text{-}DR^+$ expression in $CD8^+$ T cells was CD8 FITC (SK1), HLA-DR, PE (TU36) or IgG2bκ PE, CD4 PerCP (SK3), CD3 PE-Cy7 (SK7), CD38 APC (HB7) or IgG1κ APC, and CD45 APC-Cy7 (2D1) (all purchased from BD Biosciences). Gating was performed as follows: (step 1) forward and side scatter properties were used to set a live cell gate, (step 2) live cells were analyzed for expression of the human pan-leukocyte marker CD45, (step 3) human leukocytes were analyzed for CD3, (step 4) T cells were analyzed for CD4 and/or CD8 expression, (step 5) human $CD8^+$ T cells were analyzed for HLA-

DR and CD38 expression [186]. Gates defining HLA-DR and CD38 expression were set with isotype-matched flourophore-conjugated control antibodies.

4.3.5 *In vitro* analysis of Nef activities

The *in vivo* selected 78 base-pair deletion was introduced into JRCSF *nef* and subcloned into the retroviral vector pLXSN [93]. CEM T cells were transduced to express JRCSFNef or JRCSFNef*fs*Δ-78. Assays for CD4 downregulation and MHCI downregulation were described previously [93]. Nef expression was determined by Western blot analysis using anti-Nef AG11 monoclonal antibody [93, 152, 205].

4.3.6 Sequence analysis of plasma virion RNA

Viral RNA was extracted from 20 μl of plasma from infected mice using the QIAamp Viral RNA Mini kit (Qiagen Sciences, USA). RNA was then reverse-transcribed into cDNA, which was then subjected to nested PCR. The outer primers for *nef* amplification are 5'-AGCTTGCTCAATGCCACAGCC-3' and 5'-GCTGCATATAAGCAGCTGCTTTTTG-3'. The inner primers are 5'-TAGAGCTATTCGCCACATACC-3' and 5'-GCTTGCTACAAGGGACTTTCCGC-3'. Gel purified PCR products were sequenced and aligned to HIV_{LAI} sequences to determine if nucleotide changes had occurred.

4.3.7 Statistics

Mann-Whitney tests were performed in Prism version 5 (Graph Pad). All data were plotted as mean $\pm$ S.E.M.

4.4 Results

4.4.1 Infection of BLT humanized mice with JRCSFNef*fs*

To characterize the infection of JRCSF with a defective *nef*, we generated an inactivating mutation by generating a frame-shift, in the manner previously described [152] (Figure 4.1). JRCSF and the *nef* frame-shifted JRCSF (JRCSFNef*fs*) were injected intravenously (iv, 90,000 TCIU) into BLT mice (Figure 4.2). In Figure 4.2, wild type JRCSF-infected mice and negative control uninfected mice are compared to JRCSFNef*fs*-infected mice. JRCSFNef*fs* actively replicated, reaching a peak viral load of $3.83 \pm 2.82 \times 10^6$ (n=6), while JRCSF reached a peak viral load at $4.71 \pm 1.23 \times 10^6$ (n=6). The difference between the peak viral loads reached by these two viruses was not statistically different (p value=0.132, Mann Whitney). However, when early viral loads were compared a short delay in replication was observed for weeks 1 and 2 (p values= .0043 and .0075) (Figure 4.2 A). These results suggest that whatever replicative advantage JRCSF has over JRCSFNef*fs* is transient.

In mice infected with JRCSF, a continuous, slow decline in $CD4^+$ T cells was observed with statistically significant differences compared to $CD4^+$ T cell levels in uninfected mice from

weeks 2 through 14. JRCSFNef*fs* did not reduce $CD4^+$ T cells for 10 weeks; however, a sharp decline of 60.0% $\pm$ 13.2% was observed at 14 weeks. The difference was not statistically significant, but suggests that JRCSFNef*fs* had become capable of depleting $CD4^+$ T cells.

4.4.2 The *in vivo* evolution of *nef* leads to the reopening of the *nef* ORF

We sequenced *nef* from JRCSFNef*fs* viral RNA from blood from 8 and 14 weeks post-infection (Figure 4.3 A). At 8 weeks post-exposure, JRCSFNef*fs nef* sequence (designated "+4") was present in only two mice. *nef* sequences from the remaining four mice contained deletions ranging from 1 base to 105 bases. By 14 weeks post-exposure, JRCSFNef*fs nef* sequence could not be identified in any of the mice, suggesting that these *nef* mutants gave the viruses that express them an advantage in replication over JRCSFNef*fs*. All *nef* mutants contained deletions that restored the *nef* ORF but did not result in wild type sequence.

4.4.3 *In vitro* functional analysis of *nef* mutant that evolved *in vivo* obtained from enforced evolution

To assess *in vitro* phenotypes of ORF Nef *in vivo* generated in JRCSFNef*fs* infected mice, we chose JRCSFNef*fs*Δ-78, an *in vivo* generated *nef* that by 14 weeks replaced other *nef*s in this mouse. The coding sequence was transferred into the retroviral expression plasmid, pLXSN, used to produce a retroviral vector that in turn was used to transduce CEM T cells [26].

CEM T cells expressing wild type and mutant Nefs were analyzed for Nef expression, CD4 downregulation, and MHC Class I (MHCI) downregulation (Figure 4.3 C). Nef*fs*Δ-78 was expressed at the same level as wild type Nef (Figure 4.3 B). Flow cytometric analysis of cell surface CD4 and MHC1 expression of CEM T cells transduced with JRCSF Nef showed downregulation of both proteins (Figure 4.3 C, [26, 93, 208]). Nef*fs*Δ-78 was fully active for MHCI downregulation but completely devoid of CD4 downregulation activity.

4.4.4 Infection of BLT humanized mice with JRCSFNef*dd*

Because JRCSFNef*fs* restores the *nef* ORF by week 14, leading to the loss of $CD4^+$ T cells and wild type levels of replication, I characterized the course of infection of JRCSF with irreparable deletions in *nef* (Figure 4.4). We have demonstrated that LAI with two large deletions flanking the polypurine tract (LAINef*dd*) was indeed irreparable. We incorporated the same deletions into JRCSF *nef* (JRCSFNef*dd*) and used this virus to infect BLT humanized mice with 90,000 TCIU (Figure 4.5). Mice infected with JRCSFNef*dd* (n=6) (Figure 4.5 A), like JRCSFNef*fs* (Figure 4.2 A), harbored active viral replication. JRCSFNef*dd* reached a peak viral load of $2.29 \pm 1.67 \times 10^6$. This peak viremia was not significantly different from those of JRCSF or JRCSFNef*fs* infected mice. However, at weeks 1 and14 the viral loads of JRCSF and JRCSFNef*fs* infected mice differed: when compared to JRCSF, the JRCSFNef*dd* viral loads were statistically different at weeks 1 and 14 (p values= .0050 and .0260, Mann Whitney,

respectively) (Figure 4.2 A) and when compared to JRCSFNef*fs*, viral loads harbored by mice infected with JRCSFNef*dd* were also statistically different at week 12 and 14 (p value= .0152 and .043).

We then compared $CD4^+$ T cell levels in mice infected with JRCSFNef*dd*, JRCSF, or with JRCSFNef*fs* (Figures 4.2 B and 4.5 B). JRCSFNef*dd* infected mice did not differ from JRCSFNef*fs* in terms of $CD4^+$ T cell levels throughout the course of infection. Similarly, $CD4^+$ T cell levels throughout the course of infection did not differ statistically from uninfected mice at any point during the course of infection. At week 4 and continuing to 14 wpi, JRCSFNef*dd* infected mice maintained higher levels of peripheral blood $CD4^+$ T cells than mice infected with JRCSF (0.0043, 0.0043, 0.0043, 0.0022, 0.0022, and 0.0022, Mann Whitney, respectively).

4.4.5 Nef is required for T cell activation during JRCSF infection

T cell activation has been associated with HIV-1 disease progression [261]. One explanation for the difference in the *in vivo* phenotypes of JRCSFNef*fs* and JRCSFNef*dd* would be an inability of these mutated HIV-1s to induce systemic T cell activation [211, 212]. One of the most commonly used indicators of T cell activation is the expression of both HLA DR and CD38 [262, 263]. When we compared the percent of $CD8^+$ T cells expressing both HLA DR and CD38 in uninfected mice with the percent of $CD8^+$ T cells expressing both HLA DR and CD38 in JRCSF infected mice, we observed that the mice infected with JRCSF had a statistically

higher percentage of their $CD8^+$ T cells that expressed both HLA DR and CD38, at 6, 8, and 12 wpi (p values= .0095, .0422, and .0139, Mann Whitney, respectively). Mice infected with JRCSFNef*fs* or JRCSFNef*dd* did not differ statistically from uninfected mice nor from one another. When mice infected with JRCSF were compared to mice infected with JRCSFNef*fs,* statistically significant differences were observed at 6, 8, and 10 wpi. We compared T cell activation in mice infected with JRCSF with mice infected with JRCSFNef*dd*. We observed that mice infected with JRCSFNef*dd* had lower percentages of $CD8^+$ T cells expressing HLA DR and CD38 compared to mice infected with JRCSF at 6, 8, 10, and 12 wpi. Of interest is that no differences were seen between mice infected with JRCSFNef*dd* and mice infected with JRCSFNef*fs*. A drop in HLA DR and CD38 is observed mice infected with either JRCSFNef*fs* or wild type JRCSF, which is currently unexplainable. However longitutidal analysis of immunactivation conducted in sooty mangabeys demonstrate the extreme variability throughout out the course of SIV infection, this in addition to my data highlights our collective lack of understanding of the nuances of immune activation during viral infection [264]. Future experiments should be directed towards achieving better insight into the factors that influence chronic immune activation.

4.5 Discussion

We have demonstrated that LAI depletes $CD4^+$ T cells by 90% or more from the peripheral blood by 6 weeks post-infection [60, 152]. In this dissertation I show that JRCSF fails to deplete $CD4^+$ T cells from the peripheral blood to this extent. At 6 weeks, LAI infection resulted in a 90% reduction. Conversely, JRCSF by 6 weeks resulted in only a 24% reduction in $CD4^+$ T cells. By 14 wpi, 27.9% $\pm$ 5.9% of $CD4^+$ T cells remained relative to the pre-infection level.

We have shown that an CXCR4-tropic virus can correct a defective *nef* to regain partial function [152]; however, it is unknown if this is true for *nef* in an CCR5-tropic virus.

We established that the phenotypic differences between infection of BLT mice with wild type LAI and the *nef*-defective LAINef*dd* [60] are large and demonstrated the ability of *nef* to evolve and restore partial functionality [152]. Viruses expressing Nef have a decisive replicative advantage over the frame-shifted LAINef*fs* and replace the *nef*-defective virus within a few weeks. Here we demonstrate that this is also the case in the context of the R5-tropic virus JRCSF. In this investigation we observe the restoration of the *nef* orf with a variety of deletions; however, these deletions take out a stretch of bases required for CD4 downregulation. *In vitro* analysis demonstrates that the Δ-78 Nef, like LAI Δ-1 and Δ-13, lacks the ability to downregulate CD4.

Because *nef* ORF is quickly restored in both JRCSFNef*fs* and LAINef*fs* infections, LAINef*dd* and JRCSFNef*dd* were used to assess the role of Nef in maintaining high viral loads and in the depletion of $CD4^+$ T cells. Both the mice infected with JRCSFNef*dd* and with LAINef*dd* maintained their $CD4^+$ T cells and had lower loads than their respective wild type controls. I show that JRCSFNef*dd* infection does not induce $CD8^+$ T cell activation, in contrast to LAINef*dd* infection, which induces $CD8^+$ T cell activation to the same extent as infection with wild type JRCSF. However, unlike Zou *et al.,* I performed a longitudinal analysis of $CD8^+$ T cell activation. This difference in analyzing T cell activation may explain the difference between immune activation seen during LAINef*dd* and JRCSFNef*dd* infections.

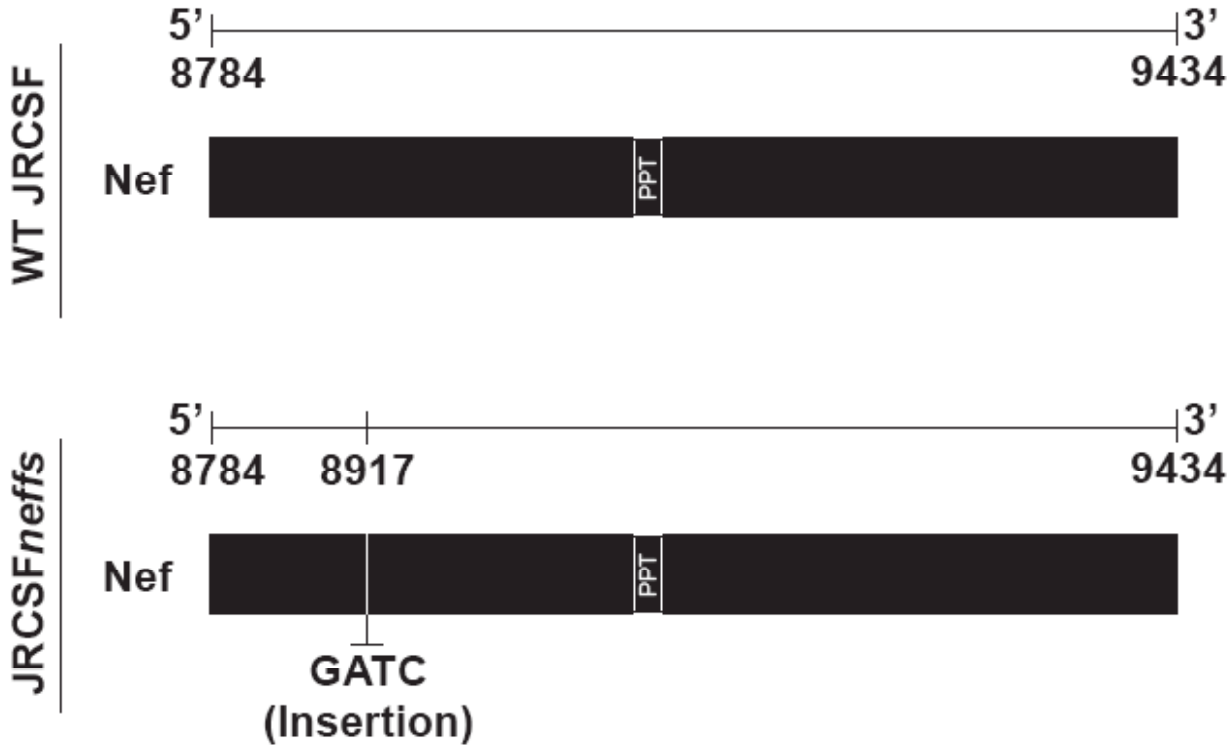

Figure 4.1. A four base insertion creates a frame shift in *nef*. *Upper Panel,* schematic representation of wild type JRCSF (WT JRCSF) is presented. Nucleotides 8784 to 9434 in NCBI accession number, M38429, represent the *nef* coding sequence. *Lower Panel*, A schematic of frame shifted *nef* (JRCSFNef*fs*) is presented. The insertion of GATC following nucleotide 8917 is indicated. PPT, polypurine tract.

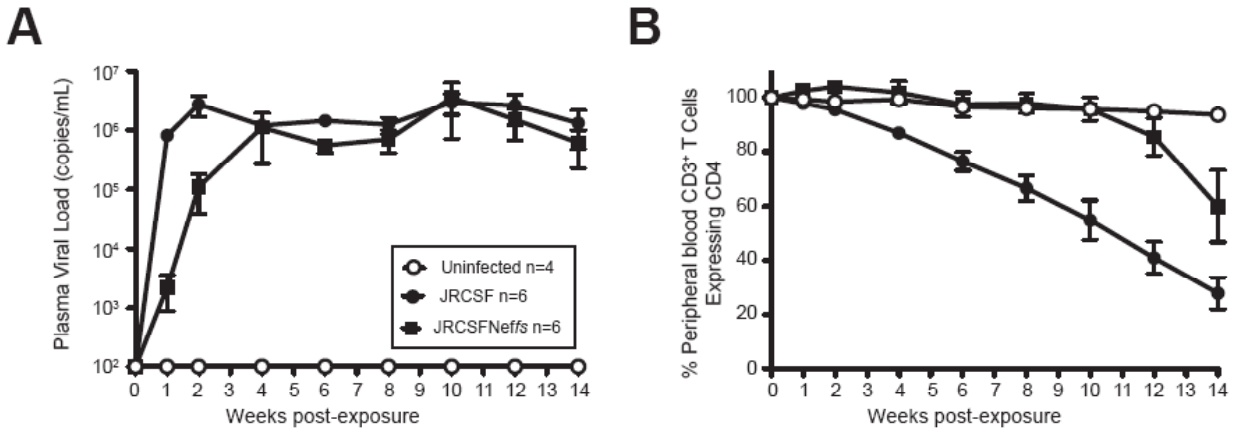

Figure 4.2. Viral load analysis and peripheral blood $CD4^+$ T cell depletion in mice infected with JRCSFNef*fs*. (A) Viral loads of BLT mice were plotted for BLT humanized mice exposed to 90,000 TCIU of JRCSF (n = 6) and JRCSFNef*fs* (n = 6). Uninfected mice (n = 4) served as negative controls. (B) The percent of $CD4^+$ T cells out of total T cells in peripheral blood are plotted for mice in (A).

A

Mouse[a]	8 Weeks[b]	14 weeks[c]
JRCSFNef*fs* 1	Δ-78/Δ-90	Δ-78
JRCSFNef*fs* 2	Δ-1	Δ-1
JRCSFNef*fs* 3	Δ-105/?	Δ-105/?
JRCSFNef*fs* 4	+4/?	Δ-1/?
JRCSFNef*fs* 5	+4/?	Δ-4
JRCSFNef*fs* 6	Δ-61/?	Δ-1/?

[a] Mouse Identification
[b] Mutations found in amplified *nef* sequences from mice at 8 weeks
[c] Mutations found in amplified *nef* sequences from mice at 14 weeks

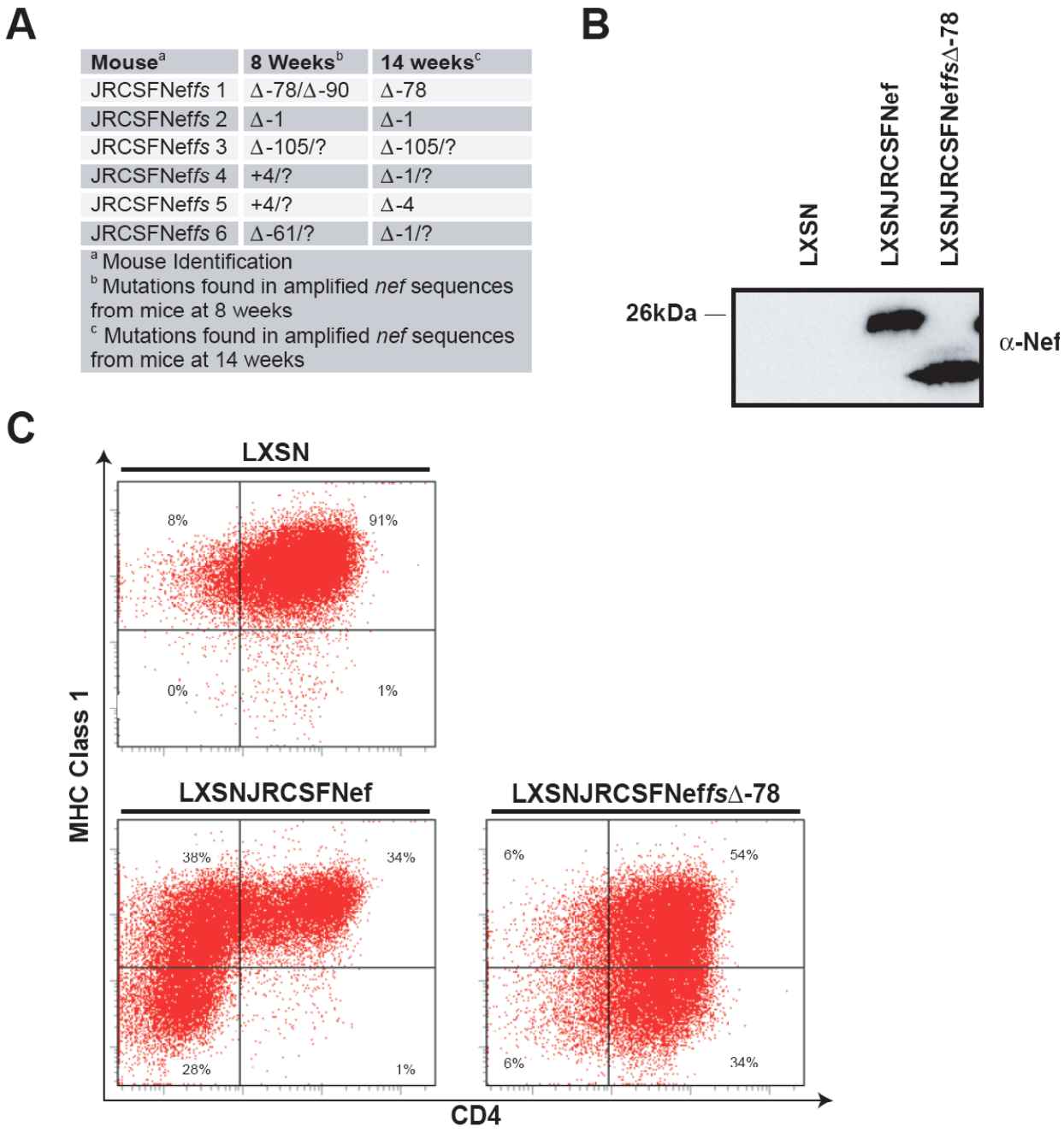

Figure 4.3. JRSCFNef*fs* restores its open reading frame. (A) At two time points during the 14 weeks of infection, plasma viral RNA was reverse transcribed, amplified by PCR, and *nef* sequenced. By 8 weeks, virus RNA from all six mice had mutations in *nef*. The original frame-

shifted *nef* was present in only two mice. By 14 weeks the original frame-shifted *nef* could no longer be identified by bulk sequencing. ? = additional sequences evident by bulk analysis (B) Nefs encoded by JRCSFNef*fs*Δ-78 and JRCSF were expressed in CEM cells. Western blot analysis confirmed the expression of the Nef*fs*Δ-78 protein. (C) CEM cells expressing JRCSF Nef, JRCSF Nef*fs*, and JRCSF Nef*fs*Δ-78 were analyzed by flow cytometry for cell surface CD4 and MHC Class 1 (MHC1) expression. JRCSF Nef*fs*Δ-78 was fully defective for CD4 downregulation but functional for MHC1 downregulation. Percentage of cells in each quadrant out of total cells is indicated.

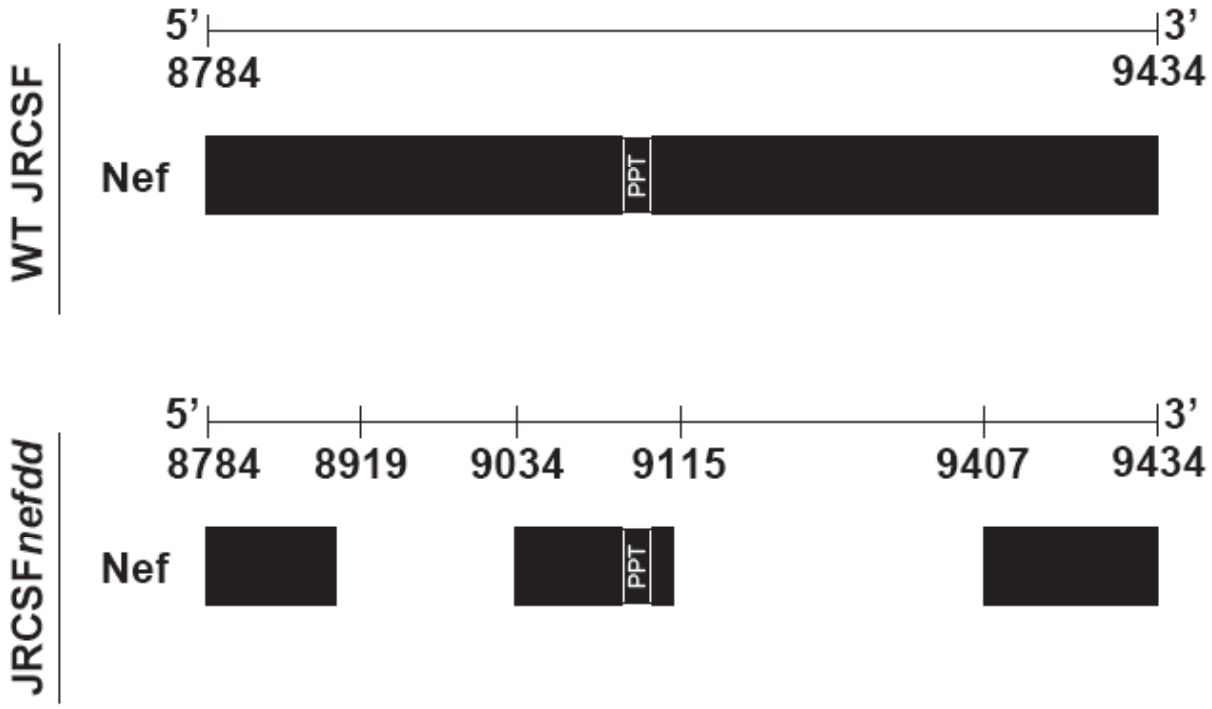

Figure 4.4. Schematic of wild type JRCSF *nef* and JRCSFNef*dd*. *Upper* Panel, *nef* ORF Lower *Panel*, three bars represent *nef* coding sequence remaining in JRCSFNef*dd*. PPT: polypurine tract. In the lower bar the 5' deletion incorporated into JRCSFNef*dd* is 115 nucleotides (8919–9034). The 3′ gap in JRCSFNef*dd* is a frame-shift deletion of 292 bases (9115–9407).

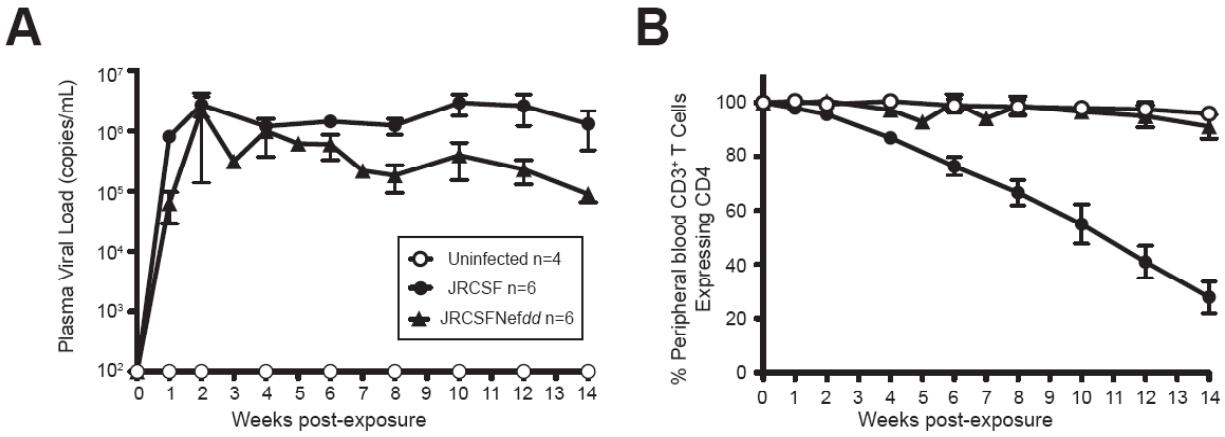

Figure 4.5. Viral load and peripheral blood $CD4^+$ T cell analysis in mice infected with JRCSFNef*dd*. (A) Viral loads of BLT mice exposed to 90,000 TCIU of JRCSF (n = 6) and JRCSFNef*dd* (n = 6). Uninfected mice (n = 4) served as negative controls. (B) The percent of $CD4^+$ T cells out of total T cells in peripheral blood are plotted for mice in (A) Uninfected and wild type controls from Figure 4.2 are shown to facilitate comparison.

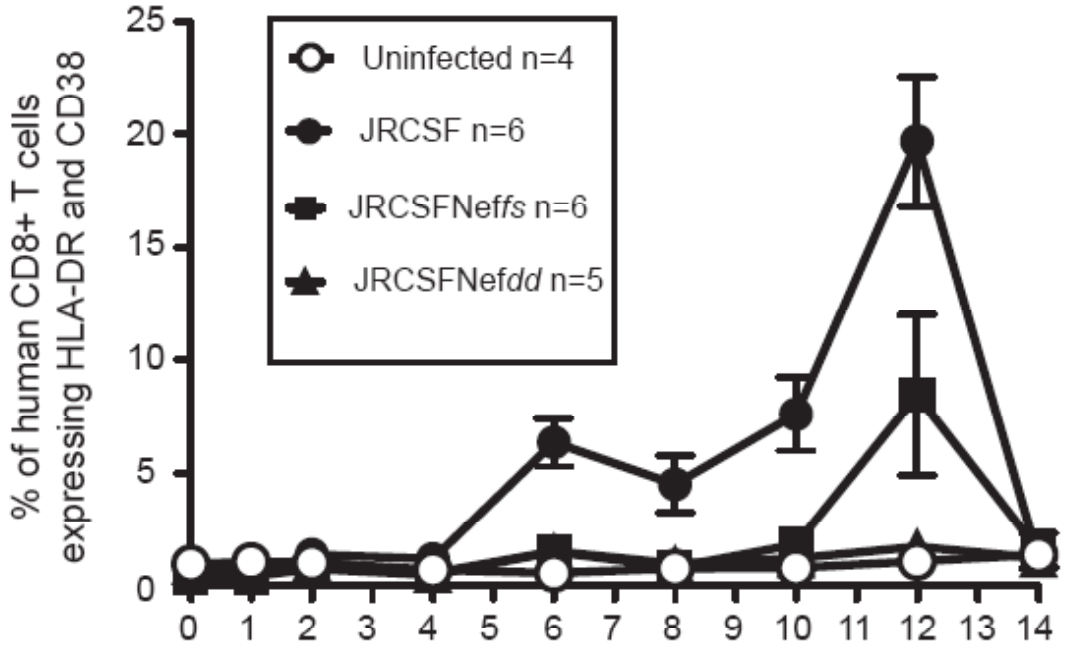

Figure 4.6. Infection with JRCSFNef*fs* and JRCSFNef*dd* do not induce T cell activation. $CD8^+$ T cell activation was measured longitudinally in peripheral blood prior to and after infection with 90,000 TCIU of JRCSF (n=6), JRCSNef*fs* (n=6), or JRCSFNef*dd* (n=5). Activation is presented as percent of total $CD8^+$ T cells in peripheral blood expressing both CD38 and HLA-DR.

CHAPTER 5: CONCLUSIONS AND FUTURE DIRECTIONS

5.1 Nef-mediated downmodulation of CD4 is critical for wild type pathogenesis and replication

Taking to account the findings of Zou *et al*., CD4 downregulation activity accounts for approximately half of Nef's capacity to enhance viral replication and deplete $CD4^+$ T cells and $CD4^+$ $CD8^+$ thymocytes, a result consistent with the high degree of conservation of the CD4 downregulation activity of Nef [8]. The identity of Nef activities that account for the remainder of Nef's effects is unknown. These yet to be identified activities present in LAINef*fs*Δ-1 and LAINef*fs*Δ-13 provide the virus a strong selective advantage over LAINef*fs*, which is fully defective for Nef expression. In addition, wild type virus, expressing a fully active Nef, outcompetes virus expressing Nef that is specifically defective for CD4 downregulation (Figure 2.2 A). We also tested the Nef activities that depend on the SH3 domain binding site because the corresponding amino acid sequence in Nef is highly conserved. However, the virus with *nef* mutated for SH3 domain binding (P72A/P75A) was essentially wild type in its ability to enhance viral replication and deplete $CD4^+$ T cells and $CD4^+$ $CD8^+$ thymocytes.

The current antivirals we have against HIV-1 are due to the intense research conducted on HIV-1. When used in combination, antiviral drugs are effective at reducing both viral loads

and the speed of disease progression [265, 266]. The vast majority of these antivirals target the enzymatic activities of reverse transcriptase, protease, and integrase [267]. Taken together, these targets represent essential elements of viral replication. HIV-1 mutates to gain back full or partial function of reverse transcriptase, protease, and integrase, which highlights the importance of identifying and designing therapies that target HIV-1 gene function as broadly as possible.

A future direction of this research should be to understand the role that less studied functions of Nef play in $CD4^+$ T cell depletion and viral replication. Some of these functions include Nef-induced elevated release of exosomes or the role of Nef in inhibiting ASK1 [214, 216].

5.2 The loss of CD4 down modulation by Nef has a similar impact on HIV-1 infection as the loss of Vpu

CD4 downregulation activity accounts for approximately half of Nef's capacity to enhance viral replication and deplete $CD4^+$ T cells and $CD4^+$ $CD8^+$ thymocytes; this dissertation concludes that the loss of Vpu has a similar effect on HIV-1 infection. This similarity raises the possibility that Nef and Vpu synergize to counter the capacity of CD4 to act as a major restrictor of viral replication. In this regard, an interesting future direction would be to characterize the course of infection of a virus lacking both Nef-mediated CD4 downregulation and Vpu. The combined effects of the absence of Nef-mediated CD4 downregulation and of Vpu can be

expected to yield a dramatic reduction in viral load and $CD4^+$ T cell cytotoxicity. This hypothesis could be tested by combining the mutation generated by the enforced evolution of LAINef*fs* with LAIΔ*vpu* (e.g., LAIΔvpuNef*fs*Δ-1) and monitoring viral loads and $CD4^+$ T cell levels in LAIΔvpuNef*fs*Δ-1 infected mice.

As mentioned in 5.1, novel antivirals that target Nef-mediated CD4 downmodulation, in combination with antivirals that disrupt less studied functions of Nef, could be effective at controlling HIV-1 infection. Conversely, another strategy for controlling HIV-1 infection could be combining antivirals that target Nef-mediated CD4 downregulation with antivirals that target Vpu. Such an approach may be effective at drastically reducing $CD4^+$ T cell cytotoxicity and viral replication during infection.

5.3 Nef is required for T cell cytotoxicity and robust viral replication of the CCR5-tropic virus JRCSF.

Wei *et al*. demonstrated through use of the highly pathogenic CXCR4-tropic virus, LAI that Nef is required for the rapid depletion of $CD4^+$ T cells and high viral loads in BLT humanized mice. CXCR4-tropic and CCR5-dual-tropic viruses appear in later stages of HIV-1 infection in about 50% of patients and the appearance of dual-tropic viruses is associated with disease progression [268-270]. However, fully CXCR4-tropic viruses in the context of natural infections rarely occur [6]. The vast majority of natural infections are infections of CCR5-tropic

viruses [6]. I was therefore interested in assessing the requirement of Nef for high viral loads and $CD4^+$ T cell depletion in the infection of the CCR5-tropic JRCSF. I leveraged a *nef* defective JRCSF virus containing a frame shift in *nef* to infect BLT humanized mice. During the course of infection the *nef* ORF was restored in all mice via a 1 base, a 78 base, a 4 base, or a 105 base pair deletion. The 78 base pair *nef* deletion was selected as a representative and was incorporated into a retroviral expression vector, which was then used to transduce CEM cells expressing both MHC1 and CD4. The Nef produced by the 78 base pair deleted *nef* was unable to downmodulate surface expression of CD4 but was fully functional for downmodulation of MHC1, which is an observation consistent with the data presented in Wei *et al* [60].

Due to the restoration of the *nef* ORF, the inactivation of *nef* through the genetic engineering of a frame shift is not sufficient for determining the necessity of a fully functional *nef* for high viral loads and $CD4^+$ T cell loss during JRCSF infection. We therefore leveraged another *nef*-defective JRCSF containing irreversible mutations in *nef* to determine the role of *nef* in $CD4^+$ T cell cytotoxicity and reaching high viral loads during JRCSF infection in humanized mice. These experiments demonstrate that Nef is required for both viral replication and $CD4^+$ T cell loss in JRCSF infected BLT humanized mice. I conclude in this thesis that as in the case with a CXCR4-tropic viral infection, the loss of $CD4^+$ T cells and high viral loads during infection with a CCR5-tropic virus requires Nef.

5.4 Induction of immune activation by HIV-1 JRCSF depends on Nef.

During the course of JRCSF virus infection, Nef is required for replication and $CD4^+$ T cell depletion. Pressure is also exerted on the virus with a frame-shifted *nef* to have an ORF. In the case of JRCSFNef*fs,* a mutated *nef* was observed that produces a partially functional Nef, which specifically lacks CD4 downmodulation. These results are similar to those seen with HIV-1 LAI, a CXCR4-tropic virus.

In the natural infection of the sooty mangabey with SIV, infection does not lead to the depletion of $CD4^+$ T cells despite chronic replication, which is in stark contrast to SIV infection in rhesus macaques and HIV-1 infection in humans [271]. HIV-1 infection in humans and SIV infection in rhesus macaques leads to an increase in immune activation, whereas SIV infection in the sooty mangabey does not induce immune activation [271]. It is suggested that this difference in immune activation underlies the pathogenic difference seen between pathogenic HIV-1 infection in humans and SIV infected macaques and non-pathogenic infection observed in SIV infected sooty mangabeys [271]. Therefore in my investigation into the role of *nef* in the depletion of $CD4^+$ T cells during the course of HIV infection in BLT humanized mice, the difference in the viral replication and $CD4^+$ T cell depletion in mice infected with either JRCSFNef*dd* or JRCSF may be due to the difference in T cell activation seen during infection. To my knowledge the experiments described in this dissertation are the first of its kind in that it

assessed T cell activation throughout the course an infection, which is experimentally manipulated to be non-cytotoxic. The longitudinal analysis of T cell activation shown here demonstrates that JRCSF infected mice have higher levels of T cell activated than those infected with JRCSFNef*dd*. I conclude from this experiment that Nef is required for T cell activation, and that T cell activation may underlie the pathogenic differences seen between wild type JRCSF and *nef*-defective JRCSF infection in humanized mice. The significance of this observation lays in the fact that in humans, activation set point early in infection determines the rate of disease progression [186, 263, 272]. Future experiments should be designed to determine the role that immune activation plays in viral replication and $CD4^+$ T cell depletion.

5.5 Nef and future applications of the BLT humanized mouse HIV/AIDS research

A perfect model for the analysis of human disease does not exist. Animal models have allowed researchers to explore aspects of human disease that involve multiple components of the *in vivo* system. However, animal models mimic only some of the nuances of human diseases. The establishment of human-animal chimeras have allowed for more of the subtleties of human disease to be appreciated and studied. The development of humanized mice through the engraftment of human tissues and immune cells into immunodeficient mice has changed biomedical research forever. Specifically, HIV research, because HIV doesn't naturally infect the mouse, has been revolutionized. Revolutionized because these mouse-human chimeras

possess necessary target cells required for sustaining an HIV infection. Now, the feasibility of complicated investigations into the dynamics of HIV infection, prevention, transmission, and treatment are simply a matter of imagination. I have described in this thesis the leveraging of the animal model the BLT humanized mouse to investigate the viral factors that influence replication and $CD4^+$ T cell loss during HIV-1 infection. I have demonstrated that both Vpu and Nef are critical determinants of rapid $CD4^+$ T cell depletion and robust viral replication during HIV infection. I have also shown that of the multiple functions of Nef, its ability to downmodulate cell surface expression of CD4 is responsible of nearly half of the *in vivo* phenotype of a wild type infection. Of interest the Nef mutant defective for SH3 domain containing proteins binding is statistically indistinguishable from a wild type infection in regards to replication and $CD4^+$ T cell cytotoxicity.

The inability of Nef to bind to SH3 domain containing proteins was made possible via mutation to the PXXP motif of Nef. This mutation also inhibits Nef-mediated downmodulation of MHC1. Dudek *et al*. have determined that BLT humanized mice are able to mount an active $CD8^+$ T cell response. However, if BLT mice have an active $CD8^+$ T cell response, how then is the replication of the PXXP motif mutant *nef* HIV unable to be controlled? An explanation could be that $CD8^+$ T cell response is in most individuals is incapable of halting HIV-1 infection even in the absence of Nef mediated downmodulation of MHC1. Some individuals are capable

of spontaneously controlling HIV-1 infection in the absence of treatment. Certain HLA's have been associated with control of viremia. HLA-B*57, specifically, has been associated with the ability to control viremia in the absence of treatment. Dudek *et al*. demonstrated that humanized BLT mice can be engineered to express HLA-B*57, and demonstrated that animals expressing the protective HLA-B*57 allele showed enhanced control of viral replication [87]. Achieving an understanding of the host and viral factors that contribute to the controller phenotype may aid in the identification of new therapies. Protective HLA alleles represent one of the host factors influencing the controller phenotype, however the viral factor influencing control of viremia could be Nef. Dyer *et al*. explores this in their investigation into a group of elite controllers and long term nonprogressors. Dyer and colleagues followed a group of five long-term non-progressors over the course of 25 years, and it was observed that protective HLA alleles were overrepresented in these five individuals in regards to these alleles frequency in the general population. Of these five, three were considered to be elite controllers. These three individuals are from the Sydney Blood Bank Cohort, a group of individuals receiving a blood transfusion contaminated with a *nef* defective virus (Table 5.1) [273].

I have helped establish the BLT humanized mouse as a model to explore the dynamics of Nef-influenced CD4 depletion and viral replication. I propose that we leverage this model to investigate the how Nef and certain HLA alleles determine the elite controller phenotype. The

genotyping of donor tissues will allow for the identification of known protective HLA alleles, specifically but not limited to HLA-B*57, HLA-B*27, and HLA-B*44. Once identified, donor tissues expressing protective HLA alleles can be used to generate BLT humanized mice similar to Dudek *et al.* These protective HLA expressing animals can then be exposed to wildtype HIV or exposed to a *nef*-defective HIV. I hypothesize that in the absence of Nef, mice that possess a protective HLA allele will be capable of controlling infection. Elite controllers are able to suppress viremia to under 100 copies of viral RNA per mL of plasma, and it will interesting to see if mice expressing protective HLA alleles are able to suppress the viremia of a *nef*-defective virus to a level that can be deemed elite controller status [274]. Dudek *et al*. observed escape mutations with a high level of reproducibility within *nef* and *env*, which he described as being one of the major advantages of the BLT humanized mouse model. However, these escape mutations were associated with reduced viral replication. In the future experiments that I propose, the monitoring of *gag*, *env*, and *nef* sequences for escape mutations be included. In the absence of Nef-mediated downmodulation of MHC1, escape mutations should be readily observed, and can be correlated to reduced viral loads.

In summary I have shown that the BLT humanized mouse model has tremendous utility, and can be leveraged towards discerning the factors that influence many aspects of HIV infection and disease progression. Specifically in determining the viral factors that influence viral

replication and T cell cytotoxicity, two of the most fundamental nuances of the progression to AIDS during HIV infection. In addition I have also demonstrated that the humanized mouse can be used in assessing what host factors influence disease progression, namely, immune activation, which here within this thesis represents the first investigation of its kind in which the pathogenesis of an HIV-1 infection can be intentionally manipulated through the ablation of the accessory protein Nef. The future of Nef and the BLT humanized mouse may hold the answer as to how some individuals are able to avoid progression to AIDS through self-suppression of HIV-1 viremia in the complete absence of therapy.

TABLE 5.1: Long-term non-progressors followed in Dyer *et al.* (from Dyer *et al*. 2008)

Current Long-term non-progressors:				
Study Subject ID	Years HIV^+	ART Status	Δnef	HLA
C49‡	23.6	naive	**Δnef**	A 2,11 B 7,60
C64‡	24.7	naive	**Δnef**	A 2,32 B 7,**44**
C135‡	26.9	naive	**Δnef**	A 1,33 B 50,**57**
C13	23.2	naive	wt	A 3,25 B 18,**27**
C53	23.4	naive	wt	A 2,24 B 15,40
‡ Sydney blood bank cohort				

REFERENCES

1. Weiss, R.A., *How does HIV cause AIDS?* Science, 1993. **260**(5112): p. 1273-9.

2. Garg, H., J. Mohl, and A. Joshi, *HIV-1 induced bystander apoptosis.* Viruses, 2012. **4**(11): p. 3020-43.

3. Stevenson, M., *HIV-1 pathogenesis.* Nat Med, 2003. **9**(7): p. 853-60.

4. Swanstrom, R. and J. Coffin, *HIV-1 Pathogenesis: The Virus.* Cold Spring Harb Perspect Med, 2012.

5. Gottlieb, M.S., et al., *Pneumocystis carinii pneumonia and mucosal candidiasis in previously healthy homosexual men: evidence of a new acquired cellular immunodeficiency.* N Engl J Med, 1981. **305**(24): p. 1425-31.

6. Cohen, M.S., et al., *Acute HIV-1 Infection.* N Engl J Med, 2011. **364**(20): p. 1943-54.

7. Observatory, G.H. *HIV/AIDS*. 2014 [cited 2014 March 4]; Available from: http://www.who.int/gho/hiv/en/.

8. Kirchhoff, F., *Immune evasion and counteraction of restriction factors by HIV-1 and other primate lentiviruses.* Cell Host Microbe, 2010. **8**(1): p. 55-67.

9. Sharp, P.M. and B.H. Hahn, *Origins of HIV and the AIDS pandemic.* Cold Spring Harb Perspect Med, 2011. **1**(1): p. a006841.

10. Gao, F., et al., *Origin of HIV-1 in the chimpanzee Pan troglodytes troglodytes.* Nature, 1999. **397**(6718): p. 436-41.

11. Bailes, E., et al., *Hybrid origin of SIV in chimpanzees.* Science, 2003. **300**(5626): p. 1713.

12. Hahn, B.H., et al., *AIDS as a zoonosis: scientific and public health implications.* Science, 2000. **287**(5453): p. 607-14.

13. Buonaguro, L., M.L. Tornesello, and F.M. Buonaguro, *Human immunodeficiency virus type 1 subtype distribution in the worldwide epidemic: pathogenetic and therapeutic implications.* J Virol, 2007. **81**(19): p. 10209-19.

14. Vidal, N., et al., *Unprecedented degree of human immunodeficiency virus type 1 (HIV-1) group M genetic diversity in the Democratic Republic of Congo suggests that the HIV-1 pandemic originated in Central Africa.* J Virol, 2000. **74**(22): p. 10498-507.

15. Lau, K.A. and J.J. Wong, *Current Trends of HIV Recombination Worldwide.* Infect Dis Rep, 2013. **5**(Suppl 1): p. e4.

16. Santiago, M.L., et al., *SIVcpz in wild chimpanzees.* Science, 2002. **295**(5554): p. 465.

17. Kenyon, J.C. and A.M. Lever, *The molecular biology of feline immunodeficiency virus (FIV).* Viruses, 2011. **3**(11): p. 2192-213.

18. Troyer, R.M., et al., *Accessory genes confer a high replication rate to virulent feline immunodeficiency virus.* J Virol, 2013. **87**(14): p. 7940-51.

19. Shimojima, M., et al., *Use of CD134 as a primary receptor by the feline immunodeficiency virus.* Science, 2004. **303**(5661): p. 1192-5.

20. Gartner, S., et al., *The role of mononuclear phagocytes in HTLV-III/LAV infection.* Science, 1986. **233**(4760): p. 215-9.

21. Pauza, C.D., *HIV persistence in monocytes leads to pathogenesis and AIDS.* Cell Immunol, 1988. **112**(2): p. 414-24.

22. de Parseval, A., et al., *Sequential CD134-CXCR4 interactions in feline immunodeficiency virus (FIV): soluble CD134 activates FIV Env for CXCR4-dependent entry and reveals a cryptic neutralization epitope.* J Virol, 2006. **80**(6): p. 3088-91.

23. Samson, M., et al., *Resistance to HIV-1 infection in caucasian individuals bearing mutant alleles of the CCR-5 chemokine receptor gene.* Nature, 1996. **382**(6593): p. 722-5.

24. Deng, H., et al., *Identification of a major co-receptor for primary isolates of HIV-1.* Nature, 1996. **381**(6584): p. 661-6.

25. Shepherd, J.C., et al., *Emergence and persistence of CXCR4-tropic HIV-1 in a population of men from the multicenter AIDS cohort study.* J Infect Dis, 2008. **198**(8): p. 1104-12.

26. Garcia, J.V. and A.D. Miller, *Serine phosphorylation-independent downregulation of cell-surface CD4 by nef.* Nature, 1991. **350**(6318): p. 508-11.

27. Hong, Y., et al., *OrfA downregulates feline immunodeficiency virus primary receptor CD134 on the host cell surface and is important in viral infection.* J Virol, 2010. **84**(14): p. 7225-32.

28. Lee, S.K., M. Potempa, and R. Swanstrom, *The Choreography of HIV-1 Proteolytic Processing and Virion Assembly.* J Biol Chem, 2012.

29. Hu, W.S. and H.M. Temin, *Retroviral recombination and reverse transcription.* Science, 1990. **250**(4985): p. 1227-33.

30. Hallenberger, S., et al., *Inhibition of furin-mediated cleavage activation of HIV-1 glycoprotein gp160.* Nature, 1992. **360**(6402): p. 358-61.

31. Zheng, Y.H., N. Lovsin, and B.M. Peterlin, *Newly identified host factors modulate HIV replication.* Immunol Lett, 2005. **97**(2): p. 225-34.

32. Pollard, V.W. and M.H. Malim, *The HIV-1 Rev protein.* Annu Rev Microbiol, 1998. **52**: p. 491-532.

33. Malim, M.H., *HIV: Ringside views.* Nature, 2014. **505**(7482): p. 167-8.

34. Malim, M.H. and P.D. Bieniasz, *HIV Restriction Factors and Mechanisms of Evasion.* Cold Spring Harb Perspect Med, 2012. **2**(5): p. a006940.

35. Kirchhoff, F., et al., *Role of Nef in primate lentiviral immunopathogenesis.* Cell Mol Life Sci, 2008. **65**(17): p. 2621-36.

36. Mansky, L.M. and H.M. Temin, *Lower in vivo mutation rate of human immunodeficiency virus type 1 than that predicted from the fidelity of purified reverse transcriptase.* Journal of Virology, 1995. **8**: p. 5087-94.

37. Wei, X., et al., *Viral dynamics in human immunodeficiency virus type 1 infection.* Nature, 1995. **373**(6510): p. 117-22.

38. Charpentier, C., et al., *Extensive recombination among human immunodeficiency virus type 1 quasispecies makes an important contribution to viral diversity in individual patients.* J Virol, 2006. **80**(5): p. 2472-82.

39. Robertson, D.L., B.H. Hahn, and P.M. Sharp, *Recombination in AIDS viruses.* J Mol Evol, 1995. **40**(3): p. 249-59.

40. Haase, A.T., et al., *Quantitative image analysis of HIV-1 infection in lymphoid tissue.* Science, 1996. **274**(5289): p. 985-9.

41. Chun, T.W., et al., *Quantification of latent tissue reservoirs and total body viral load in HIV-1 infection.* Nature, 1997. **387**(6629): p. 183-8.

42. Rodrigo, A.G., et al., *Coalescent estimates of HIV-1 generation time in vivo.* Proc Natl Acad Sci U S A, 1999. **96**(5): p. 2187-91.

43. Strebel, K., *HIV accessory proteins versus host restriction factors.* Curr Opin Virol, 2013. **3**(6): p. 692-9.

44. Malim, M.H. and M. Emerman, *HIV-1 accessory proteins--ensuring viral survival in a hostile environment.* Cell Host Microbe, 2008. **3**(6): p. 388-98.

45. Etienne, L., et al., *Gene loss and adaptation to hominids underlie the ancient origin of HIV-1.* Cell Host Microbe, 2013. **14**(1): p. 85-92.

46. Goodman, M., et al., *Primate evolution at the DNA level and a classification of hominoids.* J Mol Evol, 1990. **30**(3): p. 260-6.

47. contributors, W. 2014 3 March 2014 [cited 2014 March 4]; Available from: http://en.wikipedia.org/w/index.php?title=Primate&oldid=597991254.

48. Yap, M.W. and J.P. Stoye, *Apparent effect of rabbit endogenous lentivirus type K acquisition on retrovirus restriction by lagomorph Trim5alphas.* Philos Trans R Soc Lond B Biol Sci, 2013. **368**(1626): p. 20120498.

49. Nomaguchi, M., M. Fujita, and A. Adachi, *Role of HIV-1 Vpu protein for virus spread and pathogenesis.* Microbes Infect, 2008. **10**(9): p. 960-7.

50. Beer, B.E., et al., *Simian immunodeficiency virus (SIV) from sun-tailed monkeys (Cercopithecus solatus): evidence for host-dependent evolution of SIV within the C. lhoesti superspecies.* J Virol, 1999. **73**(9): p. 7734-44.

51. Ishikawa, J., et al., *Molecular cloning and chromosomal mapping of a bone marrow stromal cell surface gene, BST2, that may be involved in pre-B-cell growth.* Genomics, 1995. **26**(3): p. 527-34.

52. Sakuma, T., et al., *Inhibition of Lassa and Marburg virus production by tetherin.* J Virol, 2009. **83**(5): p. 2382-5.

53. Sauter, D., A. Specht, and F. Kirchhoff, *Tetherin: holding on and letting go.* Cell, 2010. **141**(3): p. 392-8.

54. Arias, J.F., et al., *Tetherin antagonism by Vpu protects HIV-infected cells from antibody-dependent cell-mediated cytotoxicity.* Proc Natl Acad Sci U S A, 2014. **111**(17): p. 6425-30.

55. Alvarez, R.A., et al., *HIV-1 Vpu Antagonism of Tetherin Inhibits Antibody-Dependent Cellular Cytotoxic Responses by Natural Killer Cells.* J Virol, 2014. **88**(11): p. 6031-46.

56. Bour, S., U. Schubert, and K. Strebel, *The human immunodeficiency virus type 1 Vpu protein specifically binds to the cytoplasmic domain of CD4: implications for the mechanism of degradation.* J Virol, 1995. **69**(3): p. 1510-20.

57. Iwabu, Y., et al., *HIV-1 accessory protein Vpu internalizes cell-surface BST-2/tetherin through transmembrane interactions leading to lysosomes.* J Biol Chem, 2009. **284**(50): p. 35060-72.

58. Foster, J.L. and J.V. Garcia, *HIV-1 Nef: at the crossroads.* Retrovirology, 2008. **5**: p. 84.

59. Geist, M.M., et al., *Heterologous Src Homology 4 Domains Support Membrane Anchoring and Biological Activity of HIV-1 Nef.* J Biol Chem, 2014.

60. Zou, W., et al., *Nef functions in BLT mice to enhance HIV-1 replication and deplete CD4+CD8+ thymocytes.* Retrovirology, 2012. **9**(1): p. 44.

61. Deacon, N.J., et al., *Genomic structure of an attenuated quasi species of HIV-1 from a blood transfusion donor and recipients.* Science, 1995. **270**(5238): p. 988-91.

62. Kirchhoff, F., et al., *Brief report: absence of intact nef sequences in a long-term survivor with nonprogressive HIV-1 infection.* N Engl J Med, 1995. **332**(4): p. 228-32.

63. Kestler, H.W., 3rd, et al., *Importance of the nef gene for maintenance of high virus loads and for development of AIDS.* Cell, 1991. **65**(4): p. 651-62.

64. Hanna, Z., et al., *Nef harbors a major determinant of pathogenicity for an AIDS-like disease induced by HIV-1 in transgenic mice.* Cell, 1998. **95**(2): p. 163-75.

65. Rahim, M.M., et al., *Adult AIDS-like disease in a novel inducible human immunodeficiency virus type 1 Nef transgenic mouse model: CD4+ T-cell activation is Nef dependent and can occur in the absence of lymphophenia.* J Virol, 2009. **83**(22): p. 11830-46.

66. Skowronski, J., D. Parks, and R. Mariani, *Altered T cell activation and development in transgenic mice expressing the HIV-1 nef gene.* Embo J, 1993. **12**(2): p. 703-13.

67. Foster, J.L. and J.V. Garcia, *Role of Nef in HIV-1 replication and pathogenesis.* Adv Pharmacol, 2007. **55**: p. 389-409.

68. Olivetta, E., et al., *HIV-1 Nef Impairs Key Functional Activities in Human Macrophages through CD36 Downregulation.* PLoS One, 2014. **9**(4): p. e93699.

69. Chandrasekaran, P., et al., *HIV-1 Nef down-modulates C-C and C-X-C chemokine receptors via ubiquitin and ubiquitin-independent mechanism.* PLoS One, 2014. **9**(1): p. e86998.

70. Weiser, K., et al., *HIV's Nef interacts with beta-catenin of the Wnt signaling pathway in HEK293 cells.* PLoS One, 2013. **8**(10): p. e77865.

71. Kyei, G.B., et al., *Autophagy pathway intersects with HIV-1 biosynthesis and regulates viral yields in macrophages.* J Cell Biol, 2009. **186**(2): p. 255-68.

72. Aqil, M., et al., *The HIV-1 Nef protein binds argonaute-2 and functions as a viral suppressor of RNA interference.* PLoS One, 2013. **8**(9): p. e74472.

73. Malbec, M., et al., *HIV-1 Nef promotes the localization of Gag to the cell membrane and facilitates viral cell-to-cell transfer.* Retrovirology, 2013. **10**: p. 80.

74. Pan, X., et al., *HIV-1 Nef disrupts membrane-microdomain-associated anterograde transport for plasma membrane delivery of selected Src family kinases.* Cell Microbiol, 2013. **15**(10): p. 1605-21.

75. Jones, E.Y., *MHC class I and class II structures.* Curr Opin Immunol, 1997. **9**(1): p. 75-9.

76. Cresswell, P., et al., *Mechanisms of MHC class I-restricted antigen processing and cross-presentation.* Immunol Rev, 2005. **207**: p. 145-57.

77. Koopmann, J.O., et al., *Export of antigenic peptides from the endoplasmic reticulum intersects with retrograde protein translocation through the Sec61p channel.* Immunity, 2000. **13**(1): p. 117-27.

78. Albring, J., et al., *Retrotranslocation of MHC class I heavy chain from the endoplasmic reticulum to the cytosol is dependent on ATP supply to the ER lumen.* Mol Immunol, 2004. **40**(10): p. 733-41.

79. Imai, J., et al., *Exogenous antigens are processed through the endoplasmic reticulum-associated degradation (ERAD) in cross-presentation by dendritic cells.* Int Immunol, 2005. **17**(1): p. 45-53.

80. Collins, K.L., et al., *HIV-1 Nef protein protects infected primary cells against killing by cytotoxic T lymphocytes.* Nature, 1998. **391**(6665): p. 397-401.

81. Williams, M., et al., *Direct binding of human immunodeficiency virus type 1 Nef to the major histocompatibility complex class I (MHC-I) cytoplasmic tail disrupts MHC-I trafficking.* J Virol, 2002. **76**(23): p. 12173-84.

82. Jia, X., et al., *Structural Basis of HIV-1 Nef mediated Down-regulation of MHC-1.* 19th Conference on Retroviruses and Opportunistic Infections, 2012. **Paper #40LB**(<http://retroconference.org/2012b/Abstracts/45450.htm>).

83. Le Gall, S., et al., *Distinct trafficking pathways mediate Nef-induced and clathrin-dependent major histocompatibility complex class I down-regulation.* J Virol, 2000. **74**(19): p. 9256-66.

84. Blagoveshchenskaya, A.D., et al., *HIV-1 Nef downregulates MHC-I by a PACS-1- and PI3K-regulated ARF6 endocytic pathway.* Cell, 2002. **111**(6): p. 853-66.

85. Dikeakos, J.D., et al., *An interdomain binding site on HIV-1 Nef interacts with PACS-1 and PACS-2 on endosomes to down-regulate MHC-I.* Mol Biol Cell, 2012. **23**(11): p. 2184-97.

86. Petersen, J.L., C.R. Morris, and J.C. Solheim, *Virus evasion of MHC class I molecule presentation.* J Immunol, 2003. **171**(9): p. 4473-8.

87. Dudek, T.E., et al., *Rapid Evolution of HIV-1 to Functional CD8+ T Cell Responses in Humanized BLT Mice.* Sci Transl Med, 2012. **4**(143): p. 143ra98.

88. Heigele, A., et al., *Viremic long-term nonprogressive HIV-1 infection is not associated with abnormalities in known Nef functions.* Retrovirology, 2014. **11**: p. 13.

89. Noviello, C.M., S. Benichou, and J.C. Guatelli, *Cooperative binding of the class I major histocompatibility complex cytoplasmic domain and human immunodeficiency virus type 1 Nef to the endosomal AP-1 complex via its mu subunit.* J Virol, 2008. **82**(3): p. 1249-58.

90. Singh, R.K., et al., *An MHC-I cytoplasmic domain/HIV-1 Nef fusion protein binds directly to the mu subunit of the AP-1 endosomal coat complex.* PLoS One, 2009. **4**(12): p. e8364.

91. Wonderlich, E.R., M. Williams, and K.L. Collins, *The tyrosine binding pocket in the adaptor protein 1 (AP-1) mu1 subunit is necessary for Nef to recruit AP-1 to the major histocompatibility complex class I cytoplasmic tail.* J Biol Chem, 2008. **283**(6): p. 3011-22.

92. Baugh, L.L., J.V. Garcia, and J.L. Foster, *Functional characterization of the human immunodeficiency virus type 1 Nef acidic domain.* J Virol, 2008. **82**(19): p. 9657-67.

93. Kuo, L.S., et al., *Overlapping effector interfaces define the multiple functions of the HIV-1 Nef polyproline helix.* Retrovirology, 2012. **9**(1): p. 47.

94. Kay, B.K., M.P. Williamson, and M. Sudol, *The importance of being proline: the interaction of proline-rich motifs in signaling proteins with their cognate domains.* FASEB J, 2000. **14**(2): p. 231-41.

95. Li, S.S., *Specificity and versatility of SH3 and other proline-recognition domains: structural basis and implications for cellular signal transduction.* Biochem J, 2005. **390**(Pt 3): p. 641-53.

96. Musacchio, A., *How SH3 domains recognize proline.* Adv Protein Chem, 2002. **61**: p. 211-68.

97. Zarrinpar, A., R.P. Bhattacharyya, and W.A. Lim, *The structure and function of proline recognition domains.* Sci STKE, 2003. **2003**(179): p. RE8.

98. Casartelli, N., et al., *The Pro78 residue regulates the capacity of the human immunodeficiency virus type 1 Nef protein to inhibit recycling of major histocompatibility complex class I molecules in an SH3-independent manner.* J Gen Virol, 2006. **87**(Pt 8): p. 2291-6.

99. Yamada, T., et al., *Proline 78 is crucial for human immunodeficiency virus type 1 Nef to down-regulate class I human leukocyte antigen.* J Virol, 2003. **77**(2): p. 1589-94.

100. Iijima, S., et al., *A noncanonical mu-1A-binding motif in the N terminus of HIV-1 Nef determines its ability to downregulate major histocompatibility complex class I in T lymphocytes.* J Virol, 2012. **86**(7): p. 3944-51.

101. Kwak, Y.T., et al., *Self-association of the Lentivirus protein, Nef.* Retrovirology, 2010. **7**: p. 77.

102. Liu, L.X., et al., *Mutation of a conserved residue (D123) required for oligomerization of human immunodeficiency virus type 1 Nef protein abolishes interaction with human thioesterase and results in impairment of Nef biological functions.* J Virol, 2000. **74**(11): p. 5310-9.

103. Dikeakos, J.D., et al., *Small molecule inhibition of HIV-1-induced MHC-I down-regulation identifies a temporally regulated switch in Nef action.* Mol Biol Cell, 2010. **21**(19): p. 3279-92.

104. Guy, B., et al., *HIV F/3' orf encodes a phosphorylated GTP-binding protein resembling an oncogene product.* Nature, 1987. **330**(6145): p. 266-9.

105. Kirchhoff, F., et al., *Nef proteins from simian immunodeficiency virus-infected chimpanzees interact with p21-activated kinase 2 and modulate cell surface expression of various human receptors.* J Virol, 2004. **78**(13): p. 6864-74.

106. Mann, J.K., et al., *Ability of HIV-1 Nef to downregulate CD4 and HLA class I differs among viral subtypes.* Retrovirology, 2013. **10**: p. 100.

107. Greenberg, M.E., et al., *Co-localization of HIV-1 Nef with the AP-2 adaptor protein complex correlates with Nef-induced CD4 down-regulation.* Embo J, 1997. **16**(23): p. 6964-76.

108. Lindwasser, O.W., et al., *A diacidic motif in human immunodeficiency virus type 1 Nef is a novel determinant of binding to AP-2.* J Virol, 2008. **82**(3): p. 1166-74.

109. Arold, S., et al., *The crystal structure of HIV-1 Nef protein bound to the Fyn kinase SH3 domain suggests a role for this complex in altered T cell receptor signaling.* Structure, 1997. **5**(10): p. 1361-72.

110. Grzesiek, S., et al., *Refined solution structure and backbone dynamics of HIV-1 Nef.* Protein Sci, 1997. **6**(6): p. 1248-63.

111. Lee, C.H., et al., *Crystal structure of the conserved core of HIV-1 Nef complexed with a Src family SH3 domain.* Cell, 1996. **85**(6): p. 931-42.

112. Chaudhuri, R., et al., *Downregulation of CD4 by human immunodeficiency virus type 1 Nef is dependent on clathrin and involves direct interaction of Nef with the AP2 clathrin adaptor.* J Virol, 2007. **81**(8): p. 3877-90.

113. Chaudhuri, R., et al., *A basic patch on alpha-adaptin is required for binding of human immunodeficiency virus type 1 Nef and cooperative assembly of a CD4-Nef-AP-2 complex.* J Virol, 2009. **83**(6): p. 2518-30.

114. O'Neill, E., et al., *Intra- and intersubtype alternative Pak2-activating structural motifs of human immunodeficiency virus type 1 Nef.* J Virol, 2006. **80**(17): p. 8824-9.

115. Coleman, S.H., et al., *Modulation of cellular protein trafficking by human immunodeficiency virus type 1 Nef: role of the acidic residue in the ExxxLL motif.* J Virol, 2006. **80**(4): p. 1837-49.

116. Yu, G. and R.L. Felsted, *Effect of myristoylation on p27 nef subcellular distribution and suppression of HIV-LTR transcription.* Virology, 1992. **187**(1): p. 46-55.

117. Doray, B., et al., *The gamma/sigma1 and alpha/sigma2 hemicomplexes of clathrin adaptors AP-1 and AP-2 harbor the dileucine recognition site.* Mol Biol Cell, 2007. **18**(5): p. 1887-96.

118. Jin, Y.J., et al., *HIV Nef-mediated CD4 down-regulation is adaptor protein complex 2 dependent.* J Immunol, 2005. **175**(5): p. 3157-64.

119. Foti, M., et al., *Nef-mediated clathrin-coated pit formation.* J Cell Biol, 1997. **139**(1): p. 37-47.

120. Burtey, A., et al., *Dynamic interaction of HIV-1 Nef with the clathrin-mediated endocytic pathway at the plasma membrane.* Traffic, 2007. **8**(1): p. 61-76.

121. Aiken, C., et al., *Nef induces CD4 endocytosis: requirement for a critical dileucine motif in the membrane-proximal CD4 cytoplasmic domain.* Cell, 1994. **76**(5): p. 853-64.

122. Rhee, S.S. and J.W. Marsh, *Human immunodeficiency virus type 1 Nef-induced down-modulation of CD4 is due to rapid internalization and degradation of surface CD4.* J Virol, 1994. **68**(8): p. 5156-63.

123. daSilva, L.L., et al., *Human immunodeficiency virus type 1 Nef protein targets CD4 to the multivesicular body pathway.* J Virol, 2009. **83**(13): p. 6578-90.

124. Foster, J.L., et al., *Mechanisms of HIV-1 Nef function and intracellular signaling.* J Neuroimmune Pharmacol, 2011. **6**(2): p. 230-46.

125. Chowers, M.Y., et al., *Optimal infectivity in vitro of human immunodeficiency virus type 1 requires an intact nef gene.* J Virol, 1994. **68**(5): p. 2906-14.

126. Miller, M.D., et al., *Expression of the human immunodeficiency virus type 1 (HIV-1) nef gene during HIV-1 production increases progeny particle infectivity independently of gp160 or viral entry.* J Virol, 1995. **69**(1): p. 579-84.

127. Goldsmith, M.A., et al., *Dissociation of the CD4 downregulation and viral infectivity enhancement functions of human immunodeficiency virus type 1 Nef.* J Virol, 1995. **69**(7): p. 4112-21.

128. Aiken, C., *Pseudotyping human immunodeficiency virus type 1 (HIV-1) by the glycoprotein of vesicular stomatitis virus targets HIV-1 entry to an endocytic pathway and suppresses both the requirement for Nef and the sensitivity to cyclosporin A.* J Virol, 1997. **71**(8): p. 5871-7.

129. Chazal, N., et al., *Human immunodeficiency virus type 1 particles pseudotyped with envelope proteins that fuse at low pH no longer require Nef for optimal infectivity.* J Virol, 2001. **75**(8): p. 4014-8.

130. Aiken, C. and D. Trono, *Nef stimulates human immunodeficiency virus type 1 proviral DNA synthesis.* J Virol, 1995. **69**(8): p. 5048-56.

131. Chowers, M.Y., et al., *The growth advantage conferred by HIV-1 nef is determined at the level of viral DNA formation and is independent of CD4 downregulation.* Virology, 1995. **212**(2): p. 451-7.

132. Schwartz, O., et al., *Human immunodeficiency virus type 1 Nef increases the efficiency of reverse transcription in the infected cell.* J Virol, 1995. **69**(7): p. 4053-9.

133. Schaeffer, E., R. Geleziunas, and W.C. Greene, *Human immunodeficiency virus type 1 Nef functions at the level of virus entry by enhancing cytoplasmic delivery of virions.* J Virol, 2001. **75**(6): p. 2993-3000.

134. Pizzato, M., et al., *Dynamin 2 is required for the enhancement of HIV-1 infectivity by Nef.* Proc Natl Acad Sci U S A, 2007. **104**(16): p. 6812-7.

135. Pizzato, M., *MLV glycosylated-Gag is an infectivity factor that rescues Nef-deficient HIV-1.* Proc Natl Acad Sci U S A, 2010. **107**(20): p. 9364-9.

136. Juompan, L.Y., et al., *Analysis of the immune responses in chimpanzees infected with HIV type 1 isolates.* AIDS Res Hum Retroviruses, 2008. **24**(4): p. 573-86.

137. Molli, P.R., et al., *PAK signaling in oncogenesis.* Oncogene, 2009. **28**(28): p. 2545-55.

138. Foster, J.L., et al., *Genetic and functional diversity of human immunodeficiency virus type 1 subtype B Nef primary isolates.* J Virol, 2001. **75**(4): p. 1672-80.

139. Schindler, M., et al., *Association of Nef with p21-activated kinase 2 is dispensable for efficient human immunodeficiency virus type 1 replication and cytopathicity in ex vivo-infected human lymphoid tissue.* J Virol, 2007. **81**(23): p. 13005-14.

140. Raney, A., et al., *Reconstitution and molecular analysis of an active human immunodeficiency virus type 1 Nef/p21-activated kinase 2 complex.* J Virol, 2005. **79**(20): p. 12732-41.

141. Karkkainen, S., et al., *Identification of preferred protein interactions by phage-display of the human Src homology-3 proteome.* EMBO Rep, 2006. **7**(2): p. 186-91.

142. Briggs, S.D., et al., *SH3-mediated Hck tyrosine kinase activation and fibroblast transformation by the Nef protein of HIV-1.* J Biol Chem, 1997. **272**(29): p. 17899-902.

143. Moarefi, I., et al., *Activation of the Src-family tyrosine kinase Hck by SH3 domain displacement.* Nature, 1997. **385**(6617): p. 650-3.

144. Trible, R.P., L. Emert-Sedlak, and T.E. Smithgall, *HIV-1 Nef selectively activates Src family kinases Hck, Lyn, and c-Src through direct SH3 domain interaction.* J Biol Chem, 2006. **281**(37): p. 27029-38.

145. Lang, S.M., et al., *Association of simian immunodeficiency virus Nef with cellular serine/threonine kinases is dispensable for the development of AIDS in rhesus macaques.* Nat Med, 1997. **3**(8): p. 860-5.

146. Arganaraz, E.R., et al., *Enhanced CD4 down-modulation by late stage HIV-1 nef alleles is associated with increased Env incorporation and viral replication.* J Biol Chem, 2003. **278**(36): p. 33912-9.

147. Tokarev, A. and J. Guatelli, *Misdirection of membrane trafficking by HIV-1 Vpu and Nef: Keys to viral virulence and persistence.* Cell Logist, 2011. **1**(3): p. 90-102.

148. Davis, K.A., et al., *Determination of CD4 antigen density on cells: role of antibody valency, avidity, clones, and conjugation.* Cytometry, 1998. **33**(2): p. 197-205.

149. Lama, J., *The physiological relevance of CD4 receptor down-modulation during HIV infection.* Curr HIV Res, 2003. **1**(2): p. 167-84.

150. Glushakova, S., et al., *CD4 down-modulation by human immunodeficiency virus type 1 Nef correlates with the efficiency of viral replication and with CD4(+) T-cell depletion in human lymphoid tissue ex vivo.* J Virol, 2001. **75**(21): p. 10113-7.

151. Carl, S., et al., *Modulation of different human immunodeficiency virus type 1 Nef functions during progression to AIDS.* J Virol, 2001. **75**(8): p. 3657-65.

152. Watkins, R.L., et al., *In vivo analysis of highly conserved Nef activities in HIV-1 replication and pathogenesis.* Retrovirology, 2013. **10**(1): p. 125.

153. Rikke Olesen , R.L.W., John F Krisko , Mingjie Liu , Lars Østergaard , John L Foster, J. Victor Garcia, *The HIV-1 Accessory Protein, Vpu, is a Major Pathogenicity Factor.* Journal of Virology, 2014. **Under review**.

154. Margottin, F., et al., *A novel human WD protein, h-beta TrCp, that interacts with HIV-1 Vpu connects CD4 to the ER degradation pathway through an F-box motif.* Mol Cell, 1998. **1**(4): p. 565-74.

155. Muthumani, K., et al., *Human immunodeficiency virus type 1 Nef induces programmed death 1 expression through a p38 mitogen-activated protein kinase-dependent mechanism.* J Virol, 2008. **82**(23): p. 11536-44.

156. Muthumani, K., et al., *HIV-1 Nef-induced FasL induction and bystander killing requires p38 MAPK activation.* Blood, 2005. **106**(6): p. 2059-68.

157. Thoulouze, M.I., et al., *Human immunodeficiency virus type-1 infection impairs the formation of the immunological synapse.* Immunity, 2006. **24**(5): p. 547-61.

158. Pan, X., et al., *HIV-1 Nef compensates for disorganization of the immunological synapse by inducing trans-Golgi network-associated Lck signaling.* Blood, 2012. **119**(3): p. 786-97.

159. Calugi, G., et al., *Entire genome of a strain of human immunodeficiency virus type 1 with a deletion of nef that was recovered 20 years after primary infection: large pool of proviruses with deletions of env.* J Virol, 2006. **80**(23): p. 11892-6.

160. Gorry, P.R., et al., *Pathogenicity and immunogenicity of attenuated, nef-deleted HIV-1 strains in vivo.* Retrovirology, 2007. **4**: p. 66.

161. Kondo, M., et al., *Identification of attenuated variants of HIV-1 circulating recombinant form 01_AE that are associated with slow disease progression due to gross genetic alterations in the nef/long terminal repeat sequences.* J Infect Dis, 2005. **192**(1): p. 56-61.

162. Abraham, L. and O.T. Fackler, *HIV-1 Nef: a multifaceted modulator of T cell receptor signaling.* Cell Commun Signal, 2012. **10**(1): p. 39.

163. Arhel, N.J. and F. Kirchhoff, *Implications of Nef: host cell interactions in viral persistence and progression to AIDS.* Curr Top Microbiol Immunol, 2009. **339**: p. 147-75.

164. Laguette, N., et al., *Human immunodeficiency virus (HIV) type-1, HIV-2 and simian immunodeficiency virus Nef proteins.* Mol Aspects Med, 2010. **31**(5): p. 418-33.

165. Mwimanzi, P., et al., *Dynamic range of Nef functions in chronic HIV-1 infection.* Virology, 2013. **439**(2): p. 74-80.

166. Heigele, A., et al., *Down-modulation of CD8alphabeta is a fundamental activity of primate lentiviral Nef proteins.* J Virol, 2012. **86**(1): p. 36-48.

167. Hrecka, K., et al., *Nef proteins from diverse groups of primate lentiviruses downmodulate CXCR4 to inhibit migration to the chemokine stromal derived factor 1.* J Virol, 2005. **79**(16): p. 10650-9.

168. Munch, J., et al., *Nef-mediated enhancement of virion infectivity and stimulation of viral replication are fundamental properties of primate lentiviruses.* J Virol, 2007. **81**(24): p. 13852-64.

169. Schindler, M., et al., *Down-modulation of mature major histocompatibility complex class II and up-regulation of invariant chain cell surface expression are well-conserved functions of human and simian immunodeficiency virus nef alleles.* J Virol, 2003. **77**(19): p. 10548-56.

170. Specht, A., et al., *Selective downmodulation of HLA-A and -B by Nef alleles from different groups of primate lentiviruses.* Virology, 2008. **373**(1): p. 229-37.

171. Fackler, O.T., et al., *Functional characterization of HIV-1 Nef mutants in the context of viral infection.* Virology, 2006. **351**(2): p. 322-39.

172. Lundquist, C.A., et al., *Nef-mediated downregulation of CD4 enhances human immunodeficiency virus type 1 replication in primary T lymphocytes.* J Virol, 2002. **76**(9): p. 4625-33.

173. Manninen, A., et al., *SH3-Domain binding function of HIV-1 Nef is required for association with a PAK-related kinase.* Virology, 1998. **250**(2): p. 273-82.

174. Olivieri, K.C., J. Mukerji, and D. Gabuzda, *Nef-mediated enhancement of cellular activation and human immunodeficiency virus type 1 replication in primary T cells is dependent on association with p21-activated kinase 2.* Retrovirology, 2011. **8**: p. 64.

175. O'Neill, E., et al., *Dynamic evolution of the human immunodeficiency virus type 1 pathogenic factor, Nef.* J Virol, 2006. **80**(3): p. 1311-20.

176. Baur, A.S., et al., *HIV-1 Nef leads to inhibition or activation of T cells depending on its intracellular localization.* Immunity, 1994. **1**(5): p. 373-84.

177. Hanna, Z., et al., *The pathogenicity of human immunodeficiency virus (HIV) type 1 Nef in CD4C/HIV transgenic mice is abolished by mutation of its SH3-binding domain, and disease development is delayed in the absence of Hck.* J Virol, 2001. **75**(19): p. 9378-92.

178. Stove, V., et al., *Signaling but not trafficking function of HIV-1 protein Nef is essential for Nef-induced defects in human intrathymic T-cell development.* Blood, 2003. **102**(8): p. 2925-32.

179. Greenberg, M.E., A.J. Iafrate, and J. Skowronski, *The SH3 domain-binding surface and an acidic motif in HIV-1 Nef regulate trafficking of class I MHC complexes.* Embo J, 1998. **17**(10): p. 2777-89.

180. Hung, C.H., et al., *HIV-1 Nef assembles a Src family kinase-ZAP-70/Syk-PI3K cascade to downregulate cell-surface MHC-I.* Cell Host Microbe, 2007. **1**(2): p. 121-33.

181. Jia, X., et al., *Structural basis of evasion of cellular adaptive immunity by HIV-1 Nef.* Nat Struct Mol Biol, 2012.

182. Xu, W., et al., *HIV-1 evades virus-specific IgG2 and IgA responses by targeting systemic and intestinal B cells via long-range intercellular conduits.* Nat Immunol, 2009. **10**(9): p. 1008-17.

183. Mangasarian, A., et al., *Nef-induced CD4 and major histocompatibility complex class I (MHC-I) down-regulation are governed by distinct determinants: N-terminal alpha helix and proline repeat of Nef selectively regulate MHC-I trafficking.* J Virol, 1999. **73**(3): p. 1964-73.

184. Brainard, D.M., et al., *Induction of robust cellular and humoral virus-specific adaptive immune responses in human immunodeficiency virus-infected humanized BLT mice.* J Virol, 2009. **83**(14): p. 7305-21.

185. Denton, P.W., et al., *Antiretroviral pre-exposure prophylaxis prevents vaginal transmission of HIV-1 in humanized BLT mice.* PLoS Med, 2008. **5**(1): p. e16.

186. Long, B.R. and C.A. Stoddart, *Alpha interferon and HIV infection cause activation of human T cells in NSG-BLT mice.* J Virol, 2012. **86**(6): p. 3327-36.

187. Murooka, T.T., et al., *HIV-infected T cells are migratory vehicles for viral dissemination.* Nature, 2012. **490**(7419): p. 283-7.

188. Kirchhoff, F., et al., *Sequence variations in human immunodeficiency virus type 1 Nef are associated with different stages of disease.* J Virol, 1999. **73**(7): p. 5497-508.

189. Lewis, M.J., et al., *Functional adaptation of Nef to the immune milieu of HIV-1 infection in vivo.* J Immunol, 2008. **180**(6): p. 4075-81.

190. Michael, N.L., et al., *Functional characterization of human immunodeficiency virus type 1 nef genes in patients with divergent rates of disease progression.* J Virol, 1995. **69**(11): p. 6758-69.

191. Denton, P.W., et al., *Systemic administration of antiretrovirals prior to exposure prevents rectal and intravenous HIV-1 transmission in humanized BLT mice.* PLoS One, 2010. **5**(1): p. e8829.

192. Denton, P.W., et al., *Generation of HIV latency in humanized BLT mice.* J Virol, 2012. **86**(1): p. 630-4.

193. Denton, P.W., et al., *One percent tenofovir applied topically to humanized BLT mice and used according to the CAPRISA 004 experimental design demonstrates partial protection from vaginal HIV infection, validating the BLT model for evaluation of new microbicide candidates.* J Virol, 2011. **85**(15): p. 7582-93.

194. Kim, S.S., et al., *RNAi-mediated CCR5 silencing by LFA-1-targeted nanoparticles prevents HIV infection in BLT mice.* Mol Ther, 2010. **18**(2): p. 370-6.

195. Lan, P., et al., *Reconstitution of a functional human immune system in immunodeficient mice through combined human fetal thymus/liver and CD34+ cell transplantation.* Blood, 2006. **108**(2): p. 487-92.

196. Melkus, M.W., et al., *Humanized mice mount specific adaptive and innate immune responses to EBV and TSST-1.* Nat Med, 2006. **12**(11): p. 1316-22.

197. Rajesh, D., et al., *Th1 and Th17 immunocompetence in humanized NOD/SCID/IL2rgammanull mice.* Hum Immunol, 2010. **71**(6): p. 551-9.

198. Sun, Z., et al., *Intrarectal transmission, systemic infection, and CD4+ T cell depletion in humanized mice infected with HIV-1.* J Exp Med, 2007. **204**(4): p. 705-14.

199. Peden, K., M. Emerman, and L. Montagnier, *Changes in growth properties on passage in tissue culture of viruses derived from infectious molecular clones of HIV-1LAI, HIV-1MAL, and HIV-1ELI.* Virology, 1991. **185**(2): p. 661-72.

200. Arora, V.K., et al., *Lentivirus Nef specifically activates Pak2.* J Virol, 2000. **74**(23): p. 11081-7.

201. Wei, B.L., et al., *Inhibition of lysosome and proteasome function enhances human immunodeficiency virus type 1 infection.* J Virol, 2005. **79**(9): p. 5705-12.

202. Palmer, S., et al., *New real-time reverse transcriptase-initiated PCR assay with single-copy sensitivity for human immunodeficiency virus type 1 RNA in plasma.* J Clin Microbiol, 2003. **41**(10): p. 4531-6.

203. Denton, P.W. and J.V. Garcia, *Mucosal HIV-1 transmission and prevention strategies in BLT humanized mice.* Trends Microbiol, 2012. **20**(6): p. 268-74.

204. Kimpton, J. and M. Emerman, *Detection of replication-competent and pseudotyped human immunodeficiency virus with a sensitive cell line on the basis of activation of an integrated beta-galactosidase gene.* J Virol, 1992. **66**(4): p. 2232-9.

205. Chang, A.H., et al., *Construction of single-chain antibodies that bind an overlapping epitope of HIV-1 Nef.* FEBS Lett, 1998. **441**(2): p. 307-12.

206. Chateau, M., M.D. Swanson, and J.V. Garcia, *Inefficient vaginal transmission of tenofovir-resistant HIV-1.* J Virol, 2012. **87**(2): p. 1274-7.

207. Krisko, J.F., et al., *HIV restriction by APOBEC3 in humanized mice.* PLoS Pathog, 2013. **9**(3): p. e1003242.

208. Schwartz, O., et al., *Endocytosis of major histocompatibility complex class I molecules is induced by the HIV-1 Nef protein.* Nat Med, 1996. **2**(3): p. 338-42.

209. Sawai, E.T., et al., *Human immunodeficiency virus type 1 Nef associates with a cellular serine kinase in T lymphocytes.* Proc Natl Acad Sci U S A, 1994. **91**(4): p. 1539-43.

210. Lundquist, C.A., J. Zhou, and C. Aiken, *Nef stimulates human immunodeficiency virus type 1 replication in primary T cells by enhancing virion-associated gp120 levels: coreceptor-dependent requirement for Nef in viral replication.* J Virol, 2004. **78**(12): p. 6287-96.

211. Schindler, M., et al., *Nef-mediated suppression of T cell activation was lost in a lentiviral lineage that gave rise to HIV-1.* Cell, 2006. **125**(6): p. 1055-67.

212. Schindler, M., et al., *Inefficient Nef-mediated downmodulation of CD3 and MHC-I correlates with loss of CD4+T cells in natural SIV infection.* PLoS Pathog, 2008. **4**(7): p. e1000107.

213. Kouwenhoven, A., V.D. Minassian, and J.W. Marsh, *HIV-1 Nef Mediates Pak Phosphorylation of Mek1 Serine298 and Elicits an Active Phospho-state of Pak2.* Curr HIV Res, 2013. **11**(3): p. 198-209.

214. Ali, S.A., et al., *Genetic characterization of HIV type 1 Nef-induced vesicle secretion.* AIDS Res Hum Retroviruses, 2010. **26**(2): p. 173-92.

215. Dinkins, C., J. Arko-Mensah, and V. Deretic, *Autophagy and HIV.* Semin Cell Dev Biol, 2010. **21**(7): p. 712-8.

216. Geleziunas, R., et al., *HIV-1 Nef inhibits ASK1-dependent death signalling providing a potential mechanism for protecting the infected host cell.* Nature, 2001. **410**(6830): p. 834-8.

217. Lenassi, M., et al., *HIV Nef is secreted in exosomes and triggers apoptosis in bystander CD4+ T cells.* Traffic, 2010. **11**(1): p. 110-22.

218. Shelton, M.N., et al., *Secretion modification region-derived peptide disrupts HIV-1 Nef's interaction with mortalin and blocks virus and Nef exosome release.* J Virol, 2012. **86**(1): p. 406-19.

219. Baur, A.S., *HIV-Nef and AIDS pathogenesis: are we barking up the wrong tree?* Trends Microbiol, 2011. **19**(9): p. 435-40.

220. Neil, S.J., et al., *An interferon-alpha-induced tethering mechanism inhibits HIV-1 and Ebola virus particle release but is counteracted by the HIV-1 Vpu protein.* Cell Host Microbe, 2007. **2**(3): p. 193-203.

221. Neil, S.J., T. Zang, and P.D. Bieniasz, *Tetherin inhibits retrovirus release and is antagonized by HIV-1 Vpu.* Nature, 2008. **451**(7177): p. 425-30.

222. Van Damme, N., et al., *The interferon-induced protein BST-2 restricts HIV-1 release and is downregulated from the cell surface by the viral Vpu protein.* Cell Host Microbe, 2008. **3**(4): p. 245-52.

223. Gotz, N., et al., *Reacquisition of Nef-mediated tetherin antagonism in a single in vivo passage of HIV-1 through its original chimpanzee host.* Cell Host Microbe, 2012. **12**(3): p. 373-80.

224. Jia, B., et al., *Species-specific activity of SIV Nef and HIV-1 Vpu in overcoming restriction by tetherin/BST2.* PLoS Pathog, 2009. **5**(5): p. e1000429.

225. Lim, E.S., H.S. Malik, and M. Emerman, *Ancient adaptive evolution of tetherin shaped the functions of Vpu and Nef in human immunodeficiency virus and primate lentiviruses.* J Virol, 2010. **84**(14): p. 7124-34.

226. Sauter, D., et al., *Tetherin-driven adaptation of Vpu and Nef function and the evolution of pandemic and nonpandemic HIV-1 strains.* Cell Host Microbe, 2009. **6**(5): p. 409-21.

227. Yang, S.J., et al., *Anti-tetherin activities in Vpu-expressing primate lentiviruses.* Retrovirology, 2010. **7**: p. 13.

228. Zhang, F., et al., *Nef proteins from simian immunodeficiency viruses are tetherin antagonists.* Cell Host Microbe, 2009. **6**(1): p. 54-67.

229. Mitchell, R.S., et al., *Vpu antagonizes BST-2-mediated restriction of HIV-1 release via beta-TrCP and endo-lysosomal trafficking.* PLoS Pathog, 2009. **5**(5): p. e1000450.

230. Douglas, J.L., et al., *Vpu directs the degradation of the human immunodeficiency virus restriction factor BST-2/Tetherin via a {beta}TrCP-dependent mechanism.* J Virol, 2009. **83**(16): p. 7931-47.

231. Goffinet, C., et al., *HIV-1 antagonism of CD317 is species specific and involves Vpu-mediated proteasomal degradation of the restriction factor.* Cell Host Microbe, 2009. **5**(3): p. 285-97.

232. Sauter, D., et al., *HIV-1 Group P is unable to antagonize human tetherin by Vpu, Env or Nef.* Retrovirology, 2011. **8**: p. 103.

233. Yang, S.J., et al., *Lack of adaptation to human tetherin in HIV-1 group O and P.* Retrovirology, 2011. **8**: p. 78.

234. Dave, V.P., et al., *Efficient BST2 antagonism by Vpu is critical for early HIV-1 dissemination in humanized mice.* Retrovirology, 2013. **10**(1): p. 128.

235. Sato, K., et al., *Vpu augments the initial burst phase of HIV-1 propagation and downregulates BST2 and CD4 in humanized mice.* J Virol, 2012. **86**(9): p. 5000-13.

236. Hatziioannou, T. and P.D. Bieniasz, *Antiretroviral restriction factors.* Curr Opin Virol, 2011. **1**(6): p. 526-32.

237. Neil, S. and P. Bieniasz, *Human immunodeficiency virus, restriction factors, and interferon.* J Interferon Cytokine Res, 2009. **29**(9): p. 569-80.

238. Neil, S.J., *The antiviral activities of tetherin.* Curr Top Microbiol Immunol, 2013. **371**: p. 67-104.

239. Andrew, A. and K. Strebel, *The interferon-inducible host factor bone marrow stromal antigen 2/tetherin restricts virion release, but is it actually a viral restriction factor?* J Interferon Cytokine Res, 2011. **31**(1): p. 137-44.

240. Sato, K., P. Gee, and Y. Koyanagi, *Vpu and BST2: Still Not There Yet?* Front Microbiol, 2012. **3**: p. 131.

241. Galao, R.P., et al., *Innate sensing of HIV-1 assembly by Tetherin induces NFkappaB-dependent proinflammatory responses.* Cell Host Microbe, 2012. **12**(5): p. 633-44.

242. Tokarev, A., et al., *Stimulation of NF-kappaB activity by the HIV restriction factor BST2.* J Virol, 2013. **87**(4): p. 2046-57.

243. Akari, H., et al., *The human immunodeficiency virus type 1 accessory protein Vpu induces apoptosis by suppressing the nuclear factor kappaB-dependent expression of antiapoptotic factors.* J Exp Med, 2001. **194**(9): p. 1299-311.

244. Bour, S., et al., *The human immunodeficiency virus type 1 Vpu protein inhibits NF-kappa B activation by interfering with beta TrCP-mediated degradation of Ikappa B.* J Biol Chem, 2001. **276**(19): p. 15920-8.

245. Gustin, J.K. and J.L. Douglas, *BST-2/tetherin: viral tether, viral sensor or both?* Future Virol, 2013. **8**(11).

246. Strebel, K., *HIV-1 Vpu - an ion channel in search of a job.* Biochim Biophys Acta, 2013. **http://dx.doi.org10.1016/j.bbamem.2013.06.029**.

247. Ruiz, A., J.C. Guatelli, and E.B. Stephens, *The Vpu protein: new concepts in virus release and CD4 down-modulation.* Curr HIV Res, 2010. **8**(3): p. 240-52.

248. Magadan, J.G. and J.S. Bonifacino, *Transmembrane domain determinants of CD4 Downregulation by HIV-1 Vpu.* J Virol, 2012. **86**(2): p. 757-72.

249. Magadan, J.G., et al., *Multilayered mechanism of CD4 downregulation by HIV-1 Vpu involving distinct ER retention and ERAD targeting steps.* PLoS Pathog, 2010. **6**(4): p. e1000869.

250. Aldrovandi, G.M. and J.A. Zack, *Replication and pathogenicity of human immunodeficiency virus type 1 accessory gene mutants in SCID-hu mice.* J Virol, 1996. **70**(3): p. 1505-11.

251. Rucker, E., et al., *Vpr and Vpu are important for efficient human immunodeficiency virus type 1 replication and CD4+ T-cell depletion in human lymphoid tissue ex vivo.* J Virol, 2004. **78**(22): p. 12689-93.

252. Denton, P.W. and J.V. Garcia, *Humanized mouse models of HIV infection.* AIDS Rev, 2011. **13**(3): p. 135-48.

253. Hout, D.R., et al., *Scrambling of the amino acids within the transmembrane domain of Vpu results in a simian-human immunodeficiency virus (SHIVTM) that is less pathogenic for pig-tailed macaques.* Virology, 2005. **339**(1): p. 56-69.

254. Li, J., et al., *Infection of cynomolgus monkeys with a chimeric HIV-1/SIVmac virus that expresses the HIV-1 envelope glycoproteins.* J Acquir Immune Defic Syndr, 1992. **5**(7): p. 639-46.

255. McCormick-Davis, C., et al., *A molecular clone of simian-human immunodeficiency virus (DeltavpuSHIV(KU-1bMC33)) with a truncated, non-membrane-bound vpu results in rapid CD4(+) T cell loss and neuro-AIDS in pig-tailed macaques.* Virology, 2000. **272**(1): p. 112-26.

256. Stephens, E.B., et al., *Deletion of the vpu sequences prior to the env in a simian-human immunodeficiency virus results in enhanced Env precursor synthesis but is less pathogenic for pig-tailed macaques.* Virology, 2002. **293**(2): p. 252-61.

257. Sauter, D., et al., *Human tetherin exerts strong selection pressure on the HIV-1 group N Vpu protein.* PLoS Pathog, 2012. **8**(12): p. e1003093.

258. Yamaguchi, J., et al., *Identification of HIV type 1 group N infections in a husband and wife in Cameroon: viral genome sequences provide evidence for horizontal transmission.* AIDS Res Hum Retroviruses, 2006. **22**(1): p. 83-92.

259. Cortes, M.J., F. Wong-Staal, and J. Lama, *Cell surface CD4 interferes with the infectivity of HIV-1 particles released from T cells.* J Biol Chem, 2002. **277**(3): p. 1770-9.

260. Koyanagi, Y., et al., *Dual infection of the central nervous system by AIDS viruses with distinct cellular tropisms.* Science, 1987. **236**(4803): p. 819-22.

261. Liu, Z., et al., *Elevated CD38 antigen expression on CD8+ T cells is a stronger marker for the risk of chronic HIV disease progression to AIDS and death in the Multicenter AIDS Cohort Study than CD4+ cell count, soluble immune activation markers, or combinations of HLA-DR and CD38 expression.* J Acquir Immune Defic Syndr Hum Retrovirol, 1997. **16**(2): p. 83-92.

262. Giorgi, J.V., et al., *CD8+ lymphocyte activation at human immunodeficiency virus type 1 seroconversion: development of HLA-DR+ CD38- CD8+ cells is associated with subsequent stable CD4+ cell levels. The Multicenter AIDS Cohort Study Group.* J Infect Dis, 1994. **170**(4): p. 775-81.

263. Deeks, S.G., et al., *Immune activation set point during early HIV infection predicts subsequent CD4+ T-cell changes independent of viral load.* Blood, 2004. **104**(4): p. 942-7.

264. Klatt, N.R., et al., *Availability of activated CD4+ T cells dictates the level of viremia in naturally SIV-infected sooty mangabeys.* J Clin Invest, 2008. **118**(6): p. 2039-49.

265. Moore, R.D. and R.E. Chaisson, *Natural history of HIV infection in the era of combination antiretroviral therapy.* AIDS, 1999. **13**(14): p. 1933-42.

266. Domingo, P. and F. Vidal, *Combination antiretroviral therapy.* Expert Opin Pharmacother, 2011. **12**(7): p. 995-8.

267. De Clercq, E., *Antivirals: past, present and future.* Biochem Pharmacol, 2013. **85**(6): p. 727-44.

268. Delobel, P., et al., *R5 to X4 switch of the predominant HIV-1 population in cellular reservoirs during effective highly active antiretroviral therapy.* J Acquir Immune Defic Syndr, 2005. **38**(4): p. 382-92.

269. Tersmette, M., et al., *Differential syncytium-inducing capacity of human immunodeficiency virus isolates: frequent detection of syncytium-inducing isolates in patients with acquired immunodeficiency syndrome (AIDS) and AIDS-related complex.* J Virol, 1988. **62**(6): p. 2026-32.

270. Weinberger, A.D. and A.S. Perelson, *Persistence and emergence of X4 virus in HIV infection.* Math Biosci Eng, 2011. **8**(2): p. 605-26.

271. Silvestri, G., et al., *Nonpathogenic SIV infection of sooty mangabeys is characterized by limited bystander immunopathology despite chronic high-level viremia.* Immunity, 2003. **18**(3): p. 441-52.

272. Giorgi, J.V., et al., *Shorter survival in advanced human immunodeficiency virus type 1 infection is more closely associated with T lymphocyte activation than with plasma virus burden or virus chemokine coreceptor usage.* J Infect Dis, 1999. **179**(4): p. 859-70.

273. Dyer, W.B., et al., *Mechanisms of HIV non-progression; robust and sustained CD4+ T-cell proliferative responses to p24 antigen correlate with control of viraemia and lack of disease progression after long-term transfusion-acquired HIV-1 infection.* Retrovirology, 2008. **5**: p. 112.

274. Blankson, J.N., *Effector mechanisms in HIV-1 infected elite controllers: highly active immune responses?* Antiviral Res, 2010. **85**(1): p. 295-302.